

Seabrook Station



**North
Atlantic**

**Updated
Final Safety
Analysis Report**

Revision 7

Seabrook Station



**North
Atlantic**

**Updated
Final Safety
Analysis Report**

Revision 7

Seabrook Station



**North
Atlantic**

**Updated
Final Safety
Analysis Report**

Revision 7

Seabrook Station



**North
Atlantic**

**Updated
Final Safety
Analysis Report**

Revision 7

CHAPTER 3DESIGN OF STRUCTURES, COMPONENTS, EQUIPMENT AND SYSTEMSTABLES

<u>Table No.</u>	<u>Title</u>
3.9(B)-5	Stress Limits for Nonactive Category I, ASME Code Class 2 and 3 Valves
3.9(B)-6	Stress Limits for Nonactive Category I, ASME Code Class 1 Valves
3.9(B)-7	Stress Limits for Category I, ASME Code Class 2 and 3 Vessels and Tanks
3.9(B)-8	ASME Section III Class 1 Piping Systems Load Combinations and Stress Limits
3.9(B)-9	ASME Section III Class 2 and 3 Essential Piping Systems Load Combinations and Stress Limits
3.9(B)-10	ASME Section III Class 2 and 3 Nonessential Piping Systems
3.9(B)-11	Terminology and Notations Used in Tables 3.9(B)-8, 3.9(B)-9 and 3.9(B)-10
3.9(B)-12	Stress Limits for Active Category I ASME Code Class 2 and 3 Pumps
3.9(B)-13	Stress Limits for Active Category I ASME Code Class 2 and 3 Valves
3.9(B)-14	Stress Limits for Active Category I ASME Code Class 1 Valves
3.9(B)-15	Stress and Deflection Analysis of Primary Component Cooling Water Pumps (14x23-S)
3.9(B)-16	Stress and Deflection Summary for Containment Spray Pumps (6x11x14B-CD)
3.9(B)-17	Stress and Deflection Summary for Emergency Feedwater Pumps (4x9 NH-10)
3.9(B)-18	Stress and Deflection Summary for Service Water Pump (30 DC 2 Stage, Johnston Pump)

CHAPTER 3DESIGN OF STRUCTURES, COMPONENTS, EQUIPMENT AND SYSTEMSTABLES

<u>Table No.</u>	<u>Title</u>
3.9(B)-19	Stress and Deflection Summary for Cooling Tower Pump (33NLC, Johnston Vertical Pump)
3.9(B)-20	Stress and Deflection Summary for Diesel Fuel Oil Transfer Pump (N 3DBS - 18 IMO Pump)
3.9(B)-21	Stress Analysis Summary - ASME III Class 1 Piping - RCS Pressurizer Safety and Relief Valves System
3.9(B)-22	Stress Analysis Summary - ASME III Class 2 and 3 Piping
3.9(B)-23	ASME Code Class 1, 2 and 3 Pipe Support Load Combinations
3.9(B)-24	Deleted
3.9(B)-25	Deleted
3.9(B)-26	Active Pumps
3.9(B)-27	Active Valve List by System
3.9(N)-1	Summary of Reactor Coolant System Design Transients
3.9(N)-2	Loading Combinations for ASME Class 1 Components and Supports
3.9(N)-3	Allowable Stresses for ASME Section III Class 1 Components
3.9(N)-4	Design Loading Combinations for ASME Code Class 2 and 3 Components and Supports
3.9(N)-5	Stress Criteria for Safety-Related ASME Class 2 and Class 3 Tanks
3.9(N)-6	Stress Criteria for Safety-Related Class 2 Tanks
3.9(N)-7	Stress Criteria for ASME Code Class 2 and 3 Inactive Pumps
3.9(N)-8	Design Criteria for Active Pumps
3.9(N)-9	Stress Criteria for Safety-Related ASME Code Class 2 and Class 3 Valves

TABLE 3.2-2
(Sheet 25 of 46)

SEISMIC AND SAFETY CLASSIFICATIONS FLUID SYSTEMS AND COMPONENTS

<u>Updated FSAR Section</u>	<u>Systems and Components</u>	<u>ANS Safety Class</u>	<u>Principal Design/Const. Codes/Std.</u>	<u>Code Class</u>	<u>Seismic Category</u>	<u>Building⁽¹¹⁾</u>	<u>Supplier</u>	<u>Notes⁽¹⁴⁾</u>
	Piping and Valves							
	Containment Penetration	2	ASME III	2	I	CS	AE	
	Other	NNS	ANSI B31.1	-	-	WB/PB/CS	AE	
9.4.1	Control Room Complex Ventilation System							
	Control Room Air Conditioning Subsystem							
	Air Conditioning/Fan	3	MFRS. STDS.	-	I	CD	AE	
	Water Chiller	3	MFRS. STDS.	-	I	CD	AE	
	Dampers	3	AMCA	-	I	CD	AE	
	Ductwork	3	SMACNA	-	I	CD	AE	See Note 13.
	Computer Room Air Conditioning Subsystem							
	Air Conditioning Unit	-	MFRS. STDS.	-	-	CD	AE	
	Condensing Unit	-	MFRS. STDS.	-	-	CD	AE	
	Cooling Coil	3	ARI 410	-	I	CD	AE	

TABLE 3.2-2
(Sheet 25a of 46)

SEISMIC AND SAFETY CLASSIFICATIONS FLUID SYSTEMS AND COMPONENTS

<u>Updated FSAR Section</u>	<u>Systems and Components</u>	<u>ANS Safety Class</u>	<u>Principal Design/Const. Codes/Stds.</u>	<u>Code Class</u>	<u>Seismic Category</u>	<u>Building⁽¹¹⁾</u>	<u>Supplier</u>	<u>Notes⁽¹⁴⁾</u>
	Chilled Water Pumps	3	MFRS. STDS.	-	I	CD	AE	
	Expansion Tank	3	ASME VIII	-	I	CD	AE	
	Piping and Valves	3	ANSI B31.1	-	I	CD	AE	

TABLE 3.2-2
(Sheet 26 of 46)

SEISMIC AND SAFETY CLASSIFICATIONS FLUID SYSTEMS AND COMPONENTS

<u>Updated FSAR Section</u>	<u>Systems and Components</u>	<u>ANS Safety Class</u>	<u>Principal Design/Const. Codes/Std.</u>	<u>Code Class</u>	<u>Seismic Category</u>	<u>Building⁽¹¹⁾</u>	<u>Supplier</u>	<u>Notes⁽¹⁴⁾</u>
	Dampers	-	AMCA	-	-	CD	AE	
	Ductwork	-	SMACNA	-	-	CD	AE	See Note 20.
	Control Room Complex Normal Makeup Air Subsystem							
	Fans	3	AMCA	-	I	CD	AE	
	Dampers	3	AMCA	-	I	CD	AE	
	Intake Piping	3	ANSI B31.1	NNS 1A	I	CD/YD	AE	See Note 19.
	Control Room Emergency Filtration Subsystem							
9.4.2	Fuel Storage Building Ventilation System							
	Ventilation Fans	-	AMCA	-	-	FB	AE	
	Dampers	3	AMCA	-	I	FB	AE	
	Ductwork	-	SMACNA	-	I	FB	AE	

rules of ASME B&PV Code, Section XI, "In-Service Inspection of Nuclear Power Plant Components."

2. Piping Systems Containing Moderate-Energy Fluids

- (a) Piping systems containing moderate-energy fluids are designed to comply with the criteria applied to high-energy fluid piping systems, as stated above, except that the piping is postulated to develop a limited-size through-wall leakage crack instead of a pipe break.
- (b) For each postulated leakage condition, design measures are provided that will provide protection from the effects of the resulting water spray and flooding.

3. Exceptions

Measures for protection against pipe whipping or jet impingement resulting from the breaks postulated in Subsection 3.6(B).2 are not provided for piping where any of the following applies:

- (a) Piping is physically separated or isolated from any essential system or component necessary for plant safety or shutdown by means of barriers, or is restrained from whipping by plant design features such as encasement.
- (b) The broken pipe cannot cause unacceptable damage to any essential system or component.
- (c) The energy associated with the whipping pipe can be demonstrated to be insufficient to impair to an unacceptable level the safety function of an essential system or component. For example, a whipping pipe is considered unable to rupture an impacted pipe of equal or larger nominal pipe size and equal or heavier wall thickness.

3.6(B).1.2 Description

High energy lines located in structures housing components essential for safe plant shutdown are listed in Table 3.6(B)-2.

Relative to possible dynamic effects of pipe failure in the Seabrook plant layout, essential systems and components are protected from the dynamic effects of rupture of high energy piping primarily by separation and redundancy. Routing of high energy lines has been arranged to provide the maximum amount of protection by using plant structural elements, such as wall or columns, and routing the high energy lines as far as practicable from essential components. In cases where separation is not possible, pipe whip

SEABROOK UPDATED FSAR

restraints are used to prevent uncontrolled whipping of the high energy piping. Compartments of primary interest are the containment structure, the main steam and feedwater pipe tunnels, and the Containment Enclosure Building and its attached compartments.

In the case of the control room, there are no high energy lines in the area which could affect habitability as a result of pipe whip. The main steam and feedwater lines on the pipe bridge are separated from the control room by the seismic Category I Control Building wall, which has been reinforced to protect the control room environment from postulated breaks in, or whip loads from, the main steam and feedwater lines. Control room habitability systems are discussed in Section 6.4.

The high energy lines outside containment whose breaks or cracks could have the greatest effect on environment within the structures housing components essential for safe plant shutdown are listed below:

- a. Primary Auxiliary Building
 - Steam generator blowdown lines
 - Auxiliary steam and condensate lines
 - Chemical and volume control system letdown line
 - Hot water heating lines
- b. Fuel Storage Building
 - Hot water heating lines
- c. Containment Enclosure and Connected Buildings
 - Hot water heating lines
- d. Main Steam and Feedwater Pipe Chase
 - Main steam lines
 - Feedwater lines
- e. Diesel Generator Building
 - Hot water heating line
- f. Control Building
 - Hot water heating line

the pipe, except where pipe whip restraints function to limit pipe separation. See Subsection 3.6(N).2.1 for exception for RCS piping.

- (b) Longitudinal splits were postulated to occur in high-energy piping four inches or larger nominal pipe size. The area of the longitudinal split was assumed to be equal to the flow area of the pipe, and the split was assumed to be parallel to the axis of the pipe. Jet impingement analysis was based on a rectangular break $2D_i$ long by $\pi D_i/8$ wide where D_i = pipe inside diameter. Breaks were oriented (but not concurrently) at two diametrically opposed points on the piping circumference such that the jet reactions produce out-of-plane bending of the piping configuration.
- (c) Certain longitudinal break orientations were excluded on the basis of the state of stress at the location considered. Specifically, where the maximum stress range in the axial direction is at least one and a half times that in the circumferential direction considering upset plant conditions, then only a circumferential break was postulated.
- (d) Longitudinal breaks were not postulated to occur in piping at terminal ends.

2. Moderate Energy Piping

Through-wall leakage cracks were postulated to occur in moderate energy piping larger than one inch nominal pipe diameter, and to have openings of one-half pipe diameter by one-half the pipe wall thickness.

d. Jet Impingement Force Criteria

The criteria used to evaluate jet impingement forces are described in Appendix 3C, Procedure for Evaluation of Jet Impingement Loads from High Energy Piping Failures. After jet forces imposed on structures or equipment have been determined, the capacity of the structures or equipment to support these loads without damage is investigated using conservative methods. Jet impingement loads are considered to be faulted condition loads and are so evaluated.

3.6(B).2.2 Analytical Methods to Define Forcing Functions and Response Models

This section presents a description of the methods used to define forcing functions and response models for pipe whip analysis. For RC Loop piping, see Subsection 3.6(N).2.2.

3.6(B).3 References

1. "Stress Report for High Energy Piping Penetrations for PSNH-Seabrook Station Units 1 and 2," Stress Report No. 9763-325-1, (Calculation 9763-C-01-ST-00-F) Rev. 1 dated September, 1976, United Engineers & Constructors Inc.
2. Moody, F.J., "Prediction of Blowdown Thrust and Jet Forces," Paper No. 69-HT-31, presented at the ASME-AICHE Heat Transfer Conference, Minneapolis, Minnesota, August 3-6, 1969.
3. Final Rule Modifying 10 CFR 50 Appendix A, GDC-4 dated October 27, 1987 [52 FR 41288].

TABLE 3.6(B)-1ESSENTIAL COMPONENTS LOCATED OUTSIDE CONTAINMENT POTENTIALLY
SUSCEPTIBLE TO EFFECTS OF PIPING FAILURE

<u>Component</u>	<u>Component Number</u>	<u>Location</u>
Residual Heat Removal Pumps	RH-P-8A	Primary Auxiliary Building
	RH-P-8B	Primary Auxiliary Building
Safety Injection Pumps	SI-P-6A	Primary Auxiliary Building
	SI-P-6B	Primary Auxiliary Building
Chemical and Volume Control Charging Pumps	CS-P-2A	Primary Auxiliary Building
	CS-P-2B	Primary Auxiliary Building
Primary Component Cooling Water Pumps	CC-P-11A	Primary Auxiliary Building
	CC-P-11B	Primary Auxiliary Building
	CC-P-11C	Primary Auxiliary Building
	CC-P-11D	Primary Auxiliary Building
Emergency Feedwater Pumps	FW-P-37A	Emergency Feedwater Pump- house
	FW-P-37B	Emergency Feedwater Pump- house
Condensate Storage Tank	CO-TK-25	Yard

TABLE 3.6(B)-2
(Sheet 1 of 13)

HIGH ENERGY LINES

<u>Line No.</u>	<u>Safety Class</u>	<u>Function</u>	<u>Essential Size</u>	<u>Yes</u>	<u>No</u>	<u>P&ID</u>
1-1	1	Primary Loop	29	X		RC-20841
1-2	1	Primary Loop	31	X		RC-20841
2-1	1	Primary Loop	31	X		RC-20841
3-1	1	Primary Loop	27½	X		RC-20842
4-1	1	Primary Loop	29	X		RC-20842
4-2	1	Primary Loop	31	X		RC-20842
5-1	1	Primary Loop	31	X		RC-20842
6-1	1	Primary Loop	27½	X		RC-20842
7-1	1	Primary Loop	29	X		RC-20843
7-2	1	Primary Loop	31	X		RC-20843
8-1	1	Primary Loop	31	X		RC-20843
9-1	1	Primary Loop	27½	X		RC-20843
10-1	1	Primary Loop	29	X		RC-20844
10-2	1	Primary Loop	31	X		RC-20844
11-1	1	Primary Loop	31	X		RC-20844
12-1	1	Primary Loop	27½	X		RC-20844
13-1	1	Reactor Coolant	12	X		RC-20841
21-1	1	Reactor Coolant	4	X		RC-20841
48-1	1	Reactor Coolant	4	X		RC-20843, 20846
48-2	1	Reactor Coolant	6	X		RC-20846
48-3	1	Reactor Coolant	4	X		RC-20846
49-1	1	Reactor Coolant	14	X		RC-20843, 20846
58-1	1	Reactor Coolant	12	X		RC-20844
74-1	1	Reactor Coolant	6	X		RC-20846
75-1	1	Reactor Coolant	6	X		RC-20846
76-1	1	Reactor Coolant	6	X		RC-20846
80-1	1	Reactor Coolant	6	X		RC-20846
80-2	1	Reactor Coolant	3	X		RC-20846
80-6	1	Reactor Coolant	3	X		RC-20846
80-15	1	Reactor Coolant	6	X		RC-20846
93-1	1	Reactor Coolant	2	X		RC-20841
94-1	1	Reactor Coolant	2	X		RC-20842
96-1	1	Reactor Coolant	2	X		RC-20843
97-1	1	Reactor Coolant	3	X		RC-20843
97-2	2	Reactor Coolant	3	X		RC-20843, CS-20722
98-1	1	Reactor Coolant	2	X		RC-20844
155-5	1	Residual Heat Removal	6	X		RH-20662, SI-20450
155-17	1	Residual Heat Removal	10	X		SI-20450
158-3	2	Residual Heat Removal	8	X		RH-20663

TABLE 3.6(B)-2
(Sheet 2 of 13)

HIGH ENERGY LINES

<u>Line No.</u>	<u>Safety Class</u>	<u>Function</u>	<u>Essential Size</u>	<u>Yes</u>	<u>No</u>	<u>P&ID</u>
158-4	2	Residual Heat Removal	6	X		RH-20663
158-5	1	Residual Heat Removal	6	X		RH-20663 SI-20450
158-17	1	Residual Heat Removal	10	X		SI-20450
160-6	1	Residual Heat Removal	6	X		RH-20663 RC-20844
160-17	1	Residual Heat	12	X		RC-20844
162-2	1	Residual Heat Removal	6	X		RH-20662 SI-20450
162-5	1	Residual Heat Removal	10	X		SI-20450
163-1	2	Residual Heat Removal	6	X		RH-20663
163-2	1	Residual Heat Removal	6	X		RH-20663 SI-20450
163-4	1	Residual Heat Removal	10	X		SI-20450
163-5	2	Residual Heat Removal	6	X		RH-20663
177-1	2	Residual Heat Removal	2	X		RH-20662 CS-20722
180-2	1	Residual Heat Removal	8	X		RH-20663
180-3	1	Residual Heat Removal	6	X		RH-20663 RC-20841
180-5	1	Residual Heat Removal	12	X		RC-20841
201-1	2	Safety Injection	10	X		SI-20450
201-2	1	Safety Injection	10	X		SI-20450, RC-20841
202-1	2	Safety Injection	10	X		SI-20450
202-2	1	Safety Injection	10	X		SI-20450, RC-20841
203-1	2	Safety Injection	10	X		SI-20450
203-2	1	Safety Injection	10	X		SI-20450, RC-20843
204-1	2	Safety Injection	10	X		SI-20450
204-2	1	Safety Injection	10	X		SI-20450, RC-20844
232-1	2	Safety Injection	2		X	SI-20450
232-2	2	Safety Injection	2		X	SI-20450
234-1	2	Safety Injection	2		X	SI-20450

TABLE 3.6(B)-2
(Sheet 3 of 13)

HIGH ENERGY LINES

<u>Line No.</u>	<u>Safety Class</u>	<u>Function</u>	<u>Essential Size</u>	<u>Yes</u>	<u>No</u>	<u>P&ID</u>
234-2	2	Safety Injection	2		X	SI-20450
236-1	2	Safety Injection	2		X	SI-20450
236-2	2	Safety Injection	2		X	SI-20450
238-1	2	Safety Injection	2		X	SI-20450
238-2	2	Safety Injection	2		X	SI-20450
240-1	2	Safety Injection	2		X	SI-20450
240-2	2	Safety Injection	2		X	SI-20450
242-1	2	Safety Injection	2		X	SI-20450
242-2	2	Safety Injection	2		X	SI-20450
244-1	2	Safety Injection	2		X	SI-20450
244-2	2	Safety Injection	2		X	SI-20450
246-1	2	Safety Injection	2		X	SI-20450
246-2	2	Safety Injection	2		X	SI-20450
251-3	2	Safety Injection	4	X		SI-20446
251-5	1	Safety Injection	2	X		SI-20446
251-6	1	Safety Injection	3	X		SI-20446
251-7	1	Safety Injection	6	X		SI-20446, RC-20843
256-3	2	Safety Injection	2	X		SI-20446
256-4	1	Safety Injection	2	X		SI-20446, RH-20663
258-1	2	Safety Injection	2	X		SI-20446
258-2	1	Safety Injection	2	X		SI-20446, RH-20663
259-3	1	Safety Injection	2	X		SI-20446, RH-20662
260-2	1	Safety Injection	2	X		SI-20446, RH-20662
261-2	1	Safety Injection	2	X		SI-20448
261-3	1	Safety Injection	3	X		SI-20448
261-4	1	Safety Injection	6	X		SI-20446, RC-20842
270-2	1	Safety Injection	2	X		SI-20446, RH-20663
272-2	2	Safety Injection	4	X		SI-20447
272-3	2	Safety Injection	3	X		SI-20447
272-4	1	Safety Injection	3	X		SI-20447
272-5	1	Safety Injection	1½	X		SI-20447, RC-20841
272-9	2	Safety Injection	4	X		SI-20447
273-1	1	Safety Injection	1½	X		SI-20447
273-5	1	Safety Injection	3	X		SI-20447

TABLE 3.6(B)-2
(Sheet 4 of 13)

HIGH ENERGY LINES

<u>Line No.</u>	<u>Safety Class</u>	<u>Function</u>	<u>Essential Size</u>	<u>Yes</u>	<u>No</u>	<u>P&ID</u>
274-1	1	Safety Injection	1½	X		SI-20447, RC-20844
274-5	1	Safety Injection	3	X		SI-20447
275-4	1	Safety Injection	1½	X		SI-20447
275-6	1	Safety Injection	3	X		SI-20447
318-1	2	Chem & Vol Control	3	X		CS-20722
318-2	2	Chem & Vol Control	2	X		CS-20722
318-9	2	Chem & Vol Control	2	X		CS-20722
324-1	2	Chem & Vol Control	3	X		CS-20722, CS-20726
325-1	2	Chem & Vol Control	2	X		CS-20726
326-1	2	Chem & Vol Control	2	X		CS-20726
327-1	2	Chem & Vol Control	3	X		CS-20726
327-2	2	Chem & Vol Control	2	X		CS-20726
328-1	2	Chem & Vol Control	2	X		CS-20726
328-2	2	Chem & Vol Control	3	X		CS-20726
328-3	2	Chem & Vol Control	2	X		CS-20726
328-6	1	Chem & Vol Control	2	X		CS-20726
328-7	1	Chem & Vol Control	1½	X		CS-20726
329-1	2	Chem & Vol Control	2	X		CS-20726
329-4	2	Chem & Vol Control	2	X		CS-20726
329-5	1	Chem & Vol Control	1½	X		CS-20726
330-1	2	Chem & Vol Control	2	X		CS-20726
330-4	1	Chem & Vol Control	2	X		CS-20726
330-5	1	Chem & Vol Control	1½	X		CS-20726
331-1	2	Chem & Vol Control	2	X		CS-20726
331-4	1	Chem & Vol Control	2	X		CS-20726
331-5	1	Chem & Vol Control	1½	X		CS-20726
348-1	NNS	Chem & Vol Control	3		X	CS-20724
354-1	NNS	Chem & Vol Control	3		X	CS-20724
355-1	2	Chem & Vol Control	3	X		CS-20722, CS-20725
355-6	2	Chem & Vol Control	3	X		CS-20722
356-1	2	Chem & Vol Control	4	X		CS-20725
356-2	2	Chem & Vol Control	3	X		CS-20725
358-1	2	Chem & Vol Control	2	X		CS-20725
358-2	2	Chem & Vol Control	3	X		CS-20725
358-3	2	Chem & Vol Control	2		X	CS-20725
360-1	2	Chem & Vol Control	3	X		CS-20722
360-2	2	Chem & Vol Control	2	X		CS-20722
360-3	2	Chem & Vol Control	2	X		CS-20722
360-4	2	Chem & Vol Control	3	X		CS-20722
360-5	2	Chem & Vol Control	2	X		CS-20722
360-6	2	Chem & Vol Control	2	X		CS-20722

TABLE 3.6(B)-2
(Sheet 5 of 13)

HIGH ENERGY LINES

<u>Line No.</u>	<u>Safety Class</u>	<u>Function</u>	<u>Essential Size</u>	<u>Essential</u>		<u>P&ID</u>
				<u>Yes</u>	<u>No</u>	
360-7	2	Chem & Vol Control	3	X		CS-20722
360-8	2	Chem & Vol Control	4	X		CS-20722
360-9	2	Chem & Vol Control	3	X		CS-20722
360-25	2	Chem & Vol Control	3	X		CS-20722
360-26	2	Chem & Vol Control	3	X		CS-20722
361-1	2	Chem & Vol Control	2	X		CS-20722
362-1	2	Chem & Vol Control	4	X		CS-20725
363-1	2	Chem & Vol Control	2	X		CS-20725
363-2	2	Chem & Vol Control	3	X		CS-20725
363-3	2	Chem & Vol Control	2	X		CS-20725
364-1	2	Chem & Vol Control	4	X		CS-20725
364-2	2	Chem & Vol Control	3	X		CS-20725
364-9	2	Chem & Vol Control	1½	X		CS-20725
365-1	2	Chem & Vol Control	2	X		CS-20725
365-2	1	Chem & Vol Control	2	X		CS-20722, RC-20846
366-1	2	Chem & Vol Control	3	X		CS-20722
366-2	1	Chem & Vol Control	3	X		CS-20722, RC-20841
367-1	2	Chem & Vol Control	2	X		CS-20725
368-1	2	Chem & Vol Control	3	X		CS-20722
368-2	1	Chem & Vol Control	3	X		CS-20722
374-1	2	Chem & Vol Control	4	X		CS-20725
376-1	NNS	Chem & Vol Control	3		X	CS-20724
431-1	2	Chem & Vol Control	3	X		CS-20727, CS-20722
431-2	2	Chem & Vol Control	4	X		CS-20727
432-1	2	Chem & Vol Control	4	X		CS-20727
432-2	2	Chem & Vol Control	3	X		CS-20727, CS-20722
525-1	NNS	Chem & Vol Control	4		X	CS-20724
525-2	NNS	Chem & Vol Control	3		X	CS-20724
525-3	NNS	Chem & Vol Control	3		X	CS-20724
526-1	NNS	Chem & Vol Control	2		X	CS-20724
526-2	NNS	Chem & Vol Control	2		X	CS-20724
526-8	NNS	Chem & Vol Control	1½		X	CS-20724
526-9	NNS	Chem & Vol Control	1½		X	CS-20724
526-10	NNS	Chem & Vol Control	3		X	CS-20724
526-13	NNS	Chem & Vol Control	2½		X	CS-20724
534-1	NNS	Chem & Vol Control	3		X	CS-20724
1301-1	2	Steam Gen Blowdown	2	X		RC-20841
1301-2	2	Steam Gen Blowdown	3	X		RC-20841, SB-20626

TABLE 3.6(B)-2
(Sheet 6 of 13)

HIGH ENERGY LINES

<u>Line No.</u>	<u>Safety Class</u>	<u>Function</u>	<u>Essential Size</u>	<u>Yes</u>	<u>No</u>	<u>P&ID</u>
1301-3	2	Steam Gen Blowdown	2	X		SB-20626
1301-4	2	Steam Gen Blowdown	3	X		SB-20626
1301-5	NNS	Steam Gen Blowdown	3		X	SB-20626
1301-16	NNS	Steam Gen Blowdown	3		X	SB-20626
1301-22	NNS	Steam Gen Blowdown	1½		X	SB-20626
1301-23	NNS	Steam Gen Blowdown	4		X	SB-20626
1303-1	2	Steam Gen Blowdown	2	X		RC-20841
1304-1	2	Steam Gen Blowdown	2	X		RC-20842
1304-2	2	Steam Gen Blowdown	3	X		RC-20842, SB-20626
1304-3	2	Steam Gen Blowdown	2	X		SB-20626
1304-4	2	Steam Gen Blowdown	3	X		SB-20626
1304-5	NNS	Steam Gen Blowdown	3		X	SB-20626
1304-17	NNS	Steam Gen Blowdown	3		X	SB-20626
1304-24	NNS	Steam Gen Blowdown	1½		X	SB-20626
1304-25	NNS	Steam Gen Blowdown	4		X	SB-20626
1306-2	2	Steam Gen Blowdown	2	X		RC-20842
1307-1	2	Steam Gen Blowdown	2	X		RC-20843
1307-2	2	Steam Gen Blowdown	3	X		RC-20843, SB-20626
1307-3	2	Steam Gen Blowdown	2	X		SB-20626
1307-4	2	Steam Gen Blowdown	3	X		SB-20626
1307-5	NNS	Steam Gen Blowdown	3		X	SB-20626
1307-17	NNS	Steam Gen Blowdown	3		X	SB-20626
1307-22	NNS	Steam Gen Blowdown	1½		X	SB-20626
1307-23	NNS	Steam Gen Blowdown	4		X	SB-20626
1309-2	2	Steam Gen Blowdown	2	X		RC-20843
1310-1	2	Steam Gen Blowdown	2	X		RC-20844
1310-2	2	Steam Gen Blowdown	3	X		RC-20844, SB-20626
1310-3	2	Steam Gen Blowdown	2	X		SB-20626
1310-4	2	Steam Gen Blowdown	3	X		SB-20626
1310-5	NNS	Steam Gen Blowdown	3		X	SB-20626
1310-16	NNS	Steam Gen Blowdown	3		X	SB-20626
1310-22	NNS	Steam Gen Blowdown	1½		X	SB-20626
1310-23	NNS	Steam Gen Blowdown	4		X	SB-20626
1312-2	2	Steam Gen Blowdown	2	X		RC-20844
1317-1	NNS	Steam Gen Blowdown	10		X	SB-20626
1317-7	NNS	Steam Gen Blowdown	14		X	SB-20626
1319-1	NNS	Steam Gen Blowdown	10		X	SB-20626
1320-1	NNS	Steam Gen Blowdown	8		X	SB-20626
1320-2	NNS	Steam Gen Blowdown	3		X	SB-20626

TABLE 3.6(B)-2
(Sheet 7 of 13)

HIGH ENERGY LINES

<u>Line No.</u>	<u>Safety Class</u>	<u>Function</u>	<u>Essential Size</u>	<u>Yes</u>	<u>No</u>	<u>P&ID</u>
1320-8	NNS	Steam Gen Blowdown	4		X	SB-20626
1321-1	NNS	Steam Gen Blowdown	3		X	SB-20626
1321-4	NNS	Steam Gen Blowdown	4		X	SB-20626
1350-3	NNS	Steam Gen Blowdown	10		X	SB-20626
2302-2	NNS	Aux Steam	8		X	AS-20570, AS-20569
2302-5	NNS	Aux Steam	4		X	AS-20570
2302-8	NNS	Aux Steam	4		X	AS-20570
2302-14	NNS	Aux Steam	2		X	AS-20571
2302-16	NNS	Aux Steam	2		X	AS-20571
2302-19	NNS	Aux Steam	4		X	AS-20570
2302-30	NNS	Aux Steam	4		X	AS-20571
2302-32	NNS	Aux Steam	8		X	AS-20570, AS-20571
2303-1	NNS	Aux Steam	6		X	AS-20570
2303-2	NNS	Aux Steam	4		X	AS-20570
2303-3	NNS	Aux Steam	4		X	AS-20570
2303-5	NNS	Aux Steam	2		X	AS-20570
2303-6	NNS	Aux Steam	3		X	AS-20570
2304-1	NNS	Aux Steam	3		X	AS-20570
2304-2	NNS	Aux Steam	1½		X	AS-20570
2304-3	NNS	Aux Steam	3		X	AS-20570
2306-1	NNS	Aux Steam	8		X	AS-20570
2306-2	NNS	Aux Steam	4		X	AS-20570
2306-4	NNS	Aux Steam	8		X	AS-20570
2306-5	NNS	Aux Steam	10		X	AS-20570
2309-1	NNS	Aux Steam	2		X	AS-20571
2309-2	NNS	Aux Steam	2		X	AS-20571
2339-1	NNS	Aux Steam	1½		X	AS-20571
2339-2	NNS	Aux Steam	1½		X	AS-20571
2341-1	NNS	Aux Steam	1½		X	AS-20571
2341-4	NNS	Aux Steam	2		X	AS-20571
2341-5	NNS	Aux Steam	1½		X	AS-20571
2364-1	NNS	Aux Steam	3		X	AS-20570
2365-6	NNS	Aux Steam	2		X	AS-20570
2366-1	NNS	Aux Steam	2		X	AS-20570
2401-1	NNS	Aux Steam Condensate	2½		X	ASC-20906
2401-2	NNS	Aux Steam Condensate	3		X	ASC-20906
2401-3	NNS	Aux Steam Condensate	2½		X	ASC-20906
2401-4	NNS	Aux Steam Condensate	1½		X	ASC-20906
2402-2	NNS	Aux Steam Condensate	2		X	ASC-20906
2402-3	NNS	Aux Steam Condensate	3		X	ASC-20906
2403-1	NNS	Aux Steam Condensate	1½		X	ASC-20906

TABLE 3.6(B)-2
(Sheet 8 of 13)

HIGH ENERGY LINES

<u>Line No.</u>	<u>Safety Class</u>	<u>Function</u>	<u>Essential Size</u>	<u>Yes</u>	<u>No</u>	<u>P&ID</u>
2404-1	NNS	Aux Steam Condensate	1½		X	ASC-20906
2404-2	NNS	Aux Steam Condensate	3		X	ASC-20906
2404-3	NNS	Aux Steam Condensate	3		X	ASC-20906
2404-4	NNS	Aux Steam Condensate	6		X	ASC-20906
2404-5	NNS	Aux Steam Condensate	3		X	ASC-20906
2404-6	NNS	Aux Steam Condensate	1½		X	ASC-20906
2404-8	NNS	Aux Steam Condensate	3		X	ASC-20906
2406-1	NNS	Aux Steam Condensate	4		X	ASC-20906, ASC-20907
2406-2	NNS	Aux Steam Condensate	6		X	ASC-20906
2406-3	NNS	Aux Steam Condensate	4		X	ASC-20906
2406-4	NNS	Aux Steam Condensate	3		X	ASC-20906
2406-5	NNS	Aux Steam Condensate	3		X	ASC-20906
2407-4	NNS	Aux Steam Condensate	1½		X	ASC-20907
2409-4	NNS	Aux Steam Condensate	1½		X	ASC-20907
2410-1	NNS	Aux Steam Condensate	2		X	ASC-20906
2410-4	NNS	Aux Steam Condensate	1½		X	ASC-20906
2433-1	NNS	Aux Steam Condensate	2		X	ASC-20906
2433-2	NNS	Aux Steam Condensate	1½		X	ASC-20906
2433-3	NNS	Aux Steam Condensate	1½		X	ASC-20906
2433-4	NNS	Aux Steam Condensate	1½		X	ASC-20906
2437-1	NNS	Aux Steam Condensate	2½		X	ASC-20906
2437-2	NNS	Aux Steam Condensate	3		X	ASC-20906
2437-3	NNS	Aux Steam Condensate	2½		X	ASC-20906
2437-4	NNS	Aux Steam Condensate	1½		X	ASC-20906
2438-2	NNS	Aux Steam Condensate	2		X	ASC-20906
2439-1	NNS	Aux Steam Condensate	1½		X	ASC-20906
2439-2	NNS	Aux Steam Condensate	1½		X	ASC-20906
2439-7	NNS	Aux Steam Condensate	1½		X	ASC-20907
2440-1	NNS	Aux Steam Condensate	1½		X	ASC-20906
2441-1	NNS	Aux Steam Condensate	1½		X	ASC-20907
2441-2	NNS	Aux Steam Condensate	1½		X	ASC-20907
2441-4	NNS	Aux Steam Condensate	2		X	ASC-20907
2441-7	NNS	Aux Steam Condensate	1½		X	ASC-20907
2442-1	NNS	Aux Steam Condensate	2		X	ASC-20906
2442-2	NNS	Aux Steam Condensate	2		X	ASC-20906
2450-1	NNS	Aux Steam Condensate	1½		X	ASC-20906
2450-2	NNS	Aux Steam Condensate	1½		X	ASC-20906
2451-1	NNS	Aux Steam Condensate	1½		X	ASC-20906
4000-1	2	Mainsteam	32	X		MS-20580, MS-20583
4000-2	2	Mainsteam	30	X		MS-20580
4000-3	NNS	Mainsteam	30		X	MS-20583

TABLE 3.6(B)-2
(Sheet 9 of 13)

HIGH ENERGY LINES

<u>Line No.</u>	<u>Safety Class</u>	<u>Function</u>	<u>Essential</u>		<u>P&ID</u>
			<u>Size</u>	<u>Yes No</u>	
4000-8	2	Mainsteam	6	X	MS-20580
4000-11	2	Mainsteam	6	X	MS-20580
4000-32	2	Mainsteam	6	X	MS-20580
4000-34	2	Mainsteam	6	X	MS-20580
4000-40	2	Mainsteam	30	X	MS-20580
4000-41	2	Mainsteam	30	X	MS-20580, MS-20583
4000-48	2	Mainsteam	2	X	MS-20580
4001-1	2	Mainsteam	32	X	MS-20581
4001-2	2	Mainsteam	30	X	MS-20581
4001-3	NNS	Mainsteam	30		X MS-20583
4001-8	2	Mainsteam	6	X	MS-20581
4001-11	2	Mainsteam	6	X	MS-20581
4001-32	2	Mainsteam	6	X	MS-20581
4001-34	2	Mainsteam	6	X	MS-20581
4001-39	2	Mainsteam	30	X	MS-20581
4001-41	2	Mainsteam	30	X	MS-20580, MS-20583
4001-46	2	Mainsteam	2	X	MS-20581
4002-1	2	Mainsteam	32	X	MS-20581
4002-2	2	Mainsteam	30	X	MS-20581
4002-3	NNS	Mainsteam	30		X MS-20583
4002-9	2	Mainsteam	6	X	MS-20581
4002-30	2	Mainsteam	6	X	MS-20581
4002-32	2	Mainsteam	6	X	MS-20581
4002-36	2	Mainsteam	30	X	MS-20581
4002-37	2	Mainsteam	30	X	MS-20581 MS-20583
4002-41	2	Mainsteam	2	X	MS-20581
4003-1	2	Mainsteam	32	X	MS-20580
4003-2	2	Mainsteam	30	X	MS-20580
4003-3	NNS	Mainsteam	30		X MS-20580
4003-9	2	Mainsteam	6	X	MS-20580
4003-30	2	Mainsteam	6	X	MS-20580
4003-32	2	Mainsteam	6	X	MS-20580
4003-36	2	Mainsteam	30	X	MS-20580
4003-37	2	Mainsteam	30	X	MS-20580 MS-20583
4003-41	2	Mainsteam	2	X	MS-20580
4004-1	NNS	Mainsteam	48		X MS-20583

TABLE 3.6(B)-2
(Sheet 10 of 13)

HIGH ENERGY LINES

<u>Line No.</u>	<u>Safety Class</u>	<u>Function</u>	<u>Essential Size</u>	<u>Yes</u>	<u>No</u>	<u>P&ID</u>
4005-1	NNS	Mainsteam	24		X	MS-20583, MS-20585
4006-1	NNS	Mainsteam	30		X	MS-20583
4006-2	NNS	Mainsteam	6		X	MS-20583
4007-1	NNS	Mainsteam	30		X	MS-20583
4007-2	NNS	Mainsteam	6		X	MS-20583
4008-1	NNS	Mainsteam	30		X	MS-20583
4008-2	NNS	Mainsteam	6		X	MS-20583
4009-1	NNS	Mainsteam	30		X	MS-20583
4009-2	NNS	Mainsteam	6		X	MS-20583
4010-1	NNS	Mainsteam	24		X	MS-20583 MS-20585
4010-33	NNS	Mainsteam	6		X	MS-20583
4366-1	3	Diesel Generator - Air	2	X		DG-20460
4367-1	3	Diesel Generator - Air	2	X		DG-20460
4368-1	3	Diesel Generator - Air	2	X		DG-20465
4369-1	3	Diesel Generator - Air	2	X		DG-20465
4454-1	NNS	Mainsteam	2		X	MS-20587
4510-3	NNS	Mainsteam Drain	2		X	MS-20587
4511-3	NNS	Mainsteam Drain	2		X	MS-20587
4511-5	NSS	Mainsteam Drain	2		X	MS-20587
4513-3	NNS	Mainsteam Drain	2		X	MS-20587
4513-4	NNS	Mainsteam Drain	2		X	MS-20583
4515-3	NNS	Mainsteam Drain	2		X	MS-20587
4515-4	NSS	Mainsteam Drain	2		X	MS-20583
4517-3	NNS	Mainsteam Drain	2		X	MS-20587
4517-4	NNS	Mainsteam Drain	2		X	MS-20583
4519-3	NNS	Mainsteam Drain	2		X	MS-20587
4519-4	NNS	Mainsteam Drain	2		X	MS-20583
4606-2	NNS	Feedwater	18		X	FW-20686
4606-3	2	Feedwater	18	X		FW-20686
4606-4	2	Feedwater	16	X		FW-20686
4606-12	2	Feedwater	2	X		FW-20686
4606-15	2	Feedwater	4	X		FW-20686, FW-20688
4607-2	NNS	Feedwater	18		X	FW-20686
4607-3	2	Feedwater	18	X		FW-20686
4607-4	2	Feedwater	16	X		FW-20686

TABLE 3.6(B)-2
(Sheet 11 of 13)

HIGH ENERGY LINES

<u>Line No.</u>	<u>Safety Class</u>	<u>Function</u>	<u>Essential Size</u>	<u>Essential</u>		<u>P&ID</u>
				<u>Yes</u>	<u>No</u>	
4607-12	2	Feedwater	2	X		FW-20686
4608-2	NNS	Feedwater	18		X	FW-20686
4608-3	2	Feedwater	18	X		FW-20686
4608-4	2	Feedwater	16	X		FW-20686
4608-12	2	Feedwater	2	X		FW-20686
4609-2	NNS	Feedwater	18		X	FW-20686
4609-3	2	Feedwater	18	X		FW-20686
4609-4	2	Feedwater	16	X		FW-20686
4609-12	2	Feedwater	2	X		FW-20686
4609-15	2	Feedwater	4	x		FW-20686, FW-20688
4614-2	2	Feedwater	4	X		FW-20686
4615-2	2	Feedwater	4	X		FW-20686
4616-2	2	Feedwater	4	X		FW-20686
4617-2	2	Feedwater	4	X		FW-20686
5198-1	NNS	Aux Steam	12		X	AS-20569
5198-2	NNS	Aux Steam	2		X	AS-20569
5198-3	NNS	Aux Steam	2		X	AS-20569
5198-8	NNS	Aux Steam	12		X	AS-20569
5198-9	NNS	Aux Steam	2		X	AS-20569
5198-11	NNS	Aux Steam	2		X	AS-20569
5198-13	NNS	Aux Steam	1½		X	AS-20569
5198-18	3	Aux Steam	12	X		AS-20569
5198-20	3	Aux Steam	12	X		AS-20569
5198-21	NNS	Aux Steam	1½		X	AS-20569
5198-22	NNS	Aux Steam	12		X	AS-20569
5230-1	NNS	Aux Steam	6		X	ASC-20908, ASC-20909, ASC-20906
5231-1	NNS	Aux Steam Condensate	2		X	ASC-20908
8751-1	NNS	Aux Steam Heat	1½		X	ASC-20908
8757-1	NNS	Aux Steam Condensate	3		X	ASC-20906
8757-2	NNS	Aux Steam Condensate	2		X	ASC-20906
8757-5	NNS	Aux Steam Heat	2½		X	ASC-20906
8767-1	NNS	Aux Steam Heat	1½		X	ASC-20908

TABLE 3.6(B)-2
(Sheet 12 of 13)

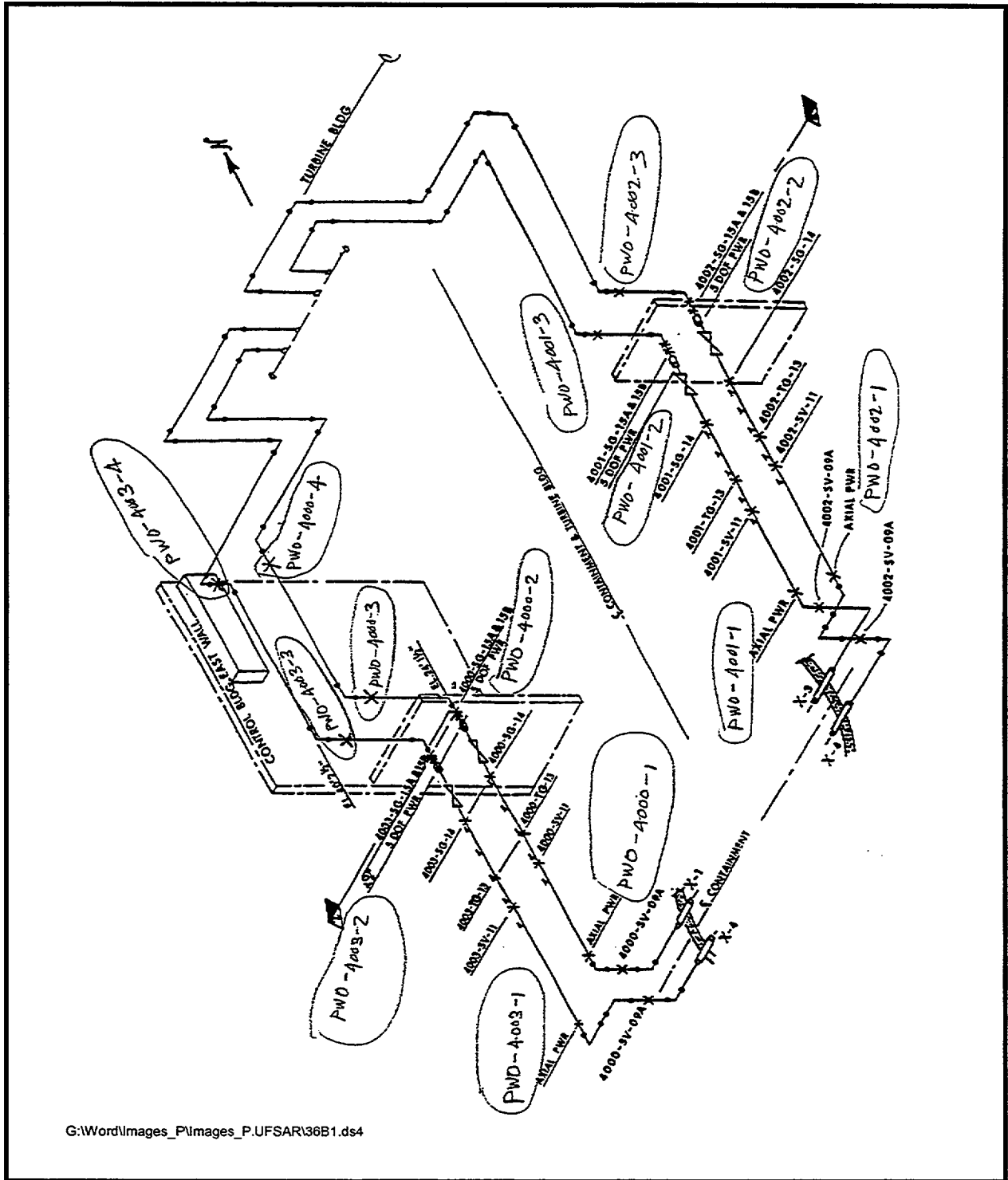
HIGH ENERGY LINES

<u>Line No.</u>	<u>Safety Class</u>	<u>Function</u>	<u>Essential Size</u>	<u>Yes</u>	<u>No</u>	<u>P&ID</u>
8863-1	NNS	Aux Steam Condensate	2		X	ASC-20906
8864-1	NNS	Aux Steam Condensate	2½		X	ASC-20906
8864-2	NNS	Aux Steam Condensate	2		X	ASC-20906
9000-1	NNS	Hot Water Supply	6		X	HW-20051
9001-1	NNS	Hot Water Supply	6		X	HW-20051
9001-2	NNS	Hot Water Supply	3		X	HW-20051
9002-1	NNS	Hot Water Supply	4		X	HW-20051
9003-1	NNS	Hot Water Supply	4		X	HW-20051
9004-1	NNS	Hot Water Supply	1½		X	HW-20051
9006-1	NNS	Hot Water Supply	2		X	HW-20051
9007-1	NNS	Hot Water Supply	4		X	HW-20051
9008-1	NNS	Hot Water Supply	4		X	HW-20051
9009-1	NNS	Hot Water Supply	1½		X	HW-20051
9011-1	NNS	Hot Water Supply	2		X	HW-20051
9012-1	NNS	Hot Water Supply	1½		X	HW-20051
9013-1	NNS	Hot Water Supply	2		X	HW-20051
9014-1	NNS	Hot Water Supply	1½		X	HW-20051
9015-1	NNS	Hot Water Supply	2		X	HW-20051
9022-1	NNS	Hot Water Supply	4		X	HW-20051
9023-1	NNS	Hot Water Supply	4		X	HW-20051
9024-1	NNS	Hot Water Supply	4		X	HW-20051
9025-1	NNS	Hot Water Supply	4		X	HW-20051
9026-1	NNS	Hot Water Supply	4		X	HW-20051
9027-1	NNS	Hot Water Supply	4		X	HW-20051
9030-1	NNS	Hot Water Supply	2		X	HW-20056
9030-2	NNS	Hot Water Supply	1½		X	HW-20056
9042-1	NNS	Hot Water Supply	2		X	HW-20051
9043-1	NNS	Hot Water Supply	2		X	HW-20051
9044-1	NNS	Hot Water Supply	2		X	HW-20051
9045-1	NNS	Hot Water Supply	2		X	HW-20051
9050-1	NNS	Hot Water Supply	2		X	HW-20051
9051-1	NNS	Hot Water Supply	2		X	HW-20051
9052-1	NNS	Hot Water Supply	2		X	HW-20051
9053-1	NNS	Hot Water Supply	2		X	HW-20051
9054-1	NNS	Hot Water Supply	2		X	HW-20051
9072-1	NNS	Hot Water Supply	2		X	HW-20051
9200-1	NNS	Hot Water Return	6		X	HWR-20051
9201-1	NNS	Hot Water Return	4		X	HWR-20051
9202-1	NNS	Hot Water Return	4		X	HWR-20051
9208-1	NNS	Hot Water Return	4		X	HWR-20051
9209-1	NNS	Hot Water Return	2		X	HWR-20051
9210-1	NNS	Hot Water Return	2		X	HWR-20051

TABLE 3.6(B)-2
(Sheet 13 of 13)

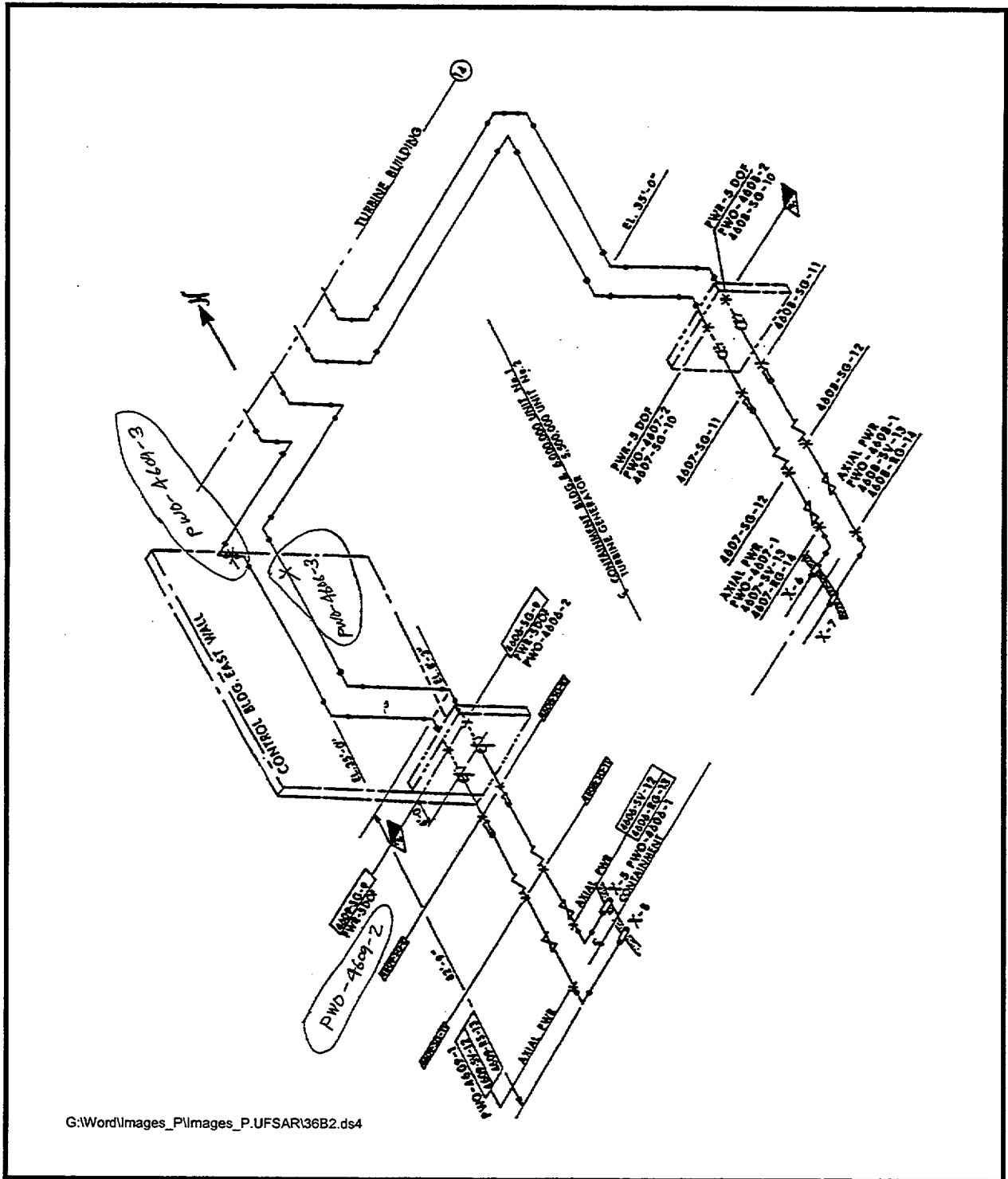
HIGH ENERGY LINES

<u>Line No.</u>	<u>Safety Class</u>	<u>Function</u>	<u>Essential Size</u>	<u>Yes</u>	<u>No</u>	<u>P&ID</u>
9211-1	NNS	Hot Water Return	2		X	HWR-20051
9212-1	NNS	Hot Water Return	2		X	HWR-20051
9213-1	NNS	Hot Water Return	2		X	HWR-20051
9214-1	NNS	Hot Water Return	4		X	HWR-20051
9215-1	NNS	Hot Water Return	2		X	HWR-20051
9216-1	NNS	Hot Water Return	2		X	HWR-20051
9217-1	NNS	Hot Water Return	2		X	HWR-20051
9218-1	NNS	Hot Water Return	2		X	HWR-20051
9219-1	NNS	Hot Water Return	2		X	HWR-20051
9220-2	NNS	Hot Water Return	1½		X	HWR-20056
9220-3	NNS	Hot Water Return	2		X	HWR-20051, HWR-20056
9221-3	NNS	Hot Water Return	1½		X	HWR-20056
9222-3	NNS	Hot Water Return	1½		X	HWR-20056
9223-2	NNS	Hot Water Return	1½		X	HWR-20056
9223-3	NNS	Hot Water Return	1½		X	HWR-20056
9268-3	NNS	Hot Water Return	1½		X	HW-20056
9270-2	NNS	Hot Water Return	1½		X	HW-20056
9270-3	NNS	Hot Water Return	1½		X	HW-20056
9271-2	NNS	Hot Water Return	1½		X	HW-20052
9271-6	NNS	Hot Water Return	1½		X	HW-20052
9272-3	NNS	Hot Water Return	1½		X	HW-20052
9273-3	NNS	Hot Water Return	1½		X	HW-20052
9274-3	NNS	Hot Water Return	1½		X	HW-20052
9275-3	NNS	Hot Water Return	1½		X	HW-20052
9826-1	NNS	Hot Water Supply	1½		X	HW-20056
9830-1	NNS	Hot Water Supply	1½		X	HW-20056
9831-1	NNS	Hot Water Supply	1½		X	HW-20056
9832-1	NNS	Hot Water Supply	1½		X	HW-20056
9833-1	NNS	Hot Water Supply	1½		X	HW-20056
9834-3	NNS	Hot Water Supply	1½		X	HW-20056
9835-1	NNS	Hot Water Supply	1½		X	HW-20056
9835-4	NNS	Hot Water Supply	1½		X	HW-20056
9836-3	NNS	Hot Water Supply	1½		X	HW-20056
9849-1	NNS	Hot Water Supply	1½		X	HW-20052
9849-7	NNS	Hot Water Supply	1½		X	HW-20052
9850-3	NNS	Hot Water Supply	1½		X	HW-20052
9851-3	NNS	Hot Water Supply	1½		X	HW-20052



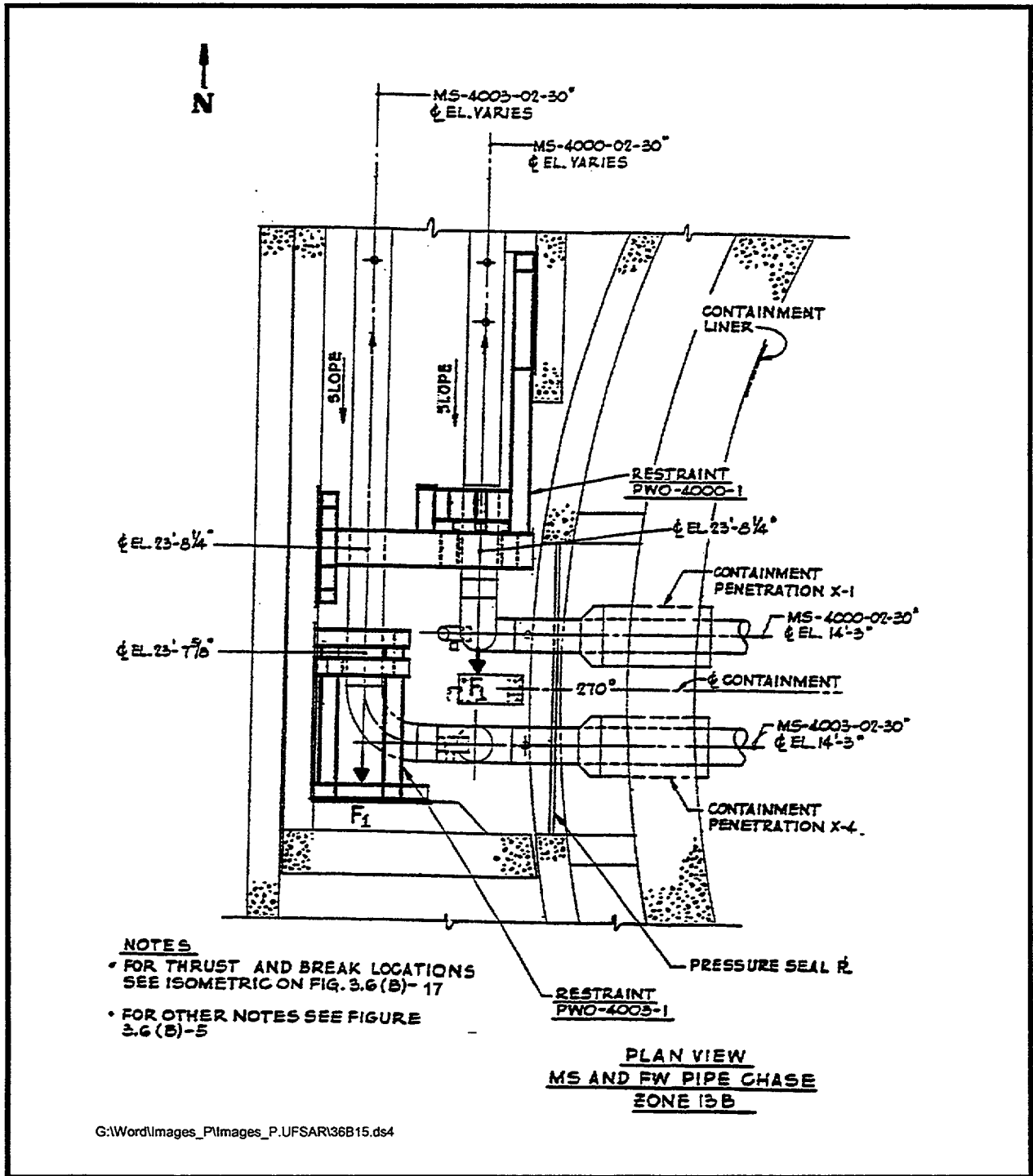
G:\Word\Images_P\Images_P.UFSAR\36B1.ds4

SEABROOK STATION UPDATED FINAL SAFETY ANALYSIS REPORT	Main Steam Piping Outside Containment	
	REV. 07	FIGURE 3.6 (B)-1

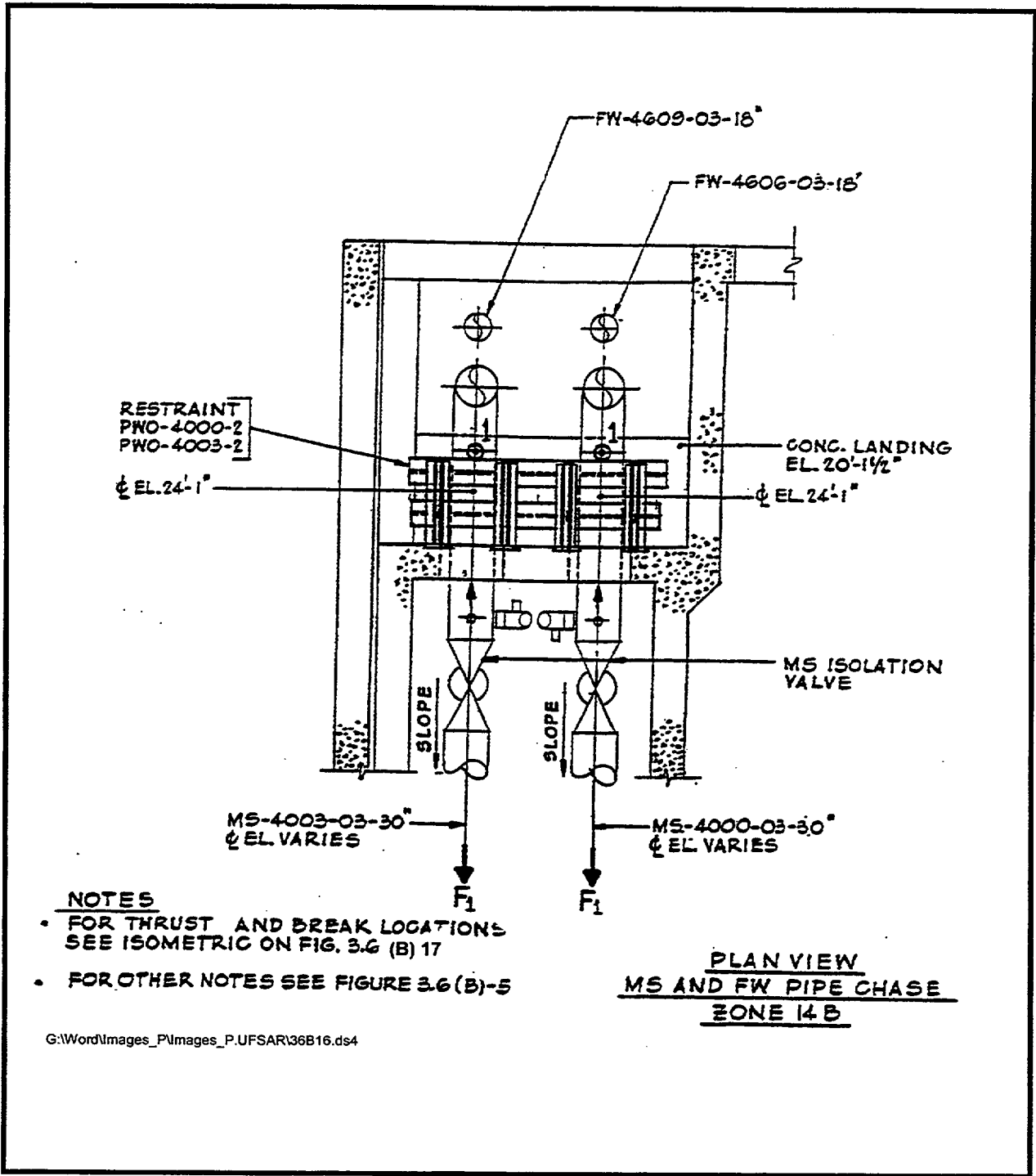


G:\Word\Images_P\Images_P.UFSAR\36B2.ds4

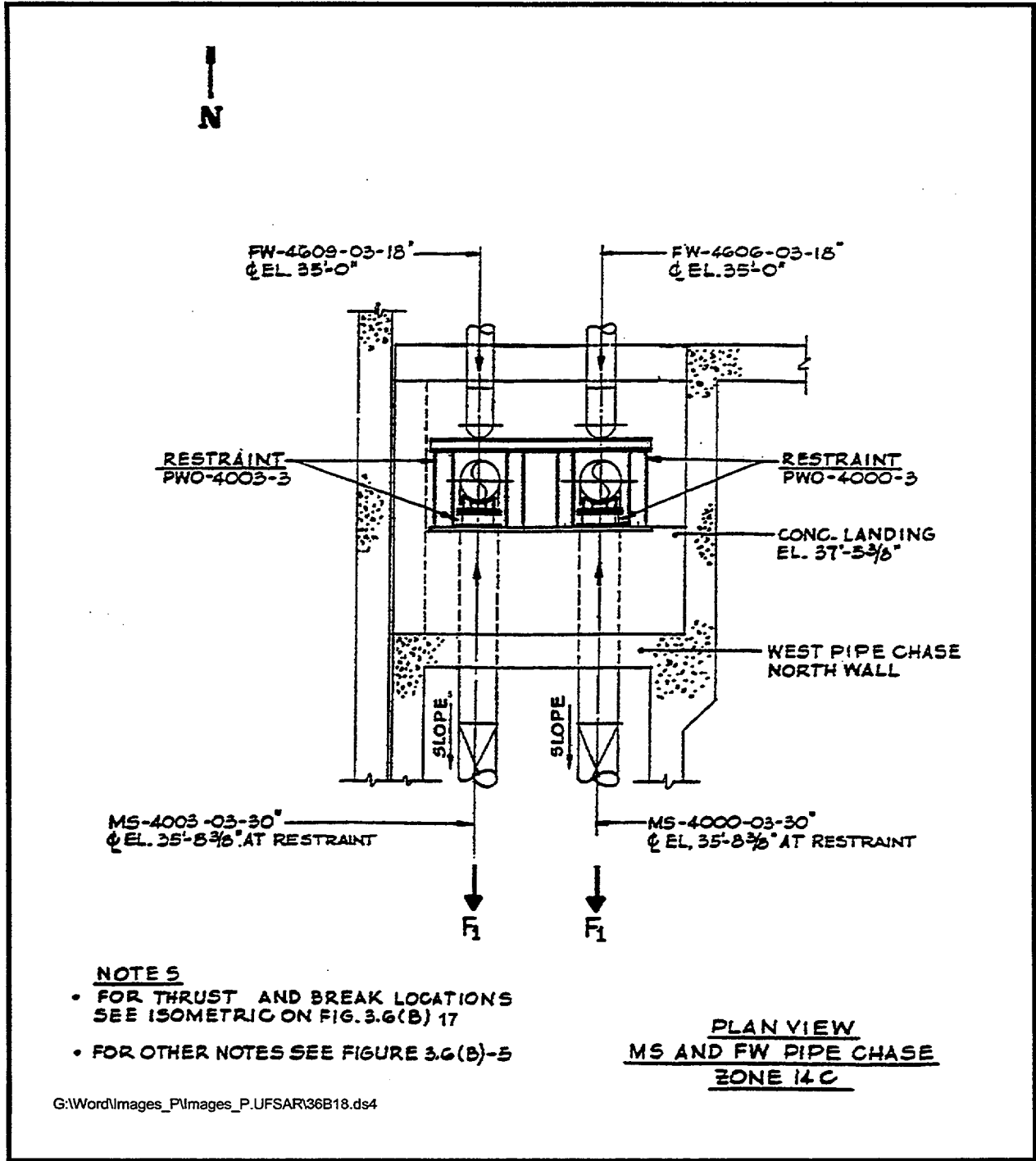
<p>SEABROOK STATION UPDATED FINAL SAFETY ANALYSIS REPORT</p>	<p>Feedwater Piping Outside Containment</p>	
	<p>REV. 07</p>	<p>FIGURE 3.6 (B)-2</p>



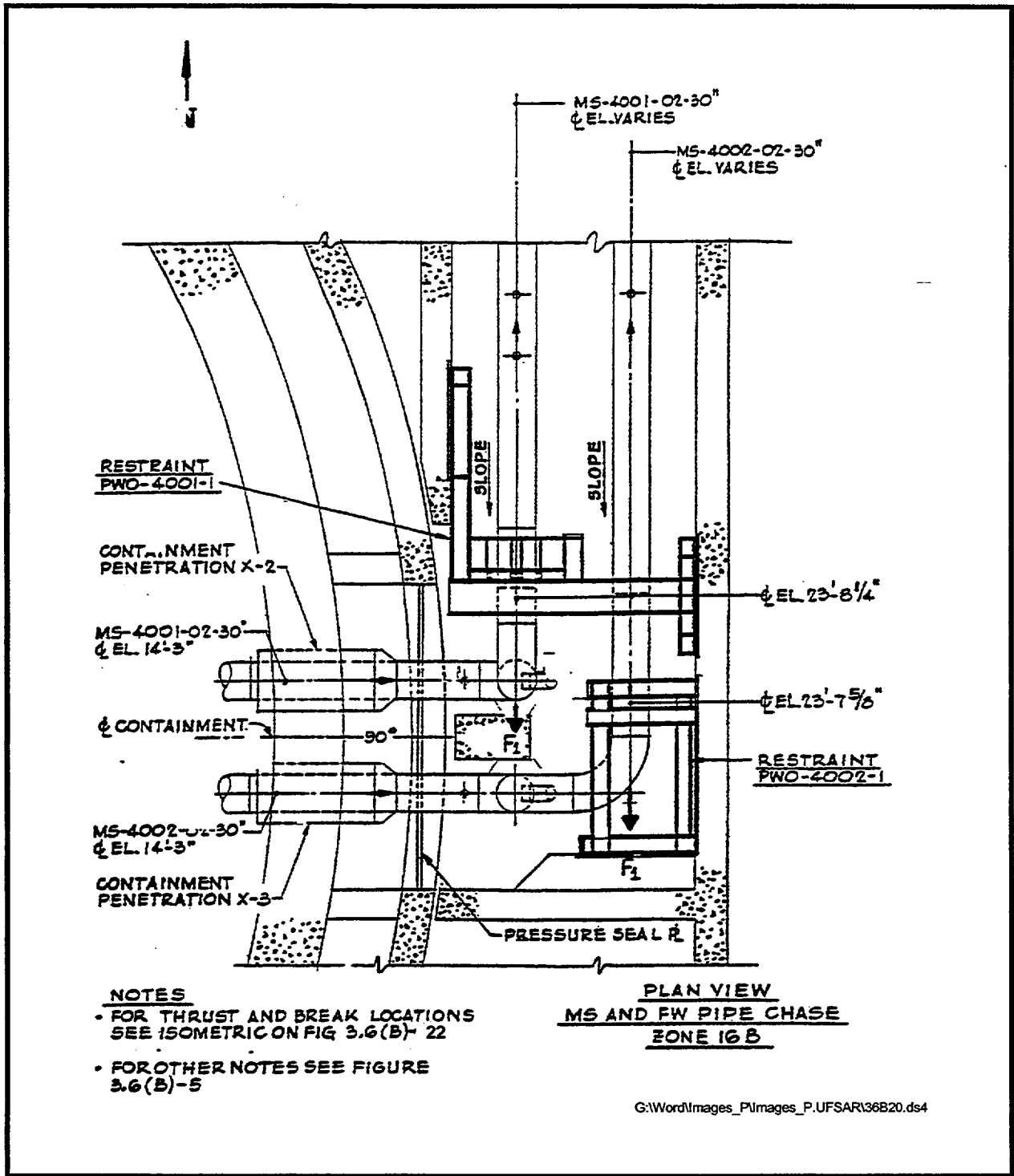
SEABROOK STATION UPDATED FINAL SAFETY ANALYSIS REPORT	Main Steam Line Axial Pipe Whip Restraints Protecting Containment Penetrations - MS and FW Pipe Chase Zone 13B	
	REV. 07	FIGURE 3.6 (B)-15



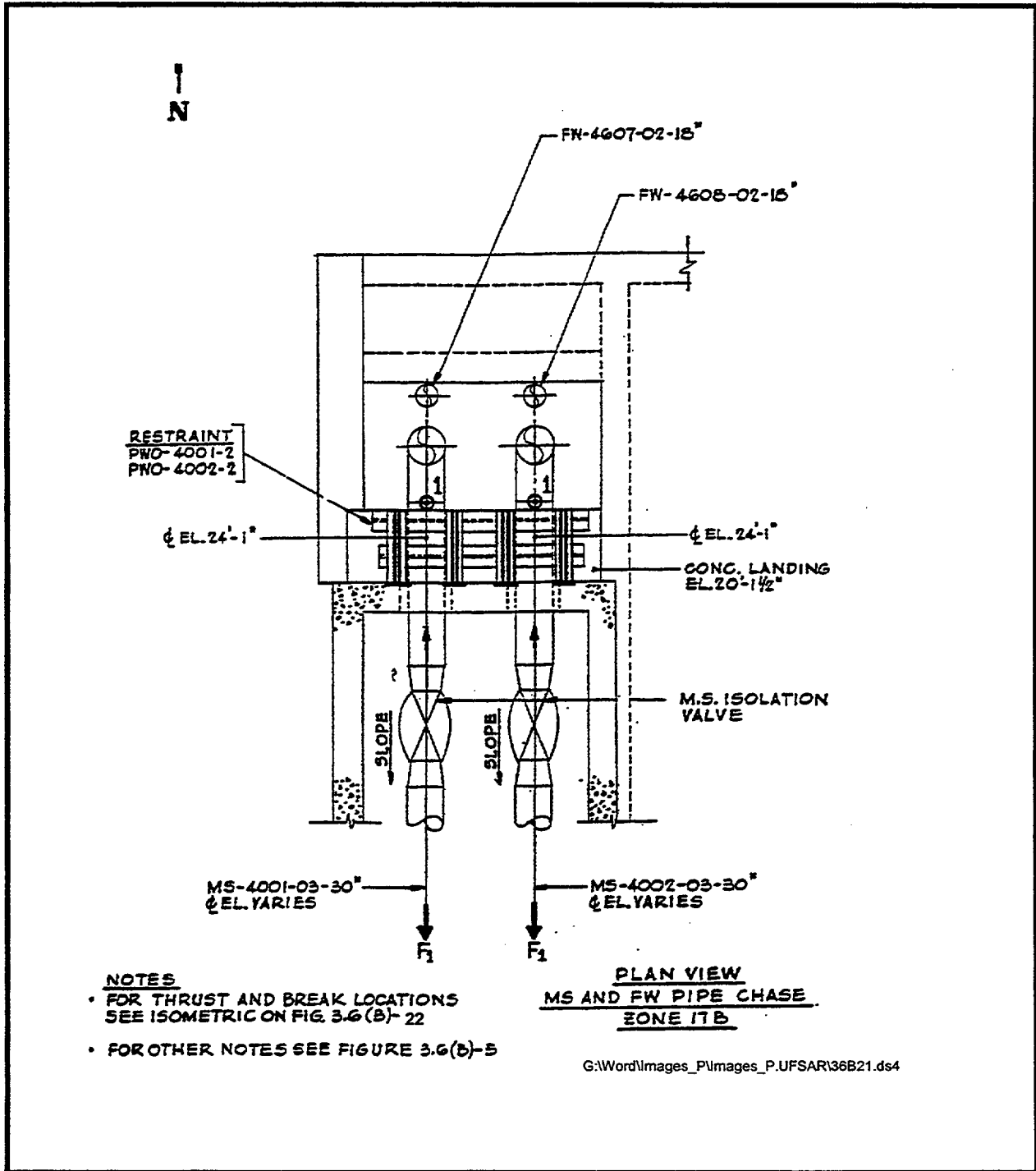
<p>SEABROOK STATION UPDATED FINAL SAFETY ANALYSIS REPORT</p>	<p>Main Steam Pipe Whip Restraints Protecting the Main Steam Isolation Valves and the Containment Penetrations - MS and FW Pipe Chase Zone 14B</p>	
	<p>REV. 07</p>	<p>FIGURE 3.6 (B)-16</p>



SEABROOK STATION UPDATED FINAL SAFETY ANALYSIS REPORT	Main Steam Line Axial Pipe Whip Restraints Protecting Containment Penetrations - MS and FW Pipe Chase Zone 16B	
	REV. 07	FIGURE 3.6 (B)-18



SEABROOK STATION UPDATED FINAL SAFETY ANALYSIS REPORT	Main Steam Line Axial Pipe Whip Restraints Protecting Containment Penetrations - MS and FW Pipe Chase Zone 16B	
	REV. 07	FIGURE 3.6 (B)-20



SEABROOK STATION UPDATED FINAL SAFETY ANALYSIS REPORT	Main Steam Line Axial Pipe Whip Restraints Protecting Containment Penetrations - MS and FW Pipe Chase Zone 17B	
	REV. 07	FIGURE 3.6 (B)-21

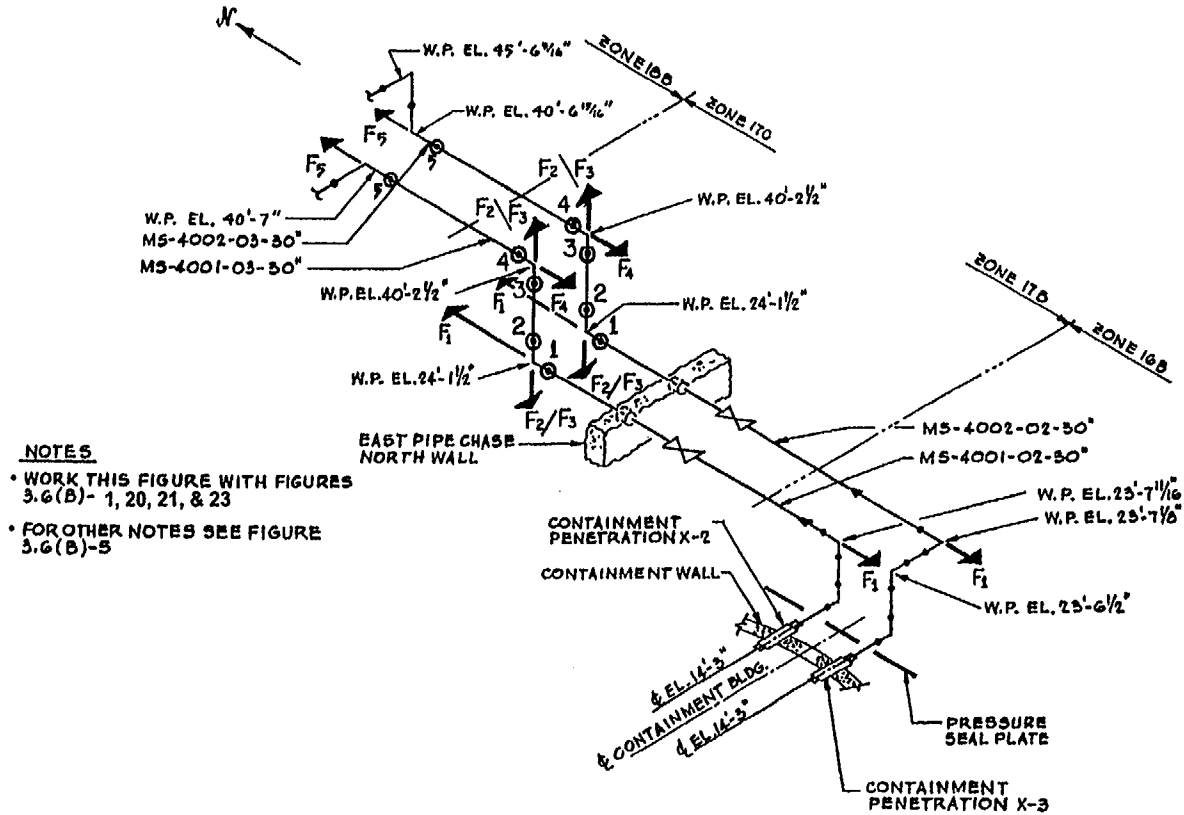
SEABROOK STATION UPDATED
FINAL SAFETY ANALYSIS REPORT

Break and Thrust Locations Isometric for MS
Pipes in East Pipe Chase

REV. 07

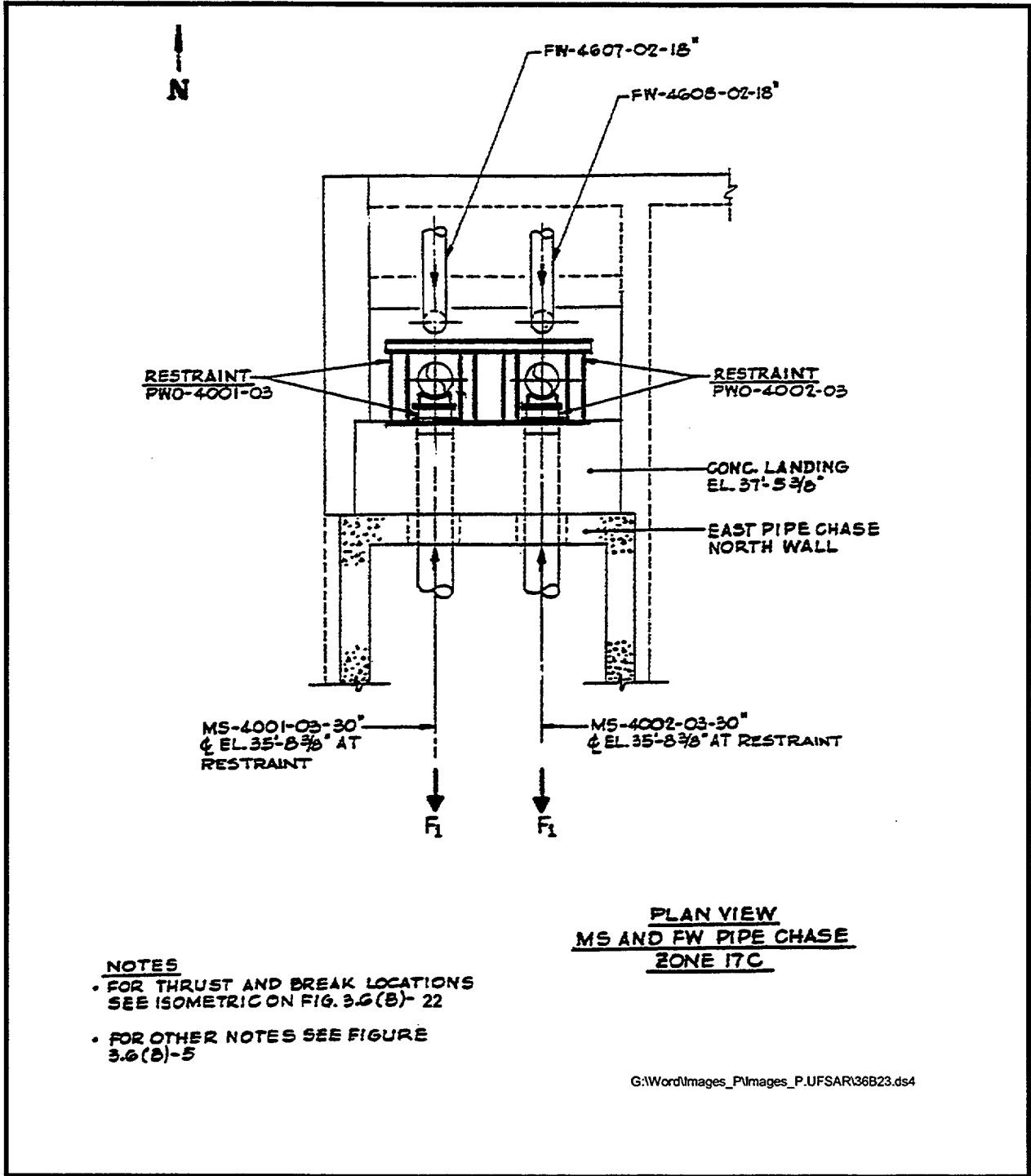
FIGURE 3.6 (B)-22

G:\WorkImages_Pictures_P\JFSAR\36B22.dwg

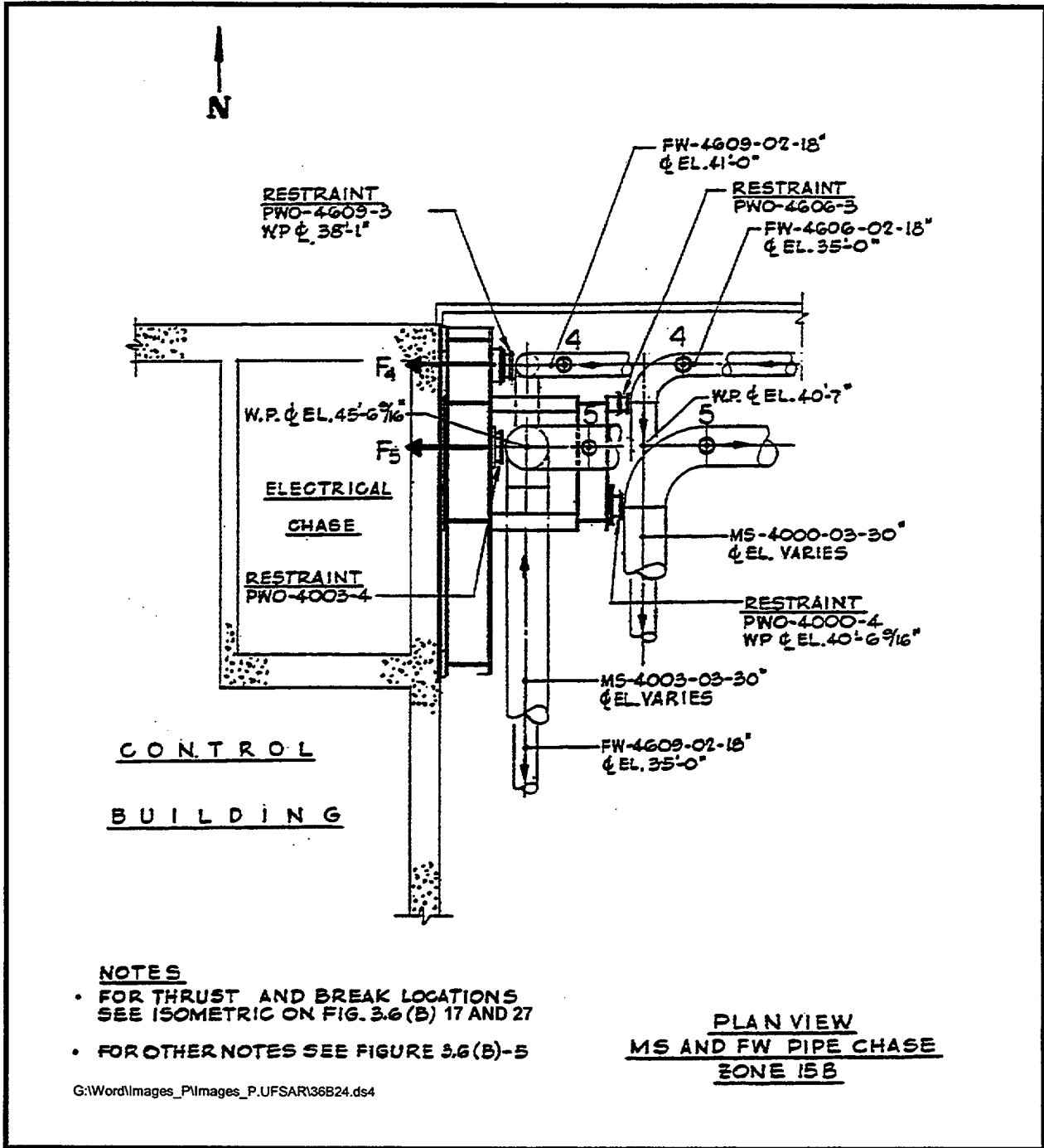


NOTES

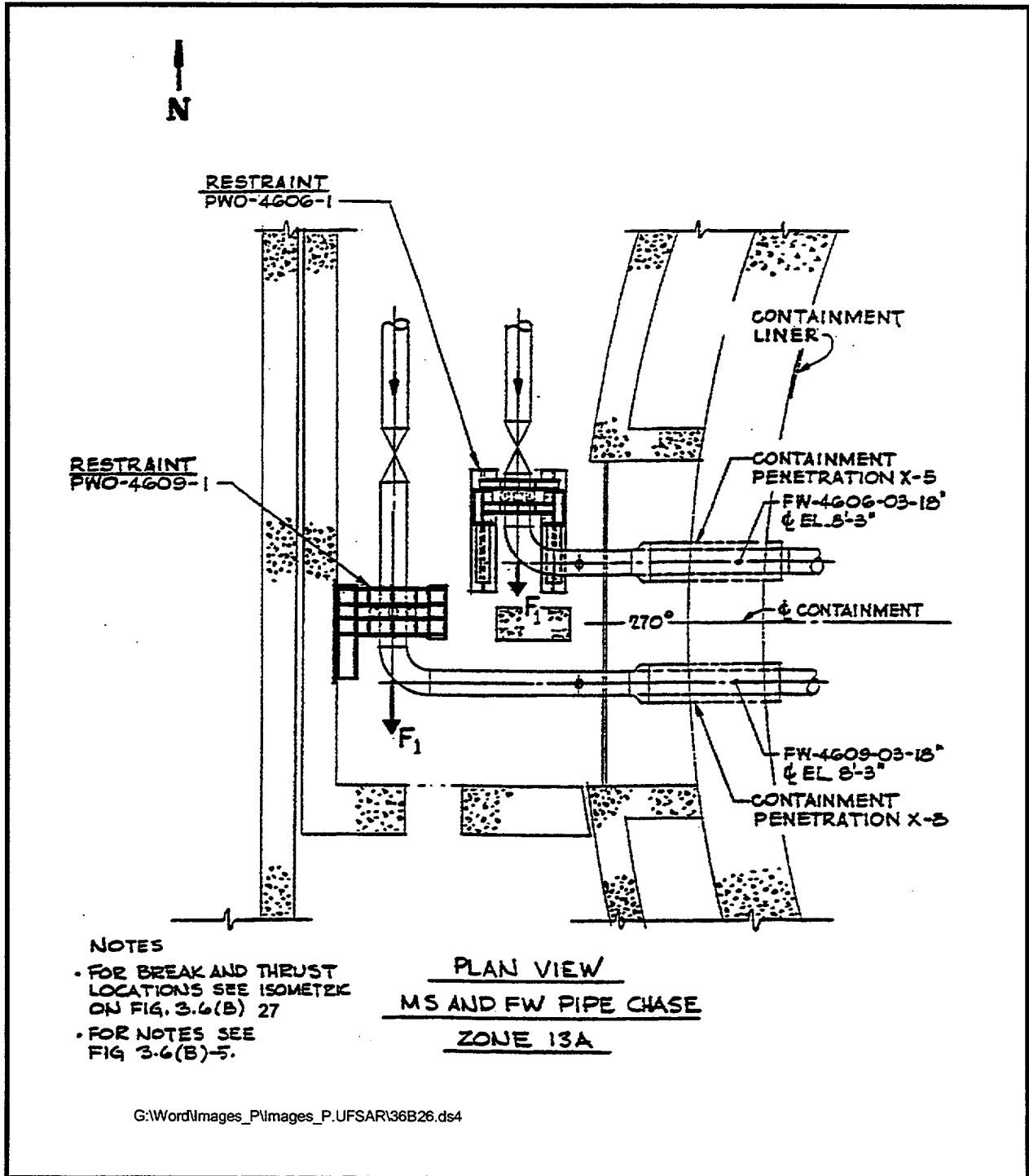
- WORK THIS FIGURE WITH FIGURES 3.6(B)-1, 20, 21, & 23
- FOR OTHER NOTES SEE FIGURE 3.6(B)-5



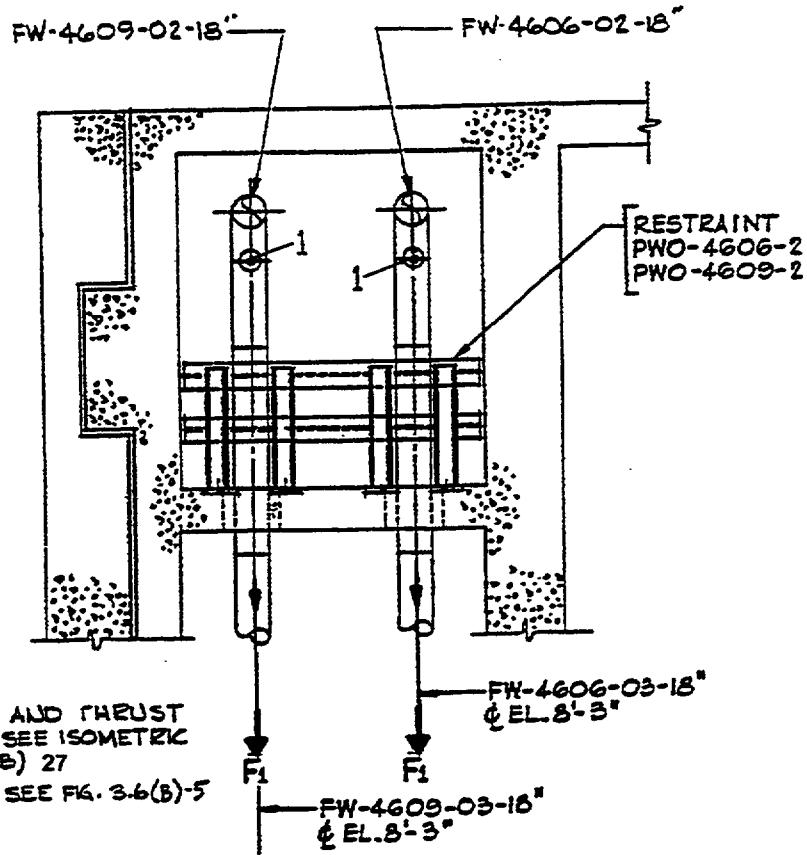
SEABROOK STATION UPDATED FINAL SAFETY ANALYSIS REPORT	Main Steam Pipe Whip Restraints Protecting West Pipe Chase North Wall MS and FW Chase Zone 17C	
	REV. 07	FIGURE 3.6 (B)-23



SEABROOK STATION UPDATED FINAL SAFETY ANALYSIS REPORT	Main Steam and Feedwater Pipe Whip Restraints Protecting East Wall of Control Building and Electrical Chase - MS and FW Pipe Chase Zone 15B	
	REV. 07	FIGURE 3.6 (B)-24



SEABROOK STATION UPDATED FINAL SAFETY ANALYSIS REPORT	Feedwater Pipe Whip Restraints Protecting Containment Liner and Penetrations - MS and FW Pipe Chase Zone 13A	
	REV. 07	FIGURE 3.6 (B)-26

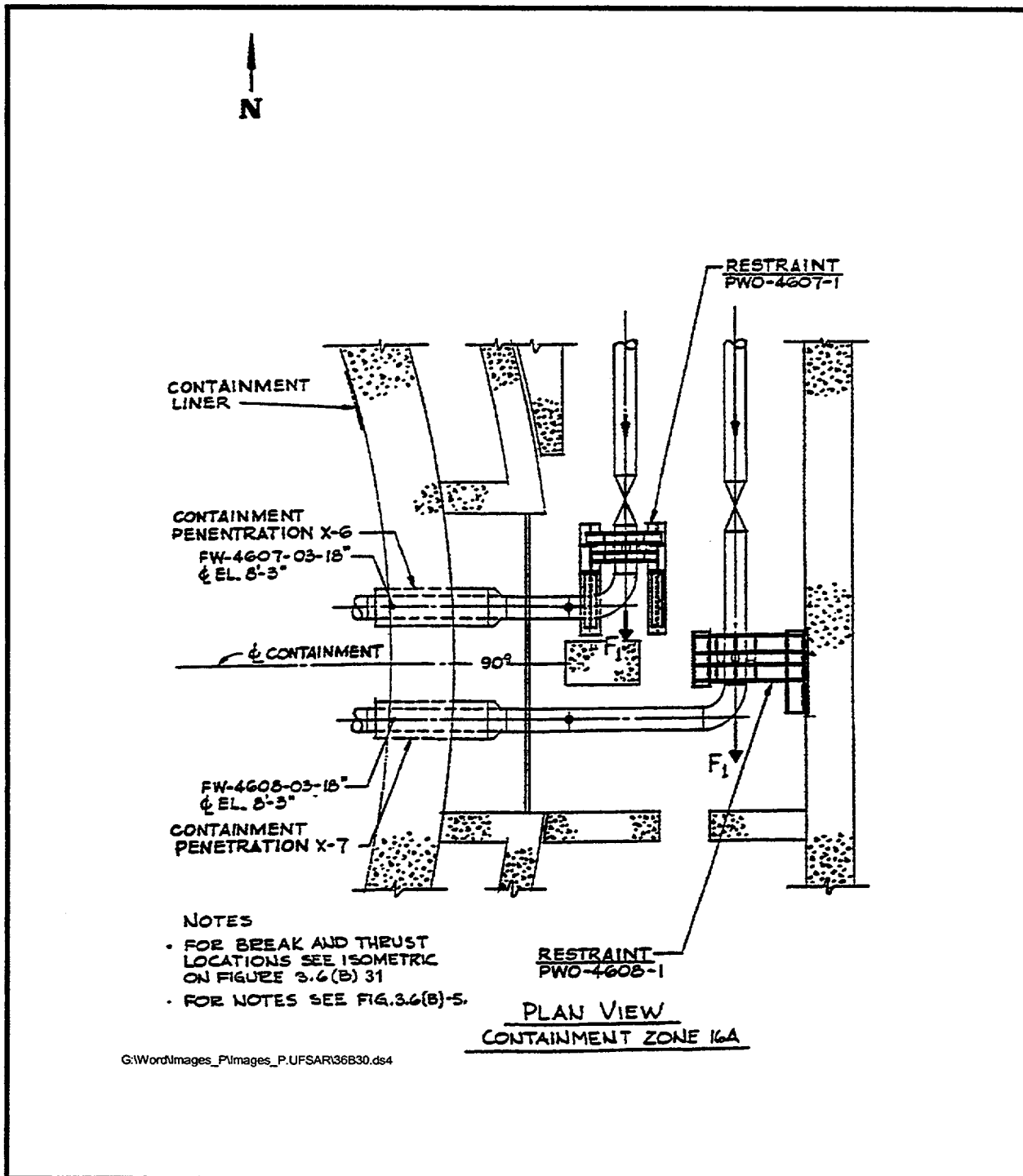


- NOTES
- FOR BREAK AND THRUST LOCATIONS SEE ISOMETRIC ON FIG. 3.6(B) 27
 - FOR NOTES SEE FIG. 3.6(B)-5

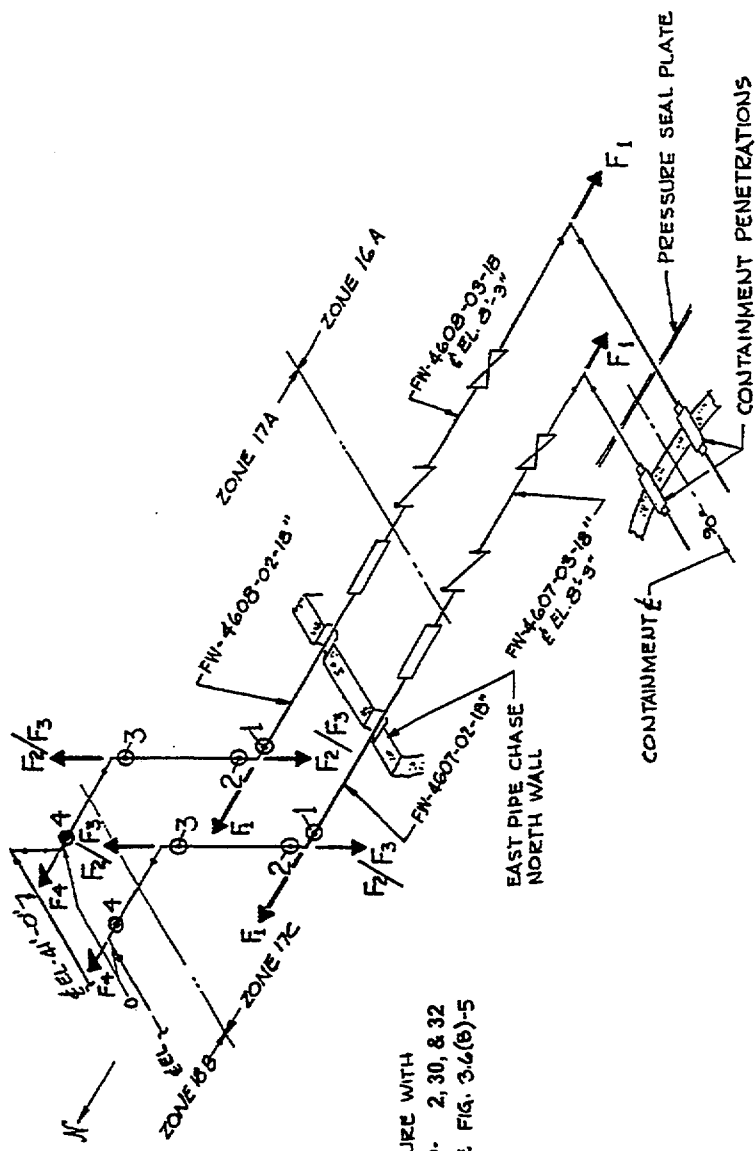
PLAN VIEW
MS AND FW PIPE CHASE
ZONE 14A

G:\Word\Images_P\Images_P\UFSAR\36B28.ds4

SEABROOK STATION UPDATED FINAL SAFETY ANALYSIS REPORT	Feedwater Pipe Whip Restraints Protecting Containment Liner and Penetrations - MS and FW Pipe Chase Zone 14A	
	REV. 07	FIGURE 3.6 (B)-28



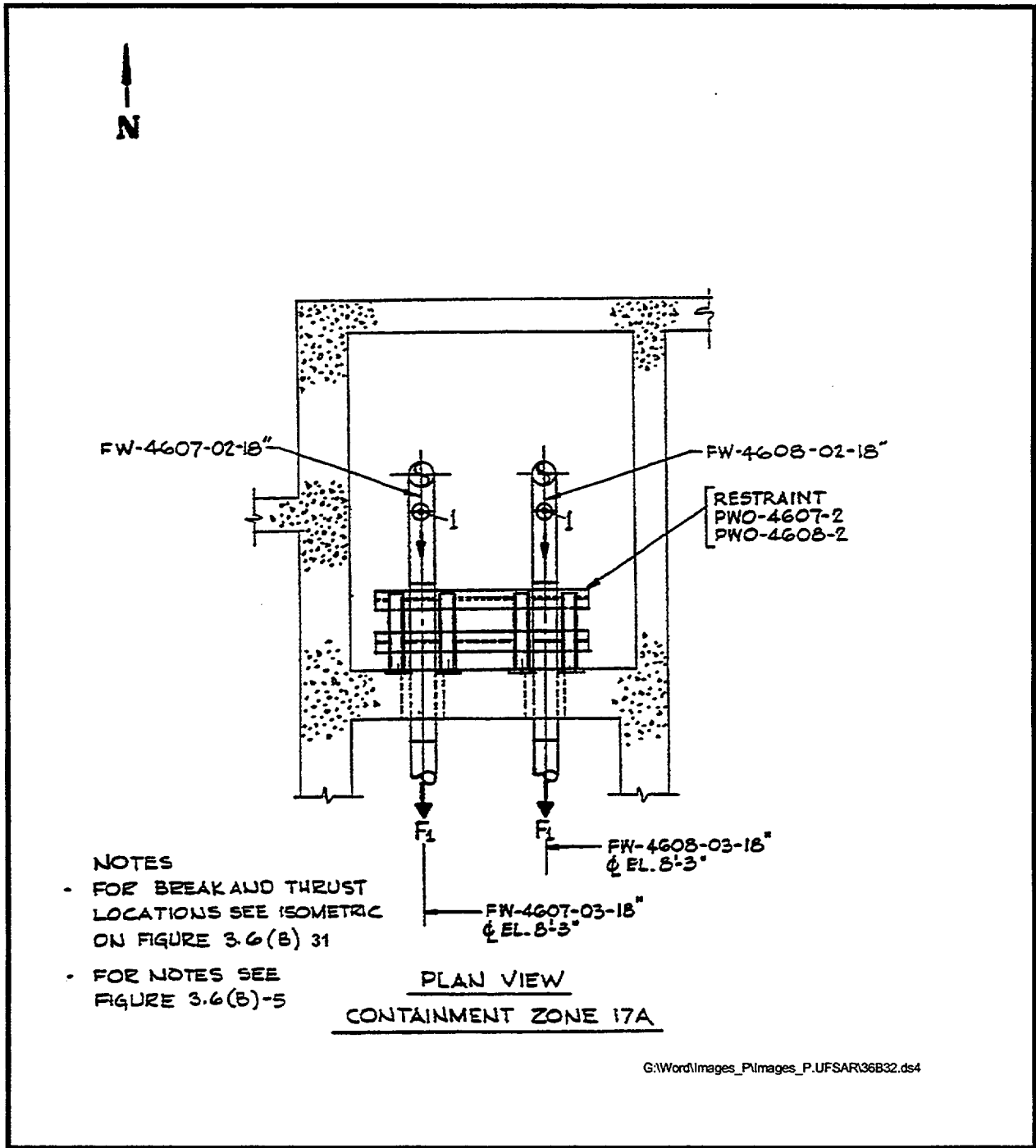
SEABROOK STATION UPDATED FINAL SAFETY ANALYSIS REPORT	Main Steam Pipe Whip Restraints Protecting Containment Liner and Penetrations - Containment Zone 16A	
	REV. 07	FIGURE 3.6 (B)-30



- NOTES
- WORK THIS FIGURE WITH FIGURES 3.6(B)- 2, 30, & 32
 - FOR NOTES SEE FIG. 3.6(B)-5

G:\Word\Images_P\Images_P.UFSAR\36B31.ds4

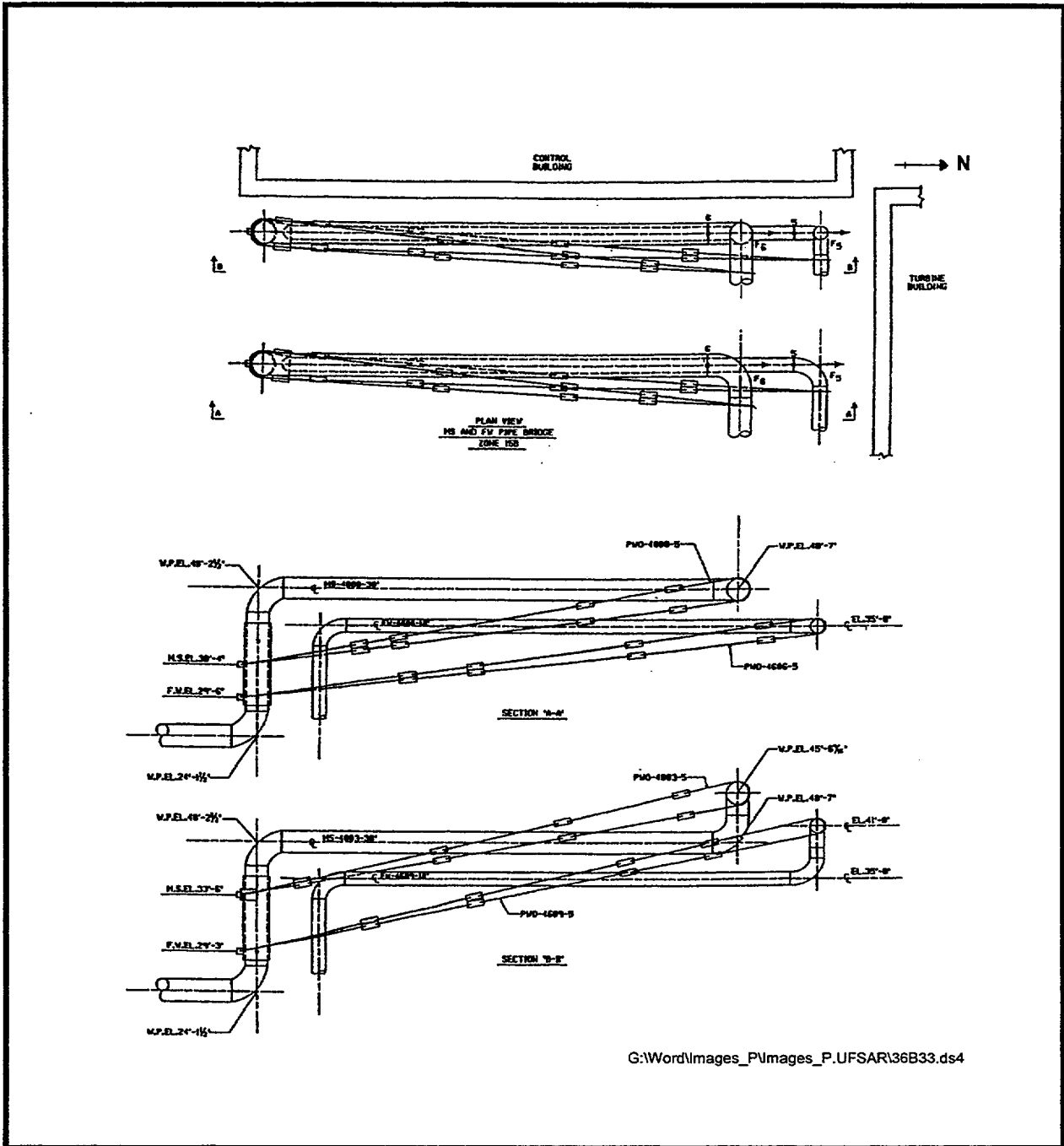
SEABROOK STATION UPDATED FINAL SAFETY ANALYSIS REPORT	Break and Thrust Locations Isometric for FW Pipes in East Chase	
	REV. 07	FIGURE 3.6 (B)-31



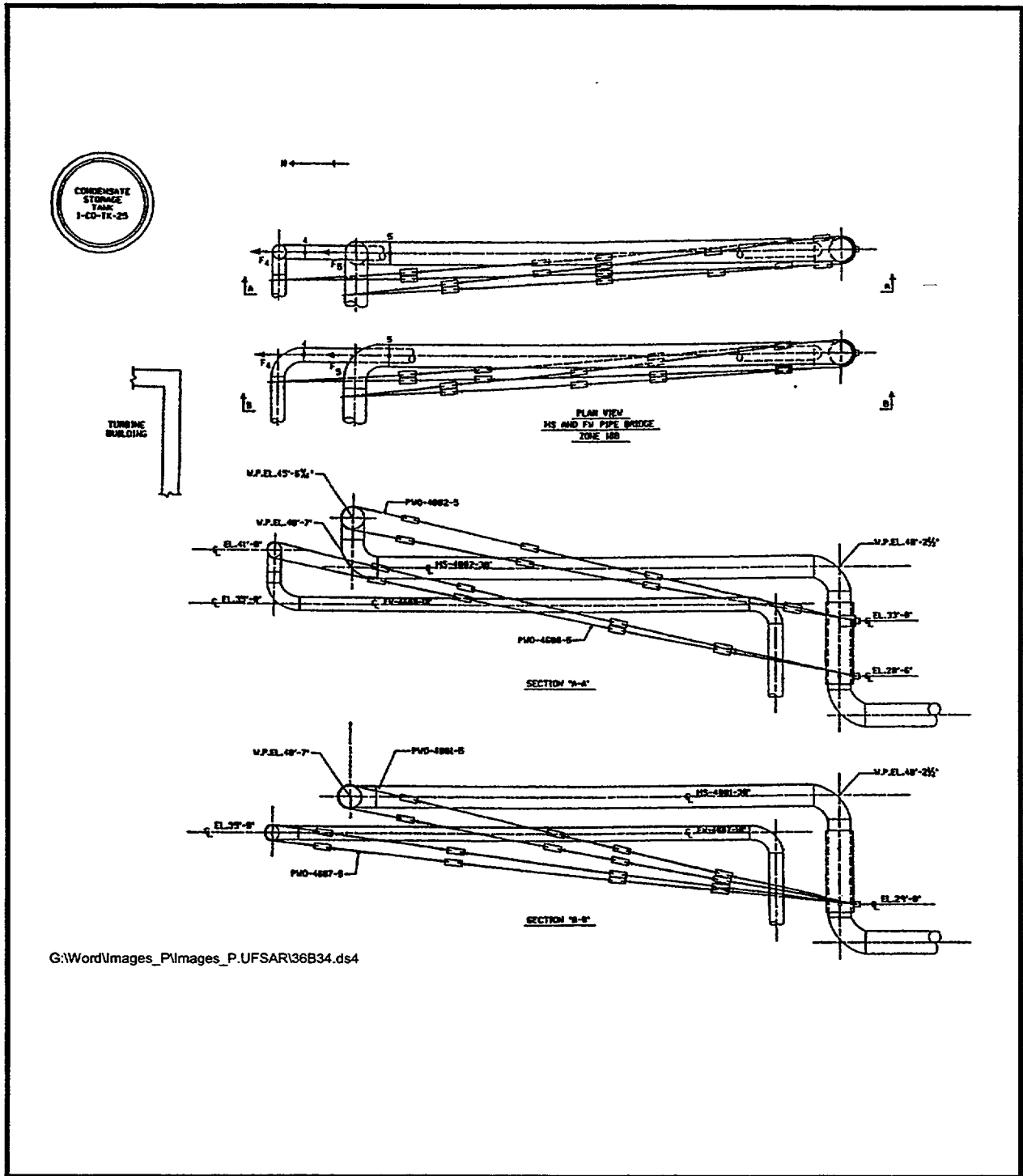
- NOTES**
- FOR BREAK AND THRUST LOCATIONS SEE ISOMETRIC ON FIGURE 3.6(B) 31
 - FOR NOTES SEE FIGURE 3.6(B)-5

G:\Word\Images_P\Images_P.UFSAR\36B32.ds4

SEABROOK STATION UPDATED FINAL SAFETY ANALYSIS REPORT	Feedwater Pipe Whip Restraints Protecting Containment Liner and Penetrations - Containment Zone 17A	
	REV. 07	FIGURE 3.6 (B)-32



<p>SEABROOK STATION UPDATED FINAL SAFETY ANALYSIS REPORT</p>	<p>Pipe Bridge West Side Main Steam and Feedwater Pipe Whip Restraints Protecting Turbine and Control Buildings</p>	
	<p>REV. 07</p>	<p>FIGURE 3.6 (B)-33</p>



G:\Word\images_P\images_P.UFSAR\36B34.ds4

<p>SEABROOK STATION UPDATED FINAL SAFETY ANALYSIS REPORT</p>	<p>Pipe Bridge East Side Main Steam and Feedwater Pipe Whip Restraints Protecting Turbine Building and Condensate Storage Tank</p>	
	<p>REV. 07</p>	<p>FIGURE 3.6 (B)-34</p>

SEABROOK UPDATED FSAR

3.9(B).2.3 Dynamic Response Analysis of Reactor Internals under Operational Flow Transients and Steady-State Conditions

Refer to Subsection 3.9(N).2.3.

3.9(B).2.4 Preoperational Flow-Induced Vibration Testing of Reactor Internals

Refer to Subsection 3.9(N).2.4.

3.9(B).2.5 Dynamic System Analysis of the Reactor Internals under Faulted Conditions

Refer to Subsection 3.9(N).2.5.

3.9(B).2.6 Correlations of Reactor Internals Vibration Tests with the Analytical Results

Refer to Subsection 3.9(N).2.6.

3.9(B).3 ASME Code Class 1, 2 and 3 Components, Component Supports and Core Support Structures

3.9(B).3.1 Loading Combinations, Design Transients, and Stress Limits

The load combinations and the design stress limits associated with the plant operating conditions which are applied to the design and analysis of the ASME III Code-constructed items, other than the NSSS items, are defined herein. The plant conditions considered were normal operation, postulated accidents and specified seismic events. Design transients are further discussed in Subsection 3.9(B).1.1. The requirements of ANSI/ANS-51.1-1983 have been satisfied by use of plant conditions and allowable stress limits imposed on active and nonactive components.

For the non-ASME component members (other than bolts) of the ASME III Code-constructed items, the design criteria limit the principal stresses to 0.6 Fy for the plant upset conditions, and to 0.9 Fy for the plant faulted condition. Refer to Subsection 3.9(B).3.4c for the bolt design criteria.

a. Valves, Pumps, Heat Exchangers, and Tanks

The loading conditions considered (where applicable) for the design of ASME Class 1, 2 and 3 components included, but were not limited to, loading effects resulting from:

1. Internal and external pressure

2. Dead load, i.e., weight of the component and normal contents, including additional pressure due to static and dynamic head of liquid
3. Superimposed loads caused by other components, such as nozzle loads
4. Environmental loads, wind loads, snow loads, and seismic loads for both an OBE and a SSE
5. Valve thrust and moments
6. Thermal and thermal transients (for Class 1 components only).

The loading combinations considered (where applicable) in the design and analysis of the ASME Code Class 1, 2 and 3 and certain non-Code safety-related components were categorized with respect to plant operating conditions defined as normal, upset, emergency and faulted conditions, as identified in Table 3.9(B)-3. The corresponding stress limits for each category of plant operating condition are presented in Table 3.9(B)-4 for nonactive pumps, Table 3.9(B)-5 for nonactive valves, Table 3.9(B)-6 for nonactive Class 1 valves and Table 3.9(B)-7 for ASME Code Class 2 and 3 pressure vessels and storage tanks. The stress limits for active pumps and valves are discussed in Subsection 3.9(B).3.2. The stress limits established for the various components are sufficiently low so that violation of the pressure boundary will not occur.

b. Piping Systems, Including In-Line Valves

The safety-related piping systems have been designed to satisfy the appropriate stress limits of the ASME III Code and those of Regulatory Guide 1.48, as delineated below:

1. For those piping systems that constitute a portion of the reactor coolant pressure boundary and have been designated as ASME III, Class 1 lines, the load combinations and stress limits for various plant operating conditions are presented in Table 3.9(B)-8.

The following are the ASME Code Class 1 pipes qualified by the original A-E, UE&C (see Subsection 3.9(N).1.1 for design transient list applicable to Class 1 components):

<u>Line No.</u>	<u>Line Size</u>	<u>Line Description</u>	<u>P&ID</u>
91-1	1"	Reactor vessel vent line	RC-20845
91-2	1"	Reactor vessel vent line	RC-20845

SEABROOK UPDATED FSAR

REVISION 7

328-6	2"	From seal inject. filters to RC-P-1A	CS-20726
328-7	1½"	From seal inject. filters to RC-P-1A	CS-20726
329-4	2"	From seal inject. filters to RC-P-1B	CS-20726
329-5	1½"	From seal inject. filters to RC-P-1B	CS-20726
330-4	2"	From seal inject. filters to RC-P-1C	CS-20726
330-5	1½"	From seal inject. filters to RC-P-1C	CS-20726
331-4	2"	From seal inject. filters to RC-P-1D	CS-20726
331-5	1½"	From seal inject. filters to RC-P-1D	CS-20726
80-1	6"	Pressurizer vent line	RC-20846
80-2	3"	Pressurizer vent line	RC-20846
80-15	6"	Pressurizer vent line	RC-20846
80-6	3"	Pressurizer vent line	RC-20846
74-1	6"	Suction line of pressur- izer relief valve	RC-20846
75-1	6"	Suction line of pressur- izer relief valve	RC-20846
76-1	6"	Suction line of pressur- izer relief valve	RC-20846

Westinghouse has responsibility for Class 1 component core support structures and specific Class 1 piping. UE&C has responsibility for pressurizer safety relief line, the reactor coolant system drain line and Class 1 reactor coolant pump seal piping.

2. For those essential piping systems which have been designated as ASME III, Class 2 and 3, and which are required for safe shutdown of the reactor, the load combinations and stress limits for various plant operating conditions are presented in Table 3.9(B)-9.
3. For those nonessential piping systems which have been designated as ASME III Class 2 and 3, but which are not required for safe shutdown of the reactor, the load combinations and stress limits for various plant operating conditions are presented in Table 3.9(B)-10.

Definitions of the symbols and notations used in Tables 3.9(B)-8, 3.9(B)-9 and 3.9(B)-10 are contained in Table 3.9(B)-11.

4. For those piping systems which are non-ASME III, design criteria were specified so that structural integrity of such systems could be maintained during the most adverse plant condition.

For any of the above piping systems which contained in-line components, such as valves, flow elements, strainers, etc., the loads imposed on such items by the piping were verified to be less than the limits established by the vendor. If operators were included on such valves, the seismic accelerations imposed were verified to be less than the levels to which the unit was qualified, either on a structural integrity criteria for nonactive valves or on an operability criteria for active valves. The latter criteria is discussed further in Subsection 3.9(B).3.2.

Analyses of all seismic Category I piping systems have been conducted using either the ADLPIPE, ADLPIPE-2 or IMAPS computer program. In each of these programs, the mathematical models employed to represent the piping system consisted of lumped masses interconnected by beam elements whose elastic properties matched those of either the piping section, or an in-line component, such as a valve. Support elements and equipment attachment points were included in such models. Lumped masses, offset from a section centerline, were included, when necessary, to model valve operators.

Structural boundaries of a mathematical model were defined by equipment connections, by support system anchors or by restraints which formed the boundary between seismic Category I and nonseismic Category I piping systems.

3.9(B).3.2 Pump and Valve Operability Assurance

The pumps and valves identified as active, whose operation is relied upon to assure safe plant shutdown or mitigate the consequences of an accident, are listed in Tables 3.9(B)-26 and 3.9(B)-27, respectively. These active pumps and valves are classified as seismic Category I, and are designed to perform their intended functions during the life of the plant under all postulated plant conditions. The operability of these active pumps and valves is assured by adherence to the design limits and supplemental stress requirements specified in NRC Regulatory Guide 1.48.

Safety-related active valves are qualified by prototype testing and analysis; safety-related active pumps are qualified by analysis and functional test. All applicable loads, such as seismic, nozzle and operating loads are considered in the test program and the analysis. Operational tests at design basis conditions are performed during plant test start-up. All active valves

The deflection of the impeller relative to the pump casing was determined by analysis to be 0.0019 in. This translates into a natural frequency of 72 Hz. The pump is, therefore, considered rigid and per FSAR commitment, seismic operability testing is not required.

The General Electric-supplied 800 HP Model 5-K 6339XC179A motor was analyzed by McDonald Engineering Analysis Company.

It is similar to the motor used for service water pump. Stress Report #266 established that the motor satisfies all of the applicable requirements.

(f) Diesel Fuel Oil Transfer Pump

Operability of the diesel fuel oil transfer pump under the most adverse applicable combination of normal loads, nozzle loads, and seismic loads has been analytically demonstrated by the pump manufacturer, Delaval IMO Pump Division. The pump assembly consists of a Delaval IMO screw-type pump (N3DBS-187) and a Westinghouse electric motor mounted on a common bedplate.

The natural frequency of the unit was calculated; the fundamental natural frequency was determined as 228 Hz. Static analysis was used to determine the structural responses and the resulting stresses; deflections are summarized in Table 3.9(B)-20.

The Westinghouse supplied 2 HP, Type T, fan-cooled AC motor was analyzed by Westinghouse Medium Motor & Gearing Division. Westinghouse Qualification Document MM-9112 and Certification letter dated February 13, 1981 assure that the motor satisfies all of the applicable requirements. The seismic analysis report is available for review at the Westinghouse Medium Motor & Gearing Division.

d. Operability Assurance Program Results for Active Valves

The results of seismic tests and analysis on active valves are provided in the document entitled, "Public Service Company of New Hampshire, Seabrook Station Units 1 & 2, Seismic Qualification Review Team (SQRT) Equipment List," which was forwarded to Mr. Frank J. Miraglia, Chief Licensing Branch #3, Division of Licensing, under cover of PSNH's letter, dated May 27, 1982.

SEABROOK UPDATED FSAR

3.9(B).3.3 Design and Installation Details for Mounting of Pressure Relief Devices

The installation and design of pressure relief devices comply with the rules of ASME III, Paragraph NB-7000, and NRC Regulatory Guide 1.67.

a. Overpressure Protection for Reactor Coolant Pressure Boundary (RCPB)

The pressurizer in the Reactor Coolant System is provided with three safety valves and two power-operated relief valves for overpressure protection. These valves discharge through a closed piping system to the pressurizer relief tank, where the steam is condensed and cooled by mixing with water. The piping system and supports are designed to satisfy the following design criteria:

1. Stress limits for load combinations listed in Table 3.9(B)-8 for safety Class 1 piping from the pressurizer to the safety and relief valves
2. Stress limits for load combinations listed in Table 3.9(B)-9 for nonsafety class piping downstream of the safety and relief valves to the pressurizer relief tank
3. Load limits on pressurizer vessel nozzles as established by the manufacturer of the pressurizer vessel
4. Load limits on valve connections as established by the manufacturer of the valves.

The three safety valves are mounted on the pressurizer nozzles with the short inlet pipe and elbow necessary to position the valves vertically. The total length of pipe, elbow and weld-neck flange is approximately 24 inches and is as short as possible to minimize the pressure drop on the inlet side of the valve.

When the valves open, the dynamic effects from the flow of water and steam are included in the design analysis.

These transient load effects on the piping system, upstream and downstream of the safety and relief valves, have been evaluated in the following manner:

1. Safety Valve Piping System

A static analysis was performed for the Safety Valve Piping System in which the peak transient loads obtained from a RELAP 5 analysis and multiplied by a dynamic load factor (DLF) were applied. The Pressurizer Safety Valve Piping System contains no water seals nor is subjected to water slugs.

2. Pressurizer Relief Valve Piping System

Both static and time history analyses were performed for the Pressurizer Relief Valve Piping System using transient loads obtained from a RELAP 5 analysis. The Pressurizer Relief Valve Piping System contains water seals and is subjected to water slugs. The effects of these two items were fully accounted for in the RELAP 5 analysis.

The RELAP 5 computer code, (Reference 1), was used to generate thermal hydraulic characteristics of the flow along the piping system, from which tables of the wave force versus time for each leg have been derived. To evaluate piping stresses and support loads, the maximum force for each leg has been selected and applied statically to the piping system in the most conservative fashion using a dynamic load factor (DLF) based on the valve opening time and the system dynamic characteristics. In cases where time history analyses were performed, the appropriate thermal hydraulic forcing function was applied to the applicable pipe segment. The developed stresses and loads on nozzles were combined with the other applicable loads from Tables 3.9(B)-8 and 3.9(B)-9. These were compared with the allowable stresses and allowable nozzle loads. The simultaneous discharge from all valves has been assumed in the thrust analyses.

b. Overpressure Protection for the Secondary (Main Steam) System

A multiple-valve installation, comprised of five safety valves, is provided in each of the four main steam lines. The valves are installed on main steam piping headers, outside of the Containment Building in a piping chase between the containment penetration and the main steam isolation valves. The safety valve discharge side is configured to minimize reaction forces at the valve branch/main header intersection point. The vertical branch line from the main steam piping header to each individual valve has a forged flange and sweepolet welded to the header. Safety valves are bolted directly to the flanges.

The effect of the valve discharge transient was obtained by static application of an assumed discharge force, as obtained from the valve manufacturer, with a dynamic load factor DLF based on the system dynamic characteristics. It has been assumed that all five valves discharge simultaneously. The system of piping supports and rigid restraints limits both dynamic and static loadings to the piping system to code allowable stresses for the load combinations listed in Table 3.9(B)-9.

c. Safety and Relief Valves for Various Auxiliary Systems

Mounting of safety and relief valves on auxiliary piping systems uses standard piping components: flanges, buttwelded or socket-welded tees, weldolets® and sockolets® for pipe branches to the valves. The valves and valve discharge piping utilize flanged joints, buttwelded and socketwelded connections. Branch connections are qualified using code standard calculations for tees with proper intensification factor (ASME III, Table NB-3682.21 or NC-3652-4). The alternative method for branch qualification is the Bijlaard method using the SPHNOZ/CYLNOZ computer program. The load combination for calculating stresses is according to Table 3.9(B)-9. These were compared with the allowable stresses.

The following basic installation of safety valves outlet piping has been utilized:

1. Open discharge with the minimum piping length, or no piping attached to the valve discharge and discharging to atmosphere.
2. Open discharge system, discharging directly to atmosphere through individual piping systems, or common header combining discharge from several valves.
3. Closed discharge system, discharging to a container through an individual piping system, or common header combining discharge from several valves.

The discharge reaction forces have been obtained from one of the following sources:

1. Valve manufacturer
2. For open steam discharge, from nonmandatory Appendix "O" of ASME III
3. For open and closed discharge systems with piping system connected to valve discharge, from UE&C proprietary computer programs MADIS, VALCLO, ELBFOR, and WATER (described in Sub-section 3.9(B).1.2).

The stress analyses of piping systems downstream and upstream of a valve have been obtained by applying the reaction forces statically with a dynamic load factor (DLF) as appropriate based on the system dynamic characteristics. Piping stresses from the safety valve discharge have been combined with the stresses from other applicable loads in accordance with the load combination from Table 3.9(B)-9. These were compared with the allowable stresses.

- (m) Load ratings shall be verified in accordance with the requirements of Article NF-3260 of the ASME B & PV Code.
- (n) Each hydraulic snubber shall be tested in compression and tension to 10 percent of its rated load and checked for leakage of the hydraulic fluid. If fluid forms droplets, drips or runs off the piston rod, the shock suppressor shall be rejected.
- (o) Shock suppressors' packaging shall be designed to protect against salt spray, rain, dust, watervapor, shock and vibration during shipping, handling and storage. Where possible, shock suppressors shall be packaged fully assembled in a single shipping container.
- (p) Mechanical units shall be designed to operate normally between 50°F and 300°F.

Hydraulic units shall be designed to operate normally between 30°F and 140°F with temperature excursions up to a maximum of 300°F.

2. Snubber Installation and Operability Verification

(a) Pre-Service Examination

A pre-service examination will be made on all snubbers. This examination will be conducted during and after snubber installation and will, as a minimum, verify the following:

- (1) There are no visible signs of damage or impaired operability as a result of storage, handling, or installation.
- (2) The snubber location, orientation, position setting, and configuration (attachments, extensions, etc.), are according to design drawings and specifications.
- (3) Small snubbers are not seized, frozen, or jammed by manual exercising during installation. Large snubbers (those that cannot be manually exercised) will be identified and examined for proper movement during preoperational testing as discussed in Subsection 3.9(B).3.4d.2(b) below.
- (4) Adequate swing clearance is provided to allow snubber movement.

- (5) If applicable, fluid is to the recommended level and is not leaking from the snubber system.
- (6) Structural connections such as pins, fasteners and other connecting hardware such as lock nuts, tabs, wire and cotter pins are installed correctly.

Prior to the performance of the thermal expansion test, an inspection of all listed snubbers covering items (1), (4) and (5) will be performed as a test prerequisite. Snubbers which are installed incorrectly or otherwise fail to meet the above requirements will be repaired or replaced and re-examined in accordance with the above criteria.

(b) Pre-Operational Testing

During thermal expansion testing, snubber thermal movements for systems whose operating temperature exceeds 250°F will be verified as follows:

- (1) During initial system heatup and cooldown, at specified temperature intervals for any system which attains operating temperature, verify the snubber expected thermal movement.
- (2) For those systems which do not attain operating temperature, verify via observation and/or calculation that the snubber will accommodate the projected thermal movement.
- (3) Verify the snubber swing clearance at specified heatup and cooldown intervals. Any discrepancies or inconsistencies shall be evaluated for cause and corrected prior to proceeding to the next specified interval.

3.9(B).4 Control Rod Drive Systems

Refer to Subsection 3.9(N).4.

3.9(B).5 Reactor Pressure Vessel Internals

Refer to Subsection 3.9(N).5.

3.9(B).6 In-Service Testing of Pumps and Valves

An ongoing in-service test program will be provided to assure the operational readiness of certain Safety Class 1, 2 and 3 pumps and valves which perform a specific

function in shutting down a reactor to a safe shutdown condition or in mitigating the consequences of an accident.

The in-service test program is based on the requirements given in the ASME OM Code, 1995 Edition, including 1996 Addenda and the requirements of 10 CFR 50.55a(f) except where specific written relief has been granted by the commission pursuant to 10 CFR Part 50, Section 50.55a(f)(6)(i). Applicability of future Code addenda will be as stated in 10 CFR 50.55a(f).

3.9(B).6.1 In-Service Testing of Pumps

In-service tests, analysis and record keeping will be performed for certain Code Class 1, 2 and 3 pumps in accordance with Subsection ISTB of the Code to assess pump operational readiness and to detect changes in pump hydraulic and mechanical performance relative to reference parameters. Reference values were established during pre-service testing and will be established after major maintenance or replacement.

Methods of measurement will be in accordance with ISTB 4.7. Installed or portable instruments employed for measuring or observing test quantities will have accuracies equal to or better than that specified in Table ISTB 4.7.1-1.

In-service test records to include test plans, documentation and required corrective action will be maintained in accordance with ISTB 7.

A listing of Class 1, 2 and 3 pumps subject to in-service testing is provided in Station procedures. The Station procedures also specify the minimum test frequency, during plant operation, in which test quantities are to be measured, analyzed and documented. Plant personnel shall maintain test plans that include the type of hydraulic circuit normally used for testing.

3.9(B).6.2 In-Service Testing of Valves

In-service tests, analyses and record keeping will be performed for certain Code Class 1, 2 and 3 valves in accordance with Subsection ISTC of the Code to assess valve operational readiness.

The in-service testing program for valves is detailed in Station procedures. Each valve to be tested is identified by system, valve number, code class, type, function, category and applicable tests and test frequencies.

Each valve, prior to service, was tested as required by those tests defined for each valve in the In-service Test Program, in effect at that time. These pre-service tests were conducted under conditions similar to those to be experienced during subsequent in-service tests, to the maximum extent practicable.

When a valve or its control system has been replaced or repaired or has undergone maintenance that could affect its performance, and prior to the time it is returned to service, it will be tested to demonstrate that the performance parameters which could be affected by the replacement, repair, or maintenance are within acceptable limits.

Valves with remote position indicators, will be visually observed at least once every 2 years to verify that remote valve indications accurately reflect valve operation.

Valves which act as an isolation boundary between high pressure reactor coolant piping and adjacent low pressure systems, and whose undetected failure or degradation could lead to an inter-system LOCA, will be considered Category A or A-C valves and tested in accordance with this section and the Technical Specifications.

Records and reports of in-service valve tests will be kept in accordance with ISTC 6 of the Code.

3.9(B).7 References

1. WREM-Water Reactor Evaluation Model, Rev. 1, NUREG-75/056, May 1975, NRC, Div. of Technical Review.
2. Public Service Company of New Hampshire letter, dated Jan. 4, 1980, to NRC, Region I, Office of Inspection and Enforcement (response to IE Bulletin No. 79-02, Rev. 2).

SEABROOK UPDATED FSAR

TABLE 3.9(B)-7

STRESS LIMITS FOR CATEGORY I
ASME CODE CLASS 2 AND 3 VESSELS AND TANKS

<u>Plant Loading Conditions</u> ⁽¹⁾	<u>Stress Limits</u> ⁽²⁾
Normal	ASME NC-3300, ND-3300 NC-3800, ND-3800
Upset	$P_m < 1.1S$ $(P_m \text{ or } P_1) + P_b < 1.65S$
Emergency	$P_m < 1.5S$ $(P_m \text{ or } P_1) + P_b < 1.8S$
Faulted	$P_m < 2.0S$ $(P_m \text{ or } P_1) + P_b < 2.4S$

NOTES

(1) Plant loading conditions are defined in Table 3.9(B)-3.

(2) S, P_m , P_1 and P_b are defined in Table 3.9(B)-4.

TABLE 3.9(B)-8

ASME SECTION III CLASS 1 PIPING
SYSTEMS LOAD COMBINATIONS AND STRESS LIMITS⁽¹⁾

Condition	Load Combination	Stress Category	Stress Limits	Stress Combination
DESIGN	P P + D + OBE	P_m $P_L + P_b$	S_m $1.5 S_m$	NB-3640 EQ(9) NB-3650
PLANT NORMAL AND UPSET	$P_{MAX} + T + TR + OBE + SAD(OBE) + Q$ <u>OR</u> $\left[\begin{array}{l} T \\ P_{MAX} + TR + OBE + Q \end{array} \right]$ <u>AND</u> U	$P_L + P_b + P_e + Q$ P_e $P_L + P_b + Q$ ----	$3 S_m$ $3 S_m$ $3 S_m$ 1.0	EQ(10) NB-3650 EQ(12) NB-3650 EQ(13) NB-3650 NB-3222.4
PLANT EMERGENCY	P_{MAX} $P_{MAX} + D + TR + DSL$	P_m $P_L + P_b$	$1.5 \times P(\text{DESIGN})$ $2.25 S_m$	NB-3655 EQ(9) NB-3655
PLANT FAULTED	P_{MAX} $P_{MAX} + D + TR + SSE + SAD + (SSE) + DSL$ + LOCA DISP.	P_m $P_L + P_b$	$2 \times P(\text{DESIGN})$ $3 S_m$	NB-3656 EQ(9) NB-3656
TEST	$P_t + D_t$ PAD + D	$P_m + P_b$ P_b	$0.9 S_y$ $1.35 S_y$	NB-3226 NB-3226

⁽¹⁾ Terminology and notations are defined in Table 3.9(B)-11

TABLE 3.9(B)-9
(Sheet 1 of 2)

ASME SECTION III CLASS 2 AND 3 ESSENTIAL PIPING
SYSTEMS LOAD COMBINATIONS AND STRESS LIMITS⁽¹⁾

Condition	Load Combination	Stress Combination	Stress Limits
DESIGN	P	NC-3640	S_h
PLANT NORMAL	$\begin{bmatrix} P + D \\ T \end{bmatrix}$	EQ(8) NC-3650 EQ(10) NC-3650	S_h S_A
	<u>OR</u> $\begin{bmatrix} P + D \\ P + D + T \end{bmatrix}$	EQ(8) NC-3650 EQ(11) NC-3650	S_h $S_h + S_A$
PLANT UPSET	$\begin{bmatrix} P_{MAX} + D + TR + OBE + SAD(OBE) \\ T \end{bmatrix}$	EQ(9) NC-3650 EQ(10) NC-3650	$1.2 S_h$ S_A
	<u>OR</u> $\begin{bmatrix} P_{MAX} + D + TR + OBE + SAD(OBE) \\ P_{MAX} + D + T \end{bmatrix}$	EQ(9) EQ(11)	$1.2 S_h$ $S_h + S_A$
	<u>OR</u> $\begin{bmatrix} P_{MAX} + D + TR + OBE \\ T + SAD(OBE) \end{bmatrix}$	EQ(9) NC-3650 EQ(10) NC-3650	$1.2 S_h$ S_A
	<u>OR</u> $\begin{bmatrix} P_{MAX} + D + TR + OBE \\ P_{MAX} + D + T + SAD(OBE) \end{bmatrix}$	EQ(9) NC-3650 EQ(11) NC-3650	$1.2 S_h$ $S_h + S_A$
	<u>AND</u> $P_{MAX} + D$	EQ(8) NC-3650	S_h
PLANT EMERGENCY	$\begin{bmatrix} P_{MAX} + D + TR + DSL \\ T \end{bmatrix}$	EQ(9) NC-3650 EQ(11) NC-3650	$1.2 S_h$ S_A
	<u>OR</u> $\begin{bmatrix} P_{MAX} + D + TR + DSL \\ P_{MAX} + D + T \end{bmatrix}$	EQ(9) NC-3650 EQ(11) NC-3650	$1.2 S_h$ $S_h + S_A$
	<u>AND</u> $P_{MAX} + D$	EQ(8) NC-3650	S_h

⁽¹⁾ Terminology and notations are defined in Table 3.9(B)-11.

SEABROOK UPDATED FSAR

TABLE 3.9(B)-9
(Sheet 2 of 2)

ASME SECTION III CLASS 2 AND 3 ESSENTIAL PIPING
SYSTEMS LOAD COMBINATIONS AND STRESS LIMITS⁽¹⁾

Condition	Load Combination	Stress Combination	Stress Limits
PLANT FAULTED	P_{MAX}	CC-1606	$2 \times P(\text{DESIGN})$
	$\left[\begin{array}{l} P_{MAX}+D+TR+SSE+SAD(SSE)+ \\ PAD+TAD+DSL \\ T \end{array} \right]$	EQ(9) NC-3650 EQ(10) NC-3650	$1.8 S_h$ S_A
	<u>OR</u>		
	$\left[\begin{array}{l} P_{MAX}+D+TR+SSE+SAD(SSE)+ \\ PAD+TAD+DSL \\ P_{MAX} + D + T \end{array} \right]$	EQ(9) NC-3650 EQ(11) NC-3650	$1.8 S_h$ $S_h + S_A$
	<u>OR</u>		
	$\left[\begin{array}{l} P_{MAX}+D+TR+SSE+DSL \\ T+SAD(SSE)+PAD+TAD \end{array} \right]$	EQ(9) NC-3650 EQ(10) NC-3650	$1.8 S_h$ S_A
<u>OR</u>			
	$\left[\begin{array}{l} P_{MAX}+D+TR+SSE+DSL \\ P_{MAX}+D+T+SAD(SSE)+PAD+TAD \end{array} \right]$	EQ(9) NC-3650 EQ(11) NC-3650	$1.8 S_h$ $S_h + S_A$
<u>AND</u>			
	$P_{MAX} + D$	EQ(8) NC-3650	S_h
TEST	$P_t + D_t$	Adopted From NB-3226	$0.9 S_y$
	$PAD + D$		$1.35 S_y$

SEABROOK UPDATED FSAR

TABLE 3.9(B)-10

ASME SECTION III CLASS 2 AND 3
NONESSENTIAL PIPING SYSTEMS⁽¹⁾

Condition	Load Combination	Stress Combination	Stress Limits
DESIGN	P	NC-3640	S_h
PLANT NORMAL	$\begin{bmatrix} P + D \\ T \end{bmatrix}$ <p style="text-align: center;"><u>OR</u></p> $\begin{bmatrix} P + D \\ P + D + T \end{bmatrix}$	EQ(8) NC-3650 EQ(10) NC-3650	S_h S_A
	$\begin{bmatrix} P_{MAX} + D + TR + OBE + SAD(OBE) \\ T \end{bmatrix}$ <p style="text-align: center;"><u>OR</u></p> $\begin{bmatrix} P_{MAX} + D + TR + OBE \\ T + SAD(OBE) \end{bmatrix}$ <p style="text-align: center;"><u>OR</u></p> $\begin{bmatrix} P_{MAX} + D + TR + OBE \\ P_{MAX} + D + T + SAD(OBE) \end{bmatrix}$ <p style="text-align: center;"><u>AND</u></p> $P_{MAX} + D$	EQ(9) NC-3650 EQ(10) NC-3650	$1.2 S_h$ S_A
PLANT UPSET	$\begin{bmatrix} P_{MAX} + D + TR + OBE \\ T + SAD(OBE) \end{bmatrix}$ <p style="text-align: center;"><u>OR</u></p> $\begin{bmatrix} P_{MAX} + D + TR + OBE \\ P_{MAX} + D + T + SAD(OBE) \end{bmatrix}$ <p style="text-align: center;"><u>AND</u></p> $P_{MAX} + D$	EQ(9) NC-3650 EQ(10) NC-3650	$1.2 S_h$ S_A
PLANT EMERGENCY	P + D + TR + DSL	EQ(9) NC-3650	$1.8 S_h$
PLANT FAULTED	P + D + TR + SSE + DSL	EQ(9) NC-3650 CC-1606	$2.4 S_h$
TEST	$P_t + D_t$ PAD + D	Adopted Form NB-3226	$0.9 S_y$ $1.35 S_y$

⁽¹⁾ Terminology and notations are defined in Table 3.9(B)-11

TABLE 3.9(B)-11
(Sheet 1 of 2)

TERMINOLOGY AND NOTATIONS USED IN
TABLES 3.9(B)-8, 3.9(B)-9 AND 3.9(B)-10

Symbols for Stress Classification and Stress Limits are in accordance with ASME Section III. Other load symbols and definitions are specified below:

- P - Internal design pressure
- P_{MAX} - Peak pressure, considered as a set pressure of over-pressure safety devices
- P_t - Test pressure
- D - Deadweight, consisting of the weight of the pipe and pipe supported elements such as valves and flanges, including weight of insulation and contained fluid
- D_t - Same as 'D' where pipe contents are fluid during pressure test
- T - Thermal loads due to:
- a. Piping thermal expansion when subjected to maximum temperature difference between the fluid and the surrounding environment in the specified plant conditions, and
 - b. Anchor displacement due to thermal movements of piping anchors
- TR - Thrust or transient due to safety valve discharge, valve trip or fluid flow
- SAD - Seismic anchor displacement (OBE or SSE), affects piping supported from different structures of relative seismic motions
- PAD - Anchor displacement due to pressure, e.g., containment building penetrations due to internal pressure during test or LOCA
- TAD - Anchor displacement due to thermal growth of the structure e.g., radial and vertical growth of Containment Building during LOCA \pm MSL-
- DSL - Dynamic System Load, Accident Load affecting piping as follows:
- Impact from missiles or pipe whip
 - Jet impingement
 - External pressure
- LOCA DISP. - Anchor displacement due to movement of primary or secondary loop during LOCA
- Q - Temperature gradient loads, ΔT_1 , ΔT_2 and $(\alpha_a T_a - \alpha_b T_b)$

TABLE 3.9(B)-11
(Sheet 2 of 2)

TERMINOLOGY AND NOTATIONS USED IN
TABLES 3.9(B)-8, 3.9(B)-9 AND 3.9(B)-10

- U - Cumulative usage factor
- OBE - Loads generated by the Operating Basis Earthquake (OBE), which is the earthquake that could reasonably be expected to affect the plant site during the operating life of the plant and which produces the vibratory ground motion for which those features of the nuclear plant necessary for continued operation without undue risk to the health and safety of the public have been designed to remain functional.
- SSE - Loads generated by the Safe Shutdown Earthquake (SSE) which is the earthquake that produces the maximum vibratory ground motion for which certain structures, systems, and components important to safety and required for safe shutdown on the plant have been designed to remain functional.

SEABROOK UPDATED FSAR

TABLE 3.9(B)-12

STRESS LIMITS FOR ACTIVE
CATEGORY I ASME CODE CLASS 2 AND 3 PUMPS

<u>Plant Loading</u> <u>Condition</u> ⁽¹⁾⁽³⁾	<u>Stress Limits</u> ⁽²⁾⁽⁴⁾
Normal	ASME Section III, Subsections NC-3400 or ND-3400
Upset	$P_m < 1.0S$ $(P_m \text{ or } P_1) + P_b < 1.5S$
Emergency	$P_m < 1.0S$ $(P_m \text{ or } P_1) + P_b < 1.5S$
Faulted	$P_m < 1.0S$ $(P_m \text{ or } P_1) + P_b < 1.5S$

NOTES

- (1) Plant loading conditions are defined in Table 3.9(B)-3.
- (2) S, P₁, P_m and P_b are defined in Table 3.9(B)-4.
- (3) Identification of the specific transients or events to be considered under each plant condition are addressed in Regulatory Guide 1.48.
- (4) For pump supports, the allowable stresses defined in AISC "Manual of Steel Construction" is used for plant condition associated with 0.5SSE. For plant conditions associated with SSE, the stresses are limited to 90 percent of yield stress for the material involved.

TABLE 3.9(B)-15STRESS AND DEFLECTION ANALYSIS OF PRIMARY
COMPONENT COOLING WATER PUMPS (14X23-S)

<u>ITEMS - SSE ANALYSIS</u>	<u>ACTUAL</u>	<u>ALLOWABLE</u>
Pump Casing, Primary Membrane, psi	5,746	17,500
Membrane and Bending, psi	15,715	26,250
Casing Flange, Normal Stress, psi	24,469	26,250
Casing Flange Bolts, psi	34,967	50,000
Suction Flange, Longitudinal Stress, psi	10,213	21,000
Discharge Flange, Longitudinal Stress, psi	9,093	21,000
Shaft Stress, psi	6,724	25,000
Shaft Deflection, at Coupling, in.	0.017	0.055
at Seal, in.	0.004	0.005
at Impeller, in.	0.009	0.0125
Casing Feet, Principal, psi	3,535	14,000
Casing Foot Bolts, Tension, psi	22,280	42,000
Casing Foot Shear Pins, Shear, psi	14,328	17,000
Bedplate, Principal psi	13,990	19,333
Bedplate, Side-Channels, tension, psi	9,534	14,500
Bedplate, Side-Channel Weld, Shear, psi	9,154	9,670
Anchor Bolts, Tension, psi	12,090	19,100
Shear, psi	8,910	12,800
Natural Frequency of Pump-Motor-Bedplate System, Hz	46.19	N/A

TABLE 3.9(B)-16STRESS AND DEFLECTION SUMMARY FOR
CONTAINMENT SPRAY PUMPS (6X11X14B-CD)

<u>ITEMS - SSE ANALYSIS</u>	<u>ACTUAL</u>	<u>ALLOWABLE</u>
Natural Frequency, Hz		
Pump	67	-
Driver	85	-
Pump Casing at Suction Nozzle, psi	2,741	27,000
Shaft Stress, psi	4,486	27,000
Pedestal Weld, psi	5,350	32,400
Pump Anchor Pin, psi	10,500	32,400
Base Cross Member, psi	20,374	32,400
Weld, psi	19,200	32,400
Bearing Load (Double Row), lbs.	1,140	17,200
(Single Row), lbs.	228	7,670
Base Hold-down bolts, Tension, psi	3,450	19,100
Shear, psi	2,430	9,900
Deflections		
Pump shaft, in.	0.0038	0.022
Coupling parallel misalignment, in.	0.0385	0.102
Coupling angular misalignment, degrees	0.264	1.5
Motor rotor, in.	0.0011	0.043

TABLE 3.9(B)-17
(Sheet 1 of 2)

STRESS AND DEFLECTION SUMMARY FOR
EMERGENCY FEEDWATER PUMPS (4x9 NH-10)

<u>ITEMS - SSE ANALYSIS</u>	<u>ACTUAL</u>	<u>ALLOWABLE</u>
A. Turbine-Driven Pump		
Natural frequency of pump-turbine, Hz		
Entire assembly	48.0	-
Shaft	93.2	-
Casing, psi		
Casing flange bolts	24,967	25,000
@ Discharge nozzle	13,444	21,000
Pump flange @ discharge	19,706	21,000
Pump foot bolt, psi		
Tension	22,700	62,500
Shear	22,800	25,800
Foundation bolt, psi		
Tension	22,500	41,300
Shear	16,500	27,500
Pump pedestal weld, psi		
Top	2,100	18,000
Bottom	16,800	18,000
Deflection, in.		
Shaft @ seal	0.0042	0.005
Coupling	0.0081	0.102
B. Motor-Driven Pump		
Natural frequency of pump-motor		
Entire assembly, Hz	49.3	-
Shaft, Hz	93.2	-
Casing, psi		
Casing flange bolts	24,967	25,000
@ discharge nozzle	14,400	21,000
Pump flange @ discharge	20,800	21,000
Pump foot bolt, psi		
Tension	19,500	62,500
Shear	22,800	25,800

TABLE 3.9(B)-17
(Sheet 2 of 2)

STRESS AND DEFLECTION SUMMARY FOR
EMERGENCY FEEDWATER PUMPS (4x9 NH-10)

<u>ITEMS - SSE ANALYSIS</u>	<u>ACTUAL</u>	<u>ALLOWABLE</u>
B. Motor-Driven Pump (cont.)		
Foundation bolt, psi		
Tension	16,720	41,300
Shear	11,000	27,500
Pump pedestal weld, psi		
Top	1,900	18,000
Bottom	15,100	18,000
Deflection, in.		
Shaft @ seal	0.0042	0.005
Coupling	0.0081	0.102

TABLE 3.9(B)-18STRESS AND DEFLECTION SUMMARY FOR
SERVICE WATER PUMP (30 DC 2 STAGE, JOHNSTON PUMP)

<u>ITEMS - SEE ANALYSIS</u>	<u>ACTUAL</u>	<u>ALLOWABLE</u>
Natural Frequency, Hz		
Horizontal	9.613	-
Vertical	24.444	-
Pump Casing, psi		
Discharge Head at Nozzle	8,046	15,700
Column at Flange	9,973	15,700
Bowls	1,413	12,500
Lineshaft, psi	13,541	18,800
Seismic Support, psi	2,448	13,345
Base Bolts, psi	9,000	19,100
Clearance, in.		
Top Impeller Wear Ring	0.0098	0.0145
Lower Impeller Wear Ring	0.0100	0.0145
Motor Air Gap	0.001808	0.035
Bearing Pressure, psi		
Seal Box	22	35
Lineshaft	32	35
Top Bowl	20	35
Inter Bowl	18	35
Suction Bowl	4	35

TABLE 3.9(B)-19STRESS AND DEFLECTION SUMMARY FOR
COOLING TOWER PUMP (33NLC, JOHNSTON VERTICAL PUMP)

<u>ITEMS - SSE ANALYSIS</u>	<u>ACTUAL</u>	<u>ALLOWABLE</u>
Natural Frequency, Hz		
Pump Assembly	14.5	-
Motor Rotor	49.7	-
Pump Casing, psi		
Discharge Head Flange	19,437	20,550
Column Flange	21,960	23,550
Pump Casing	5,644	19,800
Shaft, psi	12,265	20,000
Seismic Supports, psi	891	23,550
Anchor Bolts, Tension, psi	5,970	19,100
Shear, psi	2,380	9,900
Clearances, in.		
Impeller to Casing	0.002	0.08
Rotor/Stator	0.0172	0.035
Shaft Deflection	0.016	0.080

SEABROOK UPDATED FSAR

TABLE 3.9(B)-20

STRESS AND DEFLECTION SUMMARY FOR DIESEL
FUEL OIL TRANSFER PUMP (N 3DBS - 18 IMO PUMP)

<u>ITEMS - SSE ANALYSIS</u>	<u>ACTUAL</u>	<u>ALLOWABLE</u>
Natural Frequency, Hz	228	-
Pump Casing at Inlet Nozzle, psi	7,123	26,250
Base Plate, psi	4,147	21,750
Pump Hold-Down Bolts, psi		
Tension	2,300	19,100
Shear	1,150	9,900
Clearances, in.	0.00009	0.0005

TABLE 3.9(B)-21*

STRESS ANALYSIS SUMMARY
ASME III CLASS 1 PIPING
RCS PRESSURIZER SAFETY AND RELIEF VALVES SYSTEM
(P&ID RC-20846)
(LINE NOS: 74, 75, 76 & 80)

EVALUATION	MAX STRESS (KSI)	LINE NO. & COMPONENT	ALLOWABLE (KSI)
Eq. 9 - Design P+D+OBE	23.2	Line 76 Elbow	1.5 Sm 24.63
Eq. 9 - Faulted P+D+TR+SSE	39.1	Line 76 Elbow	3.0 Sm 49.26
Eq. 12 T	36.0	Line 80 Transition	3.0 Sm 49.26
Eq. 13 P+D+OBE+Q	37.9	Line 80 Transition	3.0 Sm 49.26
Fatigue Usage Factor	0.95	Line 80 Transition	1.0

*This table is being maintained for historical purposes only. Refer to applicable calculations for latest information.

TABLE 3.9(B)-22*
(Sheet 1 of 10)

STRESS ANALYSIS SUMMARY, ASME III CLASS 2 AND 3 PIPING
(EQUATION 9)

<u>PIPING SYSTEM</u>	SYSTEM DRAWING NO.	NORMAL & UPSET CONDITION		EMERGENCY CONDITION		FAULTED CONDITION	
		ACTUAL (KSI)	ALLOW. (KSI)	ACTUAL (KSI)	ALLOW. (KSI)	ACTUAL (KSI)	ALLOW. (KSI)
<u>REACTOR COOLANT SYSTEM</u>							
3"x4"- RC-V24 Line No. 14-1 SC 2	RC-20841	16.36	19.44	9.09	19.44	26.68	29.16
3"x4"- RC-V89 Line No. 88-1 SC 2	RC-20844	18.27	19.44	8.64	19.44	27.91	29.16
<u>REFUELING CAVITY CLEANUP SYSTEM</u>							
3/4"x1" - SF-V101 Line No. 1743-9 SC 2	SF-20484	13.24	19.08	1.17	19.08	21.66	28.62
<u>FLOOR & EQUIPMENT DRAIN SYSTEM</u>							
3/4"x1"- WLD-V209 Line No. 2076-11 SC 2	WLD-20219	10.5	22.0	2.3	22.0	21.81	33.0
<u>RESIDUAL HEAT REMOVAL SYSTEM</u>							
1"x3/4" - RH-V13 Line No. 172-1 SC 2	RH-20662	11.41	19.44	1.97	19.44	20.87	29.16
1"x3/4" - RH-V25 Line No. 169-1 SC 2	RH-20663	13.18	19.44	2.73	19.44	23.12	29.16

*This table is being maintained for historical purposes only. Refer to applicable calculations for latest information.

TABLE 3.9(B)-22
(Sheet 2 of 10)

STRESS ANALYSIS SUMMARY, ASME III CLASS 2 AND 3 PIPING
(EQUATION 9)

<u>PIPING SYSTEM</u>	SYSTEM DRAWING NO.	NORMAL & UPSET CONDITION		EMERGENCY CONDITION		FAULTED CONDITION	
		ACTUAL (KSI)	ALLOW. (KSI)	ACTUAL (KSI)	ALLOW. (KSI)	ACTUAL (KSI)	ALLOW. (KSI)
<u>SAFETY INJECTION SYSTEM</u>							
3/4"x1" - SI-V247 Line No. 248-16 SC 2	SI-20450	13.79	19.08	4.40	19.08	23.19	28.62
1"x2" - SI-V10 Line No. 220-1 SC 2	SI-20450	9.58	19.92	7.56	19.92	11.60	29.88
1"x2" - SI-V30 Line No. 221-1 SC 2	SI-20450	9.77	19.92	4.91	19.92	14.62	29.88
1"x2" - SI-V45 Line No. 222-1 SC 2	SI-20450	9.77	19.92	4.91	19.92	14.62	29.88
1"x2" - SI-V60 Line No. 223-1 SC 2	SI-20450	9.77	19.92	4.91	19.92	14.69	29.88
3/4"x1" - SI-V101 Line No. 252-1 SC 2	SI-20446	15.23	19.92	4.08	19.92	26.34	29.88
3/4"x1" - SI-V113 Line No. 253-1 SC 2	SI-20446	14.88	19.92	3.54	19.92	26.06	29.88
3/4"x1" - SI-V76 Line No. 254-1 SC 2	SI-20447	10.61	19.92	4.41	19.92	17.25	29.88
3/4"x1" - SI-V175 Line No. 278-2 SC 2	SI-20447	15.43	22.56	4.48	22.56	26.38	33.84

SEABROOK UPDATED FSAR

Prior to loading, it is assumed that the plant is at hot shutdown conditions, with 32°F feedwater cycling. During the two-hour period following the beginning of loading, the feedwater temperature increases from 32°F to 300°F due to steam dump and turbine startup heat input to the feedwater. Subsequent to unloading, feedwater heating is terminated, steam dump is reduced to residual heat removal requirements, and feedwater temperature decays from 300°F to 32°F.

The number of these loading and unloading transients is assumed to be 500 each during the 40-year plant design life, which is equivalent to about one occurrence per month.

9. Boron Concentration Equalization

Following any large change in boron concentration in the RCS, spray is initiated in order to equalize concentration between the loops and the pressurizer. This can be done by manually operating the pressurizer backup heater, thus causing a pressure increase, which will initiate spray at a compensated pressurizer pressure of approximately 2275 psia. The proportional sprays return the pressure to 2250 psia, and maintain this pressure by matching the heat input from the backup heater until the concentration is equalized. For design purposes, it is assumed that this operation is performed once after each load change in the design load follow cycle. With two load changes per day, and a 90 percent plant availability factor over the 40-year design life, the total number of occurrences is 26,400.

10. Refueling

At the end of plant cooldown, the temperature of the fluid in the RCS is less than 125°F. At this time, the vessel head is removed and the refueling canal is filled. This is done by pumping water from the refueling water storage tank, which is outside and conservatively assumed to be at 32°F, into the loops by means of the low head safety injection pumps. The refueling water flows directly into the reactor vessel via the accumulator connections and cold legs.

This operation is assumed to occur twice per year, or 80 times over the life of the plant.

11. Reduced Temperature Return to Power

The reduced temperature return to power operation is designed to improve the spinning reserve capabilities of the plant during load-follow operations without part length rods. The transient will normally begin at the ebb (50 percent) of a

load-follow cycle and will proceed at a rapid positive rate (typically 5 percent per minute) until the abilities of the control rods and the coolant temperature reduction (negative moderator coefficient) to supply reactivity are exhausted. At that point, further power increases are limited to approximately one percent per minute by the ability of the boron system to dilute the reactor coolant. The reduction in primary coolant temperature is limited by the protection system to about 20°F below the programmed value.

The reduced temperature return to power operation is not intended for daily use. It is designed to supply additional plant capabilities when required because of network fault or upset condition. Hence this mode of operation is not expected to be used more than once a week in practice (2000 times in 40 years).

12. Reactor Coolant Pumps (RCP) Startup and Shutdown

The reactor coolant pumps are started and stopped during routine operations such as RCS venting, plant heatup and cooldown, and in connection with recovery from certain transients such as Loop Out of Service and Loss of Power. Other (undefined) circumstances may also require pump starting and stopping.

Of the spectrum of RCS pressure and temperature conditions under which these operations may occur, three conditions have been selected for defining transients:

Cold condition - 70°F and 400 psig
Pump restart condition - 100°F and 400 psig
Hot condition - 557°F and 2235 psig

For RCP starting and stopping operations, it is assumed that variations in RCS primary side temperature and in pressurizer pressure and temperature are negligible, and that the steam generator secondary side is completely unaffected. The only significant variables are the primary system flow and the pressure changes resulting from the pump operations.

The following cases were considered:

Case 1 - First Pump Startup (Last Pump Shutdown)

Variations in reactor coolant loop flow accompany startup of the first pump, both in the loop containing the pump being started and in the other loops (loops in which the pumps remain idle). This case involves a higher dynamic pressure loss in the loop containing the pump being

SEABROOK UPDATED FSAR

barrel by accounting for the deflections of constraining boundaries which are represented by masses and springs. The dynamic response of the core barrel in its beam bending mode responding to blowdown forces compensates for internal pressure variation by increasing the volume of the more highly pressurized regions. The analytical methods used to develop the reactor internals hydraulics are described in WCAP-8708 (Reference 9).

d. Reactor Vessel and Internals Modeling

The reactor vessel is restrained by two mechanisms: (1) the four attached reactor coolant loops with the steam generator and reactor coolant pump primary supports and (2) four reactor vessel supports, two beneath reactor vessel inlet nozzles and two beneath reactor vessel outlet nozzles. The reactor vessel supports are described in Subsection 5.4.14 and are shown in Figures 5.4-14, and 3.8-26. The support shoe provides restraint in the horizontal directions and for downward reactor vessel motion.

The reactor vessel model consists of two nonlinear elastic models connected at a common node. One model represents the dynamic vertical characteristics of the vessel and its internals, and the other model represents the translational and rotational characteristics of the structure. These two models are combined in the DARIWOSTAS code (Reference 1) to represent motion of the reactor vessel and its internals in the plane of the vessel centerline and the broken pipe centerline.

The model for horizontal motion considers that each node has one translational and one rotational degree of freedom in the vertical plane containing the centerline of the nozzle attached to the broken pipe and the centerline of the vessel. A combination of beam elements and concentrated masses are used to represent the components including the vessel, core barrel, neutron panels, fuel assemblies, and upper support columns. Connections between the various components are either pin-pin rigid links, translational impact springs with damping, or rotational springs.

The model for vertical motion considers that each mass node has one translational degree of freedom. The structure is represented by concentrated masses, springs, dampers, gaps, and frictional elements. The model includes the core barrel, lower support columns, bottom nozzles, fuel rods, top nozzles, upper support structure, and reactor vessel.

The horizontal and vertical models are coupled at the elevation of the primary nozzle centerlines. Node 1 of the horizontal model is coupled with node 2 of the vertical model at the reactor vessel nozzle elevation. This coupled node has external restraints characterized by a 3x3 matrix which represents the reactor coolant

loop stiffness characteristics, by linear horizontal springs which describe the tangential resistance of the supports, and by individual nonlinear vertical stiffness elements which provide downward restraint only. The individual supports are located at the actual support pad locations and accurately represent the independent nonlinear behavior of each support.

e. Analytical Methods

The time-history effects of the internal loads and loops mechanical loads are combined and applied simultaneously to the appropriate nodes of the mathematical model of the reactor vessel and internals. The analysis is performed by numerically integrating the differential equations of motion to obtain the transient response. The output of the analysis includes the displacements of the reactor vessel and the loads in the reactor vessel supports which are combined with other applicable faulted condition loads and subsequently used to calculate the stresses in the supports. Also, the reactor vessel displacements are applied as a time-history input to the dynamic reactor coolant loop blowdown analysis. The resulting loads and stresses in the piping components and supports include both loop blowdown loads and reactor vessel displacements. Thus, the effect of vessel displacements upon loop response and the effect of loop blowdown upon vessel displacements are both evaluated.

f. Results of Analysis

As described, the reactor vessel and internals were analyzed for three postulated break locations. Table 3.9(N)-12 summarizes the allowable and no-loss-of-function displacements for reactor internals. Positive vertical displacement is up and positive horizontal displacement is away from and along the centerline of the vessel nozzle in the loop in which the break was postulated to occur. These displacements were calculated using an assumed break opening area for the postulated pipe ruptures of 144 in². Based on the deterministic fracture mechanics evaluation of the RCS loop piping, Westinghouse has demonstrated that postulation of pipe ruptures in the RC loop need not be made. An exemption from a portion of the requirements of General Design Criterion 4 of Appendix A to 10 CFR Part 50 has been granted to Seabrook; see Reference 14. The result of postulating rupture of one of the three branch line nozzles would be to impose reduced asymmetric loadings on the Reactor Core System. The fuel assembly grid load due to pipe ruptures was not applied to the analysis results.

SEABROOK UPDATED FSAR

- a. The pressure differential across the element
- b. Flow stagnation on, and unrecovered orifice losses across the element
- c. Friction losses along the element.

Input to the code, in addition to the blowdown pressure and velocity transients, includes the effective area of each element on which the force acts due to the pressure differential across the element, a coefficient to account for flow stagnation and unrecovered orifice losses, and the total area of the element along which the shear forces act.

The mechanical analysis (Reference 11) has been performed using conservative assumptions. Some of the more significant assumptions are:

- a. The mechanical and hydraulic analyses have considered the effect of hydroelasticity.
- b. The reactor internals are represented by a multi-mass system connected with springs and dashpots simulating the elastic response and the viscous damping of the components. The modeling is conducted in such a way that uniform masses are lumped into easily identifiable discrete masses while elastic elements are represented by springs.

The model described is considered to have a sufficient number of degrees of freedom to represent the most important modes of vibration in the vertical direction. This model is conservative in the sense that further mass-spring resolution of the system would lead to further attenuation of the shock effects obtained with the present model.

The pressure waves generated within the reactor are highly dependent on the location and nature of the postulated pipe failure. In general, the more rapid the severance of the pipe, the more severe the imposed loadings on the components. A one millisecond severance time is taken as the limiting case.

In the case of the hot leg branch line break, the vertical hydraulic forces produce an initial upward lift of the core. A rarefaction wave propagates through the reactor hot leg nozzle into the interior of the upper core barrel. Since the wave has not reached the flow annulus on the outside of the barrel, the upper barrel is subjected to an impulsive compressive wave. Thus, dynamic instability (buckling) or large deflections of the upper core barrel, or both, is a possible response of the barrel during a hot leg branch line break, and results in transverse loading on the upper core components as the fluid exits the hot leg nozzle.

In the case of the cold leg branch line break, a rarefaction wave propagates along a reactor inlet pipe, arriving first at the core barrel at the inlet nozzle of the broken loop. The upper barrel is then subjected to a non-axisymmetric expansion radial impulse which changes as the rarefaction wave propagates both around the barrel and down the outer flow annulus between vessel and barrel. After the cold leg branch line break, the initial steady-state hydraulic lift forces (upward) decrease rapidly (within a few milliseconds) and then increase in the downward direction. These cause the reactor core and lower support structure to move initially downward.

If a simultaneous seismic event with the intensity of the SSE is postulated with the loss-of-coolant accident, the imposed loading on the internals component is additive and, therefore, the combined loading is considered even though the loading imposed by the earthquake is generally small compared to the blowdown loading.

The summary of the mechanical analysis follows:

a. Mathematical Model of the Reactor Pressure Vessel and Analytical Method

The mathematical model of the RPV is a three-dimensional nonlinear finite element model which represents the dynamic characteristics of the reactor vessel and its internals in the six geometric degrees of freedom. The model was developed using the WECAN computer code. The model consists of three concentric structural submodels connected by nonlinear impact elements and stiffness matrices. The first submodel represents the reactor vessel shell and associated components. The reactor vessel is restrained by four reactor vessel supports (situated beneath alternate nozzles) and by the attached primary coolant piping. Each reactor vessel support is modeled by a linear horizontal stiffness and a vertical spring-gap element. The attached piping is represented by a stiffness matrix.

The second submodel represents the reactor core barrel (RCB), neutron panels, lower support plate, tie plates, and secondary core support components. This submodel is physically located inside the first, and is connected to it by a stiffness matrix at the internals support ledge. Core barrel to vessel shell impact is represented by nonlinear elements at the core barrel flange, core barrel nozzle, and lower radial support locations.

The third and innermost submodel represents the upper support plate, guide tubes, upper support columns, upper and lower core plates, and fuel. The third submodel is connected to the first and second by stiffness matrices and nonlinear elements.

Fluid-structure or hydro-elastic interaction is included in the reactor pressure vessel model for seismic evaluation. The horizontal hydro-elastic interaction is significant in the

cylindrical fluid flow region between the core barrel and reactor vessel (the downcomer). Mass matrices with off-diagonal terms (horizontal degrees-of-freedom only) attach between nodes on the core barrel and reactor vessel shell.

The diagonal terms of the mass matrix are similar to the lumping of water mass to the vessel shell and core barrel. The off-diagonal terms reflect the fact that all the water mass does not participate when there is no relative motion of the vessel and core barrel. It should be pointed out that the hydrodynamic mass matrix has no artificial virtual mass effect and is derived in a straight-forward, quantitative manner.

The matrices are a function of the properties of two cylinders with a fluid in the cylindrical annulus, specifically; inside and outside radius of the annulus, density of the fluid and length of the cylinders. Vertical segmentation of the RCB allows inclusion of radii variations along the RCB height and approximates the effects of RCB beam deformation. These mass matrices were inserted between selected nodes on the core barrel and reactor vessel shell.

For LOCA the time-history effects of the internals loads and loop mechanical loads are combined and applied simultaneously to the appropriate nodes of the mathematical model of the reactor vessel and internals. The analysis is performed by numerically integrating the differential equations of motion to obtain the transient response. The output of the analysis includes the displacements of the reactor vessel and the reactor internals.

dynamic stress intensities are within acceptable limits. In addition, the cumulative fatigue usage factor is also within the allowable usage factor of unity.

The stresses due to the Safe Shutdown Earthquake (vertical and horizontal components) were combined in the most unfavorable manner with the blowdown stresses to obtain the largest principal stress and deflection.

These results indicate that the maximum deflections and stresses in the critical structures are below the established allowable limits. For the transverse excitation, it is shown that the upper barrel does not buckle during a hot leg break, and that it has an allowable stress distribution during a cold leg break.

Even though control rod insertion is not required for plant shutdown, this analysis shows that most of the guide tubes will deform within the limits established experimentally to assure control rod insertion. For the guide tubes deflected above the no-loss-of-function limit, it must be assumed that the rods will not drop. However, the core will still shut down due to the negative reactivity insertion in the form of core voiding. Shutdown will be aided by the great majority of rods that do drop. Seismic deflections of the guide tubes are generally negligible by comparison with the no-loss-of-function limit.

3.9(N).2.6 Correlations of Reactor Internals Vibration Tests with the Analytical Results

As stated in Subsection 3.9(N).2.3, it is not considered necessary to conduct instrumented tests of the Seabrook reactor vessel internals. Adequacy of these internals will be verified by use of the Sequoyah and Trojan results. References 7 and 8 describe predicted vibration behavior based on studies performed prior to the plant tests. These studies, which use analytical models, scale model test results, component tests, and results of previous plant tests, are used to characterize the forcing functions and establish component structural characteristics, so that the flow induced vibratory behavior and response levels for Seabrook are estimated. These estimates are then compared to values deduced from plant test data obtained from the Sequoyah and the Trojan internals vibration measurement programs.

3.9(N).3 ASME Code Class 1, 2 and 3 Components, Component Supports and Core Support Structures

The ASME Code Class components are constructed in accordance with the ASME Boiler and Pressure Vessel Code, Section III.

Detailed discussion of ASME Code Class 1 components is provided in Section 5.4 and Subsection 3.9(N).1. For core support structures, design loading conditions are given in Subsection 3.9(N).5.

SEABROOK UPDATED FSAR

In general, for reactor internals components and for core support structures, the criteria for acceptability in regard to mechanical integrity analyses are that adequate core cooling and core shutdown must be assured. This implies that the deformation of the reactor internals must be sufficiently small so that the geometry remains substantially intact. Consequently, the limitations established on the internals are concerned principally with the maximum allowable deflections and stability of the parts, in addition to a stress criterion to assure integrity of the components.

For the loss of coolant plus the safe shutdown earthquake condition, deflections of critical internal structures are limited. In a hypothesized downward vertical displacement of the internals, energy-absorbing devices limit the displacement after contacting the vessel bottom head, ensuring that the geometry of the core remains intact.

The following mechanical functional performance criteria apply:

- a. Following the loss-of-coolant accident, the functional criterion to be met for the reactor internals is that the plant can be shutdown and cooled in an orderly fashion, so that fuel cladding temperature is kept within specified limits. This criterion implies that the deformation of critical components must be kept sufficiently small to allow core cooling.
- b. For large reactor coolant branch nozzle pipe breaks, the reduction in water density greatly reduces the reactivity of the core, thereby shutting down the core whether the control rods are tripped or not. The subsequent refilling of the core by the Emergency Core Cooling System uses borated water to maintain the core in a subcritical state. Therefore, the main requirement is to assure effectiveness of the Emergency Core Cooling System. Insertion of the control rods, although not needed, gives further assurance of ability to shut the plant down and keep it in a safe shutdown condition.
- c. The inward upper barrel deflections are controlled to insure no contacting of the nearest rod cluster control guide tube. The outward upper barrel deflections are controlled in order to maintain an adequate annulus for the coolant between the vessel inner diameter and core barrel outer diameter.
- d. The rod cluster control guide tube deflections are limited to insure operability of the control rods.
- e. To insure no column loading of rod cluster control guide tubes, the upper core plate deflection is limited.

Methods of analysis and testing for core support structures are discussed in Subsections 3.9(N).2.3, 3.9(N).2.5 and 3.9(N).2.6. Stress limits and deformation criteria are given in Subsection 3.9(N).5.

- f. Following the design basis accident, the plant shall be capable of being shut down and cooled in an orderly fashion so that fuel cladding temperature is kept within specified limits. This implies that the deformation of certain critical reactor internals must be kept sufficiently small to allow core cooling.

The functional limitations for the core structures during the design basis accident are shown in Table 3.9(N)-12. To ensure no column loading of rod cluster control guide tubes, the upper core plate deflection is limited to not exceed the value shown in Table 3.9(N)-12.

Details of the dynamic analyses, input forcing functions, and response loadings are presented in Subsection 3.9(N).2.

The basis for the design stress and deflection criteria is identified below:

a. Allowable Stresses

For normal operating conditions, Section III of the ASME Code is used as a basis for evaluating acceptability of calculated stresses. Both static and alternating stress intensities are considered.

It should be noted, that the allowable stresses in Section III of the ASME Code are based on unirradiated material properties. In view of the fact that irradiation increases the strength of the Type 304 stainless steel used for the internals, although decreasing its elongation, it is considered that use of the allowable stresses in Section III is appropriate and conservative for irradiated internal structures.

The allowable stress limits during the design basis accident used for the reactor internals are based on the draft of the 1971 edition of the ASME Code for Core Support Structures, Subsection NG, and the Criteria for Faulted Conditions.

b. Allowable Deflections

For normal operating conditions, downward vertical deflection of the lower core support plate is negligible.

For the loss-of-coolant accident plus the Safe Shutdown Earthquake condition, the deflection criteria of critical internal structures are the limiting values given in Table 3.9(N)-12. The corresponding no-loss-of-function limits are included in Table 3.9(N)-12 for comparison purposes with the allowed criteria.

The criteria for the core drop accident is based upon analyses which have to determine the total downward displacement of the internal structures following a hypothesized core drop resulting from loss of the normal core barrel supports. The initial clearance between the

secondary core support structures and the reactor vessel lower head in the hot condition is approximately $\frac{1}{2}$ inch. An additional displacement of approximately $\frac{3}{4}$ inch would occur due to strain of the energy absorbing devices of the secondary core support; thus the total drop distance is about $1\frac{1}{4}$ inches, which is insufficient to permit the tips of the Rod Cluster Control Assembly to come out of the guide thimble in the fuel assemblies.

Specifically, the secondary core support is a device which will never be used, except during a hypothetical accident of the core support (core barrel, barrel flange, etc.). There are 4 supports in each reactor. This device limits the fall of the core and absorbs much of the energy of the fall which otherwise would be imparted to the vessel. The energy of the fall is calculated assuming a complete and instantaneous failure of the primary core support and is absorbed during the plastic deformation of the controlled volume of stainless, loaded in tension. The maximum deformation of this austenitic stainless piece is limited to approximately 15 percent, after which a positive stop is provided to ensure support.

3.9(N).6 In-Service Testing of Pumps and Valves

Refer to Subsection 3.9(B).6.

3.9(N).7 References

1. "Documentation of Selected Westinghouse Structural Analysis Computer Codes," WCAP-8252, Revision 1, May 1977.
2. "Benchmark Problem Solutions Employed for Verification of the WECAN Computer Program," WCAP-8929, June 1977.
3. "Sample Analysis of a Class 1 Nuclear Piping System," prepared by ASME Working Group on Piping, ASME Publication, 1972.
4. Witt, F. J., Bamford, W. H., Esselman, T. C., "Integrity of Primary Piping Systems of Westinghouse Nuclear Power Plants during Postulated Seismic Events," WCAP-9283, March 1978.
5. Bogard, W. T., Esselman, T. C., "Combination of Safe Shutdown Earthquake and Loss-of-Coolant Accident Responses for Faulted Condition Evaluation of Nuclear Power Plants," WCAP-9279, March 1978.
6. "Prediction of the Flow-Induced Vibration of Reactor Internals by Scale Model Tests," WCAP-8303-P-A (Proprietary) and WCAP-8317A (Nonproprietary), July 1975.
7. Bloyd, C. N. and Singleton, N. R., "UHI Plant Internals Vibration Measurement Program and Pre and Post Hot Functional Examinations," WCAP-8516-P (Proprietary) and WCAP-8517 (Nonproprietary), April 1975.

8. Bloyd, C. N., Ciaramitaro, W. and Singleton, N. R., "Verification of Neutron Pad and 17x17 Guide Tube Designs by Preoperational Tests on the Trojan 1 Power Plant," WCAP-8766 (Proprietary) and WCAP-8780 (Nonproprietary), May 1976.
9. Takeuchi, K., et al., "MULTIFLEX-A Fortran-IV Computer Program for Analyzing Thermal-Hydraulic-Structure System Dynamics," WCAP-8708, (Proprietary) and WCAP-8079 (Nonproprietary), February 1976.
10. Fabric, S., "Computer Program WHAM for Calculation of Pressure, Velocity, and Force Transients in Liquid Filled Piping Networks," Kaiser Engineers Report No. 67-49-R, November 1967.
11. Bohm, G. J. and LaFaille, J. P., "Reactor Internals Response Under a Blowdown Accident," Procedures, First Intl. Conf. on Structural Mech. in Reactor Technology, Berlin, September 20-24, 1971.
12. Cooper, F. W. Jr., "17x17 Drive Line Components Tests - Phase IB, II, III, D-Loop Drop and Deflection," WCAP-8446 (Proprietary) and WCAP-8449 (Nonproprietary), December 1974.
13. Kraus, S., "Neutron Shielding Pads," WCAP-7870, May 1972.
14. Final Rule Modifying 10 CFR 50 Appendix A, GDC-4 dated October 27, 1987 [52 FR 41288].

SEABROOK UPDATED FSAR

TABLE 3.9(N)-9

STRESS CRITERIA FOR SAFETY-RELATED ASME CODE CLASS 2
AND CLASS 3 VALVES

<u>Design/Service Level</u>	<u>Stress Limits (Notes 1-4)</u>	<u>P_{max} (Note 5)</u>
Design & Service Level A	Valve bodies shall conform to ASME Section III	1.0
Service Level B	$\sigma_m \leq 1.1 S$ $(\sigma_m \text{ or } \sigma_L) + \sigma_b \leq 1.65 S$	1.1
Service Level C	$\sigma_m \leq 1.5 S$ $(\sigma_m \text{ or } \sigma_L) + \sigma_b \leq 1.80 S$	1.2
Service Level D	$\sigma_m \leq 2.0 S$ $(\sigma_m \text{ or } \sigma_L) + \sigma_b \leq 2.4 S$	1.5

Notes:

1. Valve nozzle (piping load) stress analysis is not required when both the following conditions are satisfied: (1) the section modulus and area of energy plane, normal to the flow, through the region defined as the valve body crotch are at least 110% of those for the piping connected (or joined) to the valve body inlet and outlet nozzles; and, (2) code allowable stress, S, for valve body material is equal to or greater than the code allowable stress, S, for connected piping material. If the valve body material allowable stress is less than that of the connected piping, the required acceptance criteria ratio shall be 110% multiplied by the ratio of the piping allowable stress to the valve allowable stress. If unable to comply with this requirement, an analysis in accordance with the design procedure for Class 1 valves is an acceptable alternate method.
2. Casting quality factor of 1.0 shall be used.
3. These stress limits are applicable to the pressure retaining boundary, and include the effects of loads transmitted by the extended structures, when applicable.
4. Design requirements listed in this table are not applicable to valve discs, stems, seat rings, or other parts of valves which are contained within the confines of the body and bonnet, or otherwise not part of the pressure boundary.
5. The maximum pressure resulting from upset, emergency or faulted conditions shall not exceed the tabulated factors listed under P_{max} times the design pressure. If these pressure limits are met the stress limits in Table 3.9(N)-9 are considered to be satisfied.

TABLE 3.9(N)-10ACTIVE PUMPS

<u>Pump</u>	<u>Item No.</u>	<u>System</u>	<u>ASME Safety Class</u>	<u>Normal Mode</u>	<u>Post LOCA Mode</u>	<u>Function</u>
Centrifugal charging pump No. 1	CS-P-2A	CVCS	2	ON/OFF	ON	High head safety injection
Centrifugal charging pump No. 2	CS-P-2B	CVCS	2	ON/OFF	ON	High head safety injection
Boric acid transfer pumps Nos. 1 and 2	CS-P-3A CS-P-3B	BRS	2	ON/OFF	OFF	Boration and safe shutdown
Residual heat removal pumps Nos. 1 and 2	RH-P-8A RH-P-8B	RHRS	2	OFF	ON	Low head safety injection and normal cooldown
Safety injec- tion pumps Nos. 1 and 2	SI-P-6A SI-P-6B	SIS	2	OFF	ON	Safety injection

Seabrook Station



**North
Atlantic**

**Updated
Final Safety
Analysis Report**

Revision 7

CHAPTER 4

REACTOR

CONTENTS

		<u>Page No.</u>
4.6.5	Evaluation of Combined Performance	4.6-2
4.6.6	References	4.6-2

CHAPTER 4REACTORTABLES

<u>Table No.</u>	<u>Title</u>
4.1-1	Reactor Design Comparison Table - Initial Core
4.1-2	Analytical Techniques in Core Design
4.1-3	Design Loading Conditions for Reactor Core Components
4.3-1	Reactor Core Description (Typical Low Leakage Cycle Design)
4.3-2	Nuclear Design Parameters (Typical Low Leakage Cycle Design)
4.3-3	Reactivity Requirements for Rod Cluster Control Assemblies
4.3-4	Axial Stability Index-Pressurized Water Reactor Core with a 12 Foot Height
4.3-5	Typical Neutron Flux Level (n/cm ² -sec) at Full Power
4.3-6	Deleted
4.3-7	Deleted
4.3-8	Deleted
4.3-9	Deleted
4.3-10	Deleted
4.4-1	Thermal and Hydraulic Comparison Table
4.4-2	Void Fractions at Nominal Reactor Conditions with Design Hot Channel Factors

CHAPTER 4REACTORFIGURES

<u>Figure No.</u>	<u>Title</u>
4.2-1	Fuel Assembly Cross Section - 17x17
4.2-2	Fuel Assembly Outline - 17x17
4.2-2A	Fuel Assembly Outline - 17x17 Original Core
4.2-2B	Fuel Assembly Outline - 17X17 Reload Fuel
4.2-3	Fuel Rod Schematic
4.2-3A	Fuel Rod Schematic - Original Core
4.2-3B	Fuel Rod Schematic - Reload Fuel
4.2-4	Plan View
4.2-5	Elevation View
4.2-6	Top Grid to Nozzle Attachment
4.2-6A	Top Grid to Nozzle Attachment - Original Core
4.2-6B	Removable Top Nozzle (RTN) Top Grid to Nozzle Attachment - Reload Fuel
4.2-7	Guide Thimble to Bottom Nozzle Joint
4.2-8	Rod Cluster Control and Drive Rod Assembly with Interfacing Components
4.2-9	Rod Cluster Control Assembly Outline
4.2-9A	Rod Cluster Control Assembly Outline - Original RCCAs
4.2-9B	Rod Cluster Control Assembly Outline - Replacement RDDAs
4.2-10	Ag-In-Cd Absorber Rod
4.2-10A	Ag-In-Cd Absorber Rod - Original RCCAs
4.2-10B	Ag-In-Cd Absorber Rod - Replacement RCCAs

CHAPTER 4REACTORFIGURES

<u>Figure No.</u>	<u>Title</u>
4.2-11	Burnable Poison Assembly
4.2-12	Burnable Poison Rod Cross Section
4.2-13	Primary Source Assembly
4.2-14	Secondary Source Assembly
4.2-14A	Secondary Source Assembly - Original Core
4.2-14B	Secondary Source Assembly - Additional Secondary Sources
4.2-15	Thimble Plug Assembly
4.3-1	Fuel Loading Arrangement
4.3-2	Production and Destruction of Higher Isotopes for Typical Low Leakage Cycle Design Fuel
4.3-3	Boron Concentration vs. Cycle Burnup for Typical Low Leakage Cycle Design
4.3-4	Integral Fuel Burnable Absorber Arrangement within an Assembly
4.3-5	Typical IFBA Placement in Low Leakage Fuel Loading Arrangement
4.3-6	Typical BOL Power Density Distribution Low Leakage Fuel Loading Arrangement - Conditions: BOL, ARO, HZP, Eq Xenon
4.3-7	Typical BOL Power Density Distribution Low Leakage Fuel Loading Arrangement - Conditions: BOL, ARO, HFP, Eq Xenon
4.3-8	Typical BOL Power Density Distribution Low Leakage Fuel Loading Arrangement - Conditions: BOL, Group 35% Inserted, HFP, Eq Xenon
4.3-9	Typical MOL power Density Distribution Low Leakage Fuel Loading Arrangement - Conditions: MOL, ARO, HFP, Eq Xenon
4.3-10	Typical EOL Power Density Distribution Low Leakage Fuel Loading Arrangement - Conditions: EOL, ARO, HFP, Eq Xenon

CHAPTER 4REACTORFIGURES

<u>Figure No.</u>	<u>Title</u>
4.3-11	Typical EOL Power Density Distribution Low Leakage Fuel Loading Arrangement - Conditions: EOL, Group D 35% Inserted, HFP, Eq Xenon
4.3-12	Typical Assembly Power Density Distribution Low Leakage Fuel Loading Arrangement - Conditions: BOL, ARO, HFP, Eq Xenon
4.3-13	Typical Assembly Power Density Distribution Low Leakage Fuel Loading Arrangement - Conditions: EOL, ARO, HFP, Eq Xenon
4.3-14	Typical Axial Power Shapes at BOL During Normal Operation for Typical Low Leakage Cycle Design
4.3-15	Typical Axial Power Shapes at EOL During Normal Operation for Typical Low Leakage Cycle Design
4.3-16	Typical Axial Power Shapes During Rodded Operation for Typical Low Leakage Cycle Design
4.3-17	Comparison of Assembly Axial Power Distribution with Core Average Axial Distribution - D Bank Slightly Inserted
4.3-18	Deleted
4.3-19	Deleted
4.3-20	Deleted
4.3-21	Normalized Maximum F_0 versus Axial Height during Normal Operation for Typical Low Leakage Cycle Design
4.3-22	Illustration of Required Overpower ΔT Setpoint for a Typical Reload core Versus Axial Flux Difference
4.3-23	Illustration of Required Overtemperature ΔT Setpoint at Nominal conditions for a Typical Reload Core versus Axial Flux Difference
4.3-24	Example of a Typical Comparison between Calculated and Measured Relative Fuel Assembly Power Distribution - Conditions: BOL, HFP, ARO

CHAPTER 4REACTORFIGURES

<u>Figure No.</u>	<u>Title</u>
4.3-25	Example of a Typical Comparison between Calculated and Measured Core Average Axial Power - Conditions; BOL, HFP, ARO
4.3-26	All-Rods-Out Nuclear Enthalpy Rise Hot Channel Factor versus Power Level
4.3-27	Typical Low Leakage Core Design Doppler Temperature Coefficient at BOL and EOL
4.3-28	Typical Low Leakage Core Design Doppler-Only Power Coefficient - BOL, & EOL
4.3-29	Typical Low Leakage Core Design Doppler-Only Power Defect - BOL, & EOL
4.3-30	Typical Low Leakage Core Design Moderator Temperature Coefficient at BOL, ARO
4.3-31	Typical Low Leakage Core Design Moderator Temperature Coefficient at EOL, ARO
4.3-32	Typical Low Leakage Core Design Moderator Temperature Coefficient at BOL versus Boron Concentration
4.3-33	Typical Low Leakage Core Design Moderator Temperature Coefficient versus cycle Burnup
4.3-34	Typical Low Leakage Core Design Total Power Coefficient at BOL & EOL
4.3-35	Typical Low Leakage Core Design Total Power Defect at BOL & EOL
4.3-36	Rod Cluster Control Assembly Pattern
4.3-37	Accident Simulated Withdrawal of Two Control Banks - EOL, HZP, Banks C and B Moving in Same Plane
4.3-38	Design Trip Curve
4.3-39	Normalized RCCA Reactivity Worth versus Fraction of Travel

CHAPTER 4REACTORFIGURES

<u>Figure No.</u>	<u>Title</u>
4.3-40	Axial Offset vs. Time - PWR Core with a 12-Ft Height and 121 Assemblies
4.3-41	XY Xenon Test Thermocouple Response - Quadrant Tilt Difference vs. Time
4.3-42	Calculated and Measured Doppler Defect and Coefficient at BOL, 2-Loop Plant, 121 Assemblies, 12-Ft Core
4.3-43	Typical Low Leakage Core Design Comparison of Calculated and Measured Boron Concentration
4.4-1	TDC vs. Reynolds Number for 26 Inch Grid Spacing
4.4-2	Normalized Radial Flow and Enthalpy Distribution at 4-Ft Elevation for Cycle 1
4.4-3	Normalized Radial Flow and Enthalpy Distribution at 8-Ft Elevation for Cycle 1
4.4-4	Normalized Radial Flow and Enthalpy Distribution at 12-Ft Elevation - Core Exit for Cycle 1
4.4-5	Deleted
4.4-6	Reactor Coolant System Temperature - Percent Power Map
4.4-7	Distribution of Incore Instrumentation

CHAPTER 4REACTOR4.1 SUMMARY DESCRIPTION

This chapter describes: (1) the mechanical components of the reactor and reactor core including the fuel rods and fuel assemblies, (2) the nuclear design, and (3) the thermal-hydraulic design.

The reactor core comprises multiple regions of fuel assemblies which are similar in mechanical design, but different in fuel enrichment. Reload fuel is similar in mechanical design to the initial core; the differences are described in the following sections. The initial core design employed three enrichments in a three-region core, whereas more enrichments may be employed for a particular refueling scheme. Fuel cycle times of six months to over eighteen months are possible, and may be employed with the core described herein.

The core is cooled and moderated by light water at a pressure of 2250 pounds per square inch absolute (psia) in the Reactor Coolant System. The moderator coolant contains boron as a neutron poison. The concentration of boron in the coolant is varied as required to control relatively slow reactivity changes including the effects of fuel burnup. Additional boron, in the form of burnable poison rods, were employed in the initial core to establish the desired initial reactivity. Integral Fuel Burnable Absorbers (IFBA) are employed in reload fuel for this purpose. IFBAs are fuel rods in which a thin zirconium diboride coating is applied directly to the fuel pellets.

Two hundred and sixty four fuel rods are mechanically joined in a square, 17x17 array to form a fuel assembly. The fuel rods are supported at intervals along their length by grid assemblies and intermediate flow mixer (IFM) grids (for the V5H (w IFMs) design) which maintain the lateral spacing between the rods throughout the design life of the assembly. The grid assembly consists of an "egg-crate" arrangement of interlocked straps. The straps contain springs and dimples for fuel rod support as well as coolant mixing vanes. The fuel rods consist of enriched uranium dioxide ceramic cylindrical pellets contained in hermetically sealed zirconium alloy tubing. All fuel rods are pressurized with helium during fabrication to reduce stresses and strains and to increase fatigue life.

The center position in the assembly is reserved for use by the incore instrumentation, while the remaining 24 positions in the array are equipped with guide thimbles joined to the grids and the top and bottom nozzles. The guide thimbles may be used as core locations for Rod Cluster Control Assemblies (RCCAs), neutron source assemblies, or burnable poison rods. Otherwise, the guide thimbles can be fitted with plugging devices to limit bypass flow.

The bottom nozzle is a bottom structural element of the fuel assembly, and admits the coolant flow to the assembly.

The top nozzle assembly is a box-like structure which serves as the upper structural element of the fuel assembly, in addition to providing a partial protective housing for the RCCA or other components.

The RCCAs each consist of a group of individual absorber rods fastened at the top end to a common hub called a spider assembly. These assemblies contain absorber material to control the reactivity of the core, and to control axial power distribution.

The nuclear design analyses and evaluations established physical locations for control rods, burnable poison rods and physical parameters such as fuel enrichments and boron concentration in the coolant. The nuclear design evaluation established that the reactor core has inherent characteristics which, together with corrective actions of the reactor control and protective systems, provide adequate reactivity control even if the highest reactivity worth RCCA is stuck in the fully withdrawn position.

The design also provides for inherent stability against diametral and azimuthal power oscillations and for control of induced axial power oscillation through the use of control rods.

The thermal-hydraulic design analyses and evaluations establish coolant flow parameters which assure that adequate heat transfer is provided between the fuel cladding and the reactor coolant. The thermal design takes into account local variations in dimensions, power generation, flow distribution and mixing. The mixing vanes incorporated in the fuel assembly spacer grid design and the VF5 (w IFMs) IFMs induce additional flow mixing between the various flow channels within a fuel assembly as well as between adjacent assemblies.

Instrumentation is provided in and out of the core to monitor the nuclear, thermal-hydraulic, and mechanical performance of the reactor and to provide inputs to automatic control functions.

Table 4.1-1 presents a comparison of the principal nuclear, thermal-hydraulic and mechanical design parameters between Seabrook Station Unit 1 and the W. B. McGuire Nuclear Station Units 1 and 2 (Docket Nos. 50-369 and 50-370).

Fuel densification was evaluated in Reference 1 which concludes that Westinghouse fuel will not densify. However fuel densification effects have been considered in safety evaluations.

The analytical techniques employed in the core design are tabulated in Table 4.1-2. The loading conditions considered in general for the core internals and components are tabulated in Table 4.1-3. Specific or limiting loads considered for design purposes of the various components are listed as follows: fuel assemblies in Subsection 4.2.1.5; neutron absorber rods, burnable poison rods, neutron source rods and thimble plug assemblies in

Subsection 4.2.1.6. The dynamic analyses, input forcing functions, and response loadings are presented in Section 3.9(N).

4.1.1 References

1. Oelrich, R. L., and Kersting, P. J., "Assessment of Clad Flattening and Densification Power Spike Factor Elimination in Westinghouse Nuclear Fuel," WCAP-13589, January 1993.

TABLE 4.1-1
(Sheet 3 of 3)

REACTOR DESIGN COMPARISON TABLE
INITIAL CORE

<u>Thermal and Hydraulic Design Parameters</u>	<u>Seabrook Unit 1</u>	<u>W. B. McGuire Units 1 & 2</u>
Rod Cluster Control Assemblies		
Neutron absorber		
Full length	Ag-In-Cd	Ag-In-Cd
Part length	---	Ag-In-Cd
Cladding Material	Austenitic SS	Type 304 SS-cold worked
Clad thickness		
Ag-In-Cd (in.)	0.0185	---
Number of clusters, full length/ part length	57/0	53/8
Number of absorber rods per cluster	24	24
Core Structure		
Core barrel, I.D./O.D. (in.)	148.0/152.5	148.0/152.5
Thermal shield	Neutron pad design	Neutron pad design
Structure Characteristics		
Core diameter, equivalent (in.)	132.7	132.7
Core height, active fuel (in.)	144.0	144.0
Reflector Thickness and Composition		
Top, water plus steel (in.)	-10	-10
Bottom, water plus steel (in.)	-10	-10
Side, water plus steel (in.)	-15	-15
H ₂ O/U molecular ratio lattice (cold)	2.41	2.41

- a. This limit is associated with the maximum value of F_Q for normal operation.
b. This is the maximum value of F_Q for normal operation.

TABLE 4.1-2
(Sheet 1 of 2)

ANALYTICAL TECHNIQUES IN CORE DESIGN

<u>Analysis</u>	<u>Technique</u>	<u>Computer Code</u>	<u>Section Referenced</u>
Mechanical design core internals loads, deflections, and stress analysis	Static and dynamic modeling	Blowdown code, FORCE, finite element, structural analysis code, and others	3.7(N) - 3.9(N) 3.9(N)
Fuel rod design			
Fuel performance characteristics (temperature, internal pressure, clad stress, etc.)	Semi-empirical thermal model of fuel rod with consideration of fuel changes, heat transfer, fission gas release, etc.	Westinghouse fuel rod design model	4.2 4.3 4.4
Nuclear design			
1. Cross sections	40 Group 2D neutron transport theory	CASMO-3 PHOENIX-P	4.3
2. 3D power dis- tributions, bo- ron concentra- tions, reacti- vity coefficients, kinetic parameters, control rod worths, reactor and fuel assembly criticality	3D 2 Group advanced	SIMULATE-3 ANC	4.3
3. Steam line break, rod ejec- tion doppler flat- tening factor	3D space-time kinetics	STAR	15.0

4.2 FUEL SYSTEM DESIGN

The plant design conditions are divided into four categories in accordance with their anticipated frequency of occurrence and risk to the public: Condition I - Normal Operation; Condition II - Incidents of Moderate Frequency; Condition III - Infrequent Incidents; and Condition IV - Limiting Faults. Chapter 15 describes bases and plant operation and events involving each condition.

The reactor is designed so that its components meet the following performance and safety criteria:

- a. The mechanical design of the reactor core components and their physical arrangement, together with corrective actions of the reactor control, protection, and emergency cooling systems (when applicable) ensure that:
 1. Fuel damage (defined as penetration of the fission product barrier i.e., the fuel rod clad) is not expected during Condition I and Condition II events. It is not possible, however, to preclude a very small number of rod failures. These are within the capability of the plant cleanup system and are consistent with plant design bases.
 2. The reactor can be brought to a safe state following a Condition III event with only a small fraction of fuel rods damaged (in any case, the fraction of fuel rods damaged must be limited to meet the dose guidelines of 10 CFR 100) although sufficient fuel damage might occur to preclude immediate resumption of operation.
 3. The reactor can be brought to a safe state and the core can be kept subcritical with acceptable heat transfer geometry following transients arising from \Condition IV events.
- b. The fuel assemblies are designed to withstand loads induced during shipping, handling, and core loading without exceeding the criteria of Subsection 4.2.1.5.
- c. The fuel assemblies are designed to accept control rod insertions to provide the required reactivity control for power operations and reactivity shutdown conditions.
- d. All fuel assemblies have provisions for the insertion of incore instrumentation necessary for plant operation.

- e. The reactor internals, in conjunction with the fuel assemblies and incore control components, direct reactor coolant through the core. This achieves acceptable flow distribution and restricts bypass flow so that the heat transfer performance requirements can be met for all modes of operation.

4.2.1 Design Bases

The 17 x 17 STD and V5H fuel rod and fuel assembly design bases are established to satisfy the general performance and safety criteria presented in Section 4.2.

The fuel rods are designed for a peak rod burnup of approximately 60,000 megawatt days per metric ton of uranium (MWd/Mtu) in the fuel cycle equilibrium condition.

Design values for the properties of the materials which comprise the fuel rod, fuel assembly and incore control components are given in Reference 2 for Zircaloy clad in Reference 16 for ZIRLO™ clad fuel. Other supplementary fuel design criteria/limits are given in Reference 20.

4.2.1.1 Cladding

a. Material and Mechanical Properties

Zircaloy-4 and ZIRLO™ combine neutron economy (low absorption cross section); high corrosion resistance to coolant, fuel, and fission products; and high strength and ductility at operating temperatures. Reference 1 documents the operating experience with Zircaloy-4 and ZIRLO™ as a clad material. Information on the material chemical and mechanical properties of the cladding is given in Reference 2 and Reference 16 with due consideration of temperature and irradiation effects.

b. Stress-Strain Limits

1. Clad Stress

The von Mises criterion is used to calculate the effective stresses. The cladding stresses under Condition I and II events are less than the Zircaloy 0.2% offset yield stress, with due consideration of temperature and irradiation effects. While the cladding has some capability for accommodating plastic strain, the yield stress has been accepted as a conservative design basis.

2. Clad Tensile Strain

The total tensile creep strain is less than 1 percent from the unirradiated condition. The elastic tensile strain during a transient is less than 1 percent from the pretransient value. These limits are consistent with proven practice.

c. Vibration and Fatigue

1. Strain Fatigue

The cumulative strain fatigue cycles are less than the design strain fatigue life. This basis is consistent with proven practice.

2. Vibration

Potential fretting wear due to vibration is prevented by design of the fuel assembly grid springs and dimples, assuring that the stress-strain limits are not exceeded during design life. Fretting of the clad surface can occur due to flow-induced vibration between the fuel rods and fuel assembly grid springs. Vibration and fretting forces vary during the fuel life due to clad diameter creepdown combined with grid spring relaxation.

d. Chemical Properties

Chemical properties of the cladding are discussed in Reference 2 for Zircaloy-4 and Reference 16 for ZIRLO™.

4.2.1.2 Fuel Material/Integral Fuel Burnable Absorber (IFBA)

a. Thermal-Physical Properties

The thermal-physical properties of UO₂ are described in Reference 2 with due consideration of temperature and irradiation effects.

Fuel pellet temperatures - The center temperature of the hottest pellet is to be below the melting temperature of the UO₂ (melting point of 5080 F (Reference 2) unirradiated and decreasing by 58°F per 10,000 MWd/Mtu). While a limited amount of center melting can be tolerated, the design conservatively precludes center melting. A calculated fuel centerline temperature of 4700 F has been selected as an overpower limit to assure no fuel melting. This provides sufficient margin for uncertainties as described in Subsection 4.4.2.9.

The normal design density of the fuel is approximately 95 percent of theoretical. Additional information on fuel properties is given in Reference 2.

b. Fuel Densification and Fission Product Swelling

The design bases and models used for fuel densification and swelling are provided in References 4 and 17.

c. Chemical Properties

References 2 and 14 provide the basis for justifying that no adverse chemical interactions occur between the fuel and adjacent cladding material.

4.2.1.3 Fuel Rod Performance

The detailed fuel rod design establishes such parameters as pellet size and density, cladding-pellet diameter gap, gas plenum size, and helium prepressurization level. The design also considers effects such as fuel density changes, fission gas release, cladding creep, and other physical properties which vary with burnup. The integrity of the fuel rods is ensured by designing to prevent excessive fuel temperatures, excessive internal rod gas pressures due to fission gas releases, and excessive cladding stresses and strains. This is achieved by designing the fuel rods to satisfy the conservative design basis in the following subsections during Condition I and II events over the fuel lifetime. For each design basis, the performance of the limiting fuel rod must not exceed the limits specified.

a. Fuel Rod Models

The basic fuel rod models and the ability to predict operating characteristics are given in Reference 17 and Subsection 4.2.3.

b. Mechanical Design Limits

Fuel rod design methodology described in Reference 18 demonstrates that clad flattening will not occur in Westinghouse fuel designs. The rod internal gas pressure will remain below the value which causes the fuel/clad diametral gap to increase due to outward cladding creep during steady state operation. The maximum rod pressure is also limited so that extensive Departure from Nucleate

internals assembly is lowered into place.

All components in the thimble plug assembly, except for the springs, are constructed from austenitic stainless steel or Inconel.

4.2.3 Design Evaluation

The fuel assemblies, fuel rods and incore control components are designed to satisfy the performance and safety criteria of the introduction to Section 4.2, the mechanical design bases of Subsection 4.2.1, and other interfacing nuclear and thermal hydraulic design bases specified in Sections 4.3 and 4.4. Effects of Conditions II, III, IV or Anticipated Transients without Trip on fuel integrity are presented in Chapter 15 or supporting topical reports.

The initial step in fuel rod design evaluation for a region of fuel is to determine the limiting rod(s). Limiting rods are defined as those rod(s) whose predicted performance provides the minimum margin to each of the design criteria. For a number of design criteria, the limiting rod is the lead burnup rod of a fuel region. In other instances it may be the maximum power or the minimum burnup rod. For the most part, no single rod will be limiting with respect to all design criteria.

After identifying the limiting rod(s), a worst-case performance evaluation is made which uses the limiting rod design basis power history and considers the effects of model uncertainties and dimensional variations. Furthermore, to verify adherence to the design criteria, the conservative case evaluation also considers the effects of postulated transient power increases which are achievable during operation consistent with Conditions I and II events. These transient power increases can affect both rod and local power levels. The analytical methods used in the evaluation result in performance parameters which demonstrate the fuel rod behavior. Examples of parameters considered include rod internal pressure, fuel temperature, clad stress, and clad strain. In fuel rod design analyses, these performance parameters provide the basis for comparison between expected fuel rod behavior and the corresponding design criteria limits.

Fuel rod and fuel assembly models used for the various evaluations are documented and maintained under an appropriate control system. Properties of materials used in the design evaluations are given in Reference 2.

4.2.3.1 Cladding

a. Vibration and Wear

Fuel rod vibrations are flow induced. The effect of the vibration on the fuel assembly and individual fuel rods is minimal. The cyclic stress range associated with deflections of such small magnitude is insignificant and has no effect on the structural integrity of the fuel rod.

The reaction force on the grid supports due to rod vibration motions is also small and is much less than the spring preload. Firm fuel clad spring contact is maintained. No significant wear of the clad or grid supports is expected during the life of the fuel assembly, based on out-of-pile flow tests performance of similarly designed fuel in operating reactors, and design analysis.

Clad fretting and fuel vibration has been experimentally investigated as shown in Reference 10.

b. Fuel Rod Internal Pressure and Cladding Stresses

The burnup dependent fission gas release model (Reference 17) is used in determining the internal gas pressures as a function of irradiation time. The plenum volume of the fuel rod has been established to ensure that the maximum internal pressure of the fuel rod will not exceed the value which would cause (1) the fuel/clad diametral gap to increase during steady state operation and (2) extensive DNB propagation to occur (see Subsection 4.2.1.3b). The clad stresses at a constant local fuel rod power are low. Compressive stresses are created by the pressure differential between the coolant pressure and the rod internal gas pressure.

Because of the prepressurization with helium, the volume average effective stresses are always less than approximately 10,000 psi at the pressurization level used in the fuel rod design. Stresses due to the temperature gradient are not included in this average effective stress because thermal stresses are, in general, negative at the clad inside diameter and positive at the clad outside diameter and their contribution to the clad volume average stress is small. Furthermore, the thermal stress decreases with time during steady state operation due to stress relaxation. The stress due to pressure differential is highest in the minimum power rod at the beginning-of-life due to low internal gas pressure. The thermal stress is highest in the maximum power rod due to steep temperature gradient.

Tensile stresses could be created once the clad has come in contact with the pellet. These stresses would be induced by the fuel pellet swelling during irradiation. Fuel swelling can result in small clad strains (< 1 percent) for expected discharge burnups but the associated clad stresses are very low because of clad creep (thermal and irradiation-induced creep). The 1 percent strain criterion is extremely conservative for fuel-swelling driven clad strain because the strain rate associated with solid fission products swelling is very slow. A detailed discussion on fuel rod performance is given in Subsection 4.2.3.3.

c. Materials and Chemical Evaluation

Zircaloy-4 and ZIRLO™ clad has a high corrosion resistance to the coolant, fuel and fission products. As shown in Reference 1, there is pressurized water reactor operating experience on the capability of Zircaloy-4 and ZIRLO™ as a clad material. Controls on fuel fabrication specify maximum moisture levels to preclude clad hydriding.

Metallographic examination of irradiated commercial fuel rods have shown occurrences of fuel/clad chemical interaction. Reaction layers of 1 mil in thickness have been observed between fuel and clad at limited points around the circumference. Metallographic data indicate that this interface layer remains very thin even at high burnup. Thus, there is no indication of propagation of the later and eventual clad penetration.

Stress corrosion cracking is another postulated phenomenon related to fuel/clad chemical interaction. Out-of-pile tests have shown that in the presence of high clad tensile stresses, large concentrations of selected fission products (such as iodine) can chemically attack the tubing and can lead to eventual clad cracking. Extensive post-irradiation examination has produced no inpile evidence that this mechanism is operative in Westinghouse produced commercial fuel.

d. Rod Bowing

Reference 11 presents the model used for evaluation of fuel rod bowing. The effects of rod bowing or DNBR are described in Subsection 4.4.2.2e. Also refer to item e in Section 4.2.

e. Consequences of Power-Coolant Mismatch

This subject is discussed in Chapter 15.

f. Creep Collapse and Creepdown

This subject and the associated irradiation stability of cladding have been evaluated using the models described in Reference 6. It has been established that the design basis of no clad collapse during planned core life can be satisfied by limiting fuel densification and by having a sufficiently high initial internal rod pressure.

g. Irradiation Stability of the Cladding

As shown in Reference 1, there is PWR operating experience on the capability of Zircaloy and ZIRLO™ as a cladding material. Extensive experience with irradiated Zircaloy-4 is summarized in Reference 2 and Reference 16 for ZIRLO™.

h. Cycling and Fatigue

A comprehensive review of the available strain fatigue models was conducted by Westinghouse as early as 1968. This review included the Langer-O'Donnell model (Reference 12), the Yao-Munse model and the Manson-Halford model. Upon completion of this review and using the results of the Westinghouse experimental programs discussed below, it was concluded that the approach defined by Langer-O'Donnell would be retained and the empirical factors of their correlation modified in order to conservatively bound the results of the Westinghouse testing program.

The Westinghouse testing program was subdivided into the following subprograms:

1. A rotating bend fatigue experiment on unirradiated Zircaloy-4 specimens at room temperature and at 725°F. Both hydrided and non-hydrided Zircaloy-4 cladding were tested.
2. A biaxial fatigue experiment in gas autoclave on unirradiated Zircaloy-4 cladding, both hydrided and non-hydrided.

3. A fatigue test program on irradiated cladding from the CVS and Yankee Core V conducted at Battelle Memorial institute.

The results of these test programs provided information on different cladding conditions including the effects of irradiation, of hydrogen levels and of temperature.

The design equations followed the concept for the fatigue design criterion according to the ASME Boiler and Pressure Vessel Code, Section III.

it is recognized that a possible limitation to the satisfactory behavior of the fuel rods in a reactor which is subjected to daily load follow is the failure of the cladding by low cycle strain fatigue. During their normal residence time in reactor, the fuel rods may be subjected to ~1000 cycles with typical changes in power level from 50% to 100% of their steady-state values.

The assessment of the fatigue life of the fuel rod cladding is subject to a considerable uncertainty due to the difficulty of evaluating the strain range which results from the cyclic interaction of the fuel pellets and cladding. This difficulty arises, for example, from such high unpredictable phenomena as pellet cracking, fragmentation, and relocation. Since early 1968, this particular phenomenon has been investigated analytically and experimentally.

Strain fatigue tests on irradiated and non-irradiated hydrided Zr-4 claddings were performed, which permitted a definition of a conservative fatigue life limit and recommendation on a methodology to treat the strain fatigue evaluation of Westinghouse reference fuel rod designs.

It is believed that the final proof of the adequacy of a given fuel rod design to meet the load follow requirements can only come from incore experiments performed on actual reactors. Experience in load follow operation dates back to early 1970 with the load follow operation of the Saxton reactor. Successful load follow operation has been performed on reactor A (>400 load follow cycles) and reactor B (>500 load follow cycles). In both cases, there was no significant coolant activity increase that could be associated with the load follow mode of operation.

4.2.3.2 Fuel Materials Considerations

Sintered, high density uranium dioxide fuel reacts only slightly with the clad at core operating temperatures and pressures. In the event of clad defects, the high resistance of uranium dioxide to attack by water protects against fuel deterioration although limited fuel erosion can

occur. As has been shown by operating experience and extensive experimental work, the thermal design parameters conservatively account for changes in the thermal performance of the fuel elements due to pellet fracture which may occur during power operation. The consequences of defects in the clad are greatly reduced by the ability of uranium dioxide to retain fission products, including those which are gaseous or highly volatile. Observations from several operating Westinghouse-supplied pressurized water reactors (Reference 9) have shown that fuel pellets can densify under irradiation to a density higher than the manufactured values. Fuel densification and subsequent settling of the fuel pellets can result in local and distributed gaps in the fuel rods. Fuel densification has been minimized by improvements in the fuel manufacturing process and by specifying a nominal 95 percent initial fuel density.

The evaluation of fuel densification effects and its consideration in fuel design are described in References 4 and 5. The treatment of fuel swelling and fission gas release are described in Reference 5.

The effects of waterlogging on fuel behavior are discussed in Subsection 4.2.3.3.

4.2.3.3 Fuel Rod Performance

In the calculation of the steady state performance of a nuclear fuel rod, the following interacting factors must be considered:

- a. Clad creep and elastic deflection
- b. Pellet density changes, thermal expansion, gas release, and thermal properties as a function of temperature and fuel burnup
- c. Internal pressure as a function of fission gas release, rod geometry, and temperature distribution.

These effects are evaluated using a fuel rod design model (Reference 17). The model modifications for time dependent fuel densification are also given in Reference 17. With the above interacting factors considered, the model determines the fuel rod performance characteristics for a given rod geometry, power history, and axial power shape. In particular, internal gas pressure, fuel and clad temperatures, and clad deflections are calculated. The fuel rod is divided into several axial sections and radially into a number of annular zones. Fuel density changes are calculated separately for each segment. The effects are integrated to obtain the internal rod pressure.

The initial rod internal pressure is selected to delay fuel/clad mechanical interaction and to avoid the potential for flattened rod formation. It is limited, however, by the design criteria for the rod internal pressure (see Subsection 4.2.1.3).

The gap conductance between the pellet surface and the clad inner diameter is calculated as a function of the composition, temperature, and pressure of the gas mixture, and the gap size or contact pressure between clad and pellet. After computing the fuel temperature for each pellet annular zone, the fractional fission gas release is assessed using an empirical model derived from experimental data (Reference 17). The total amount of gas released is based on the average fractional release within each axial and radial zone and the gas generation rate which in turn is a function of burnup. Finally, the gas released is summed over all zones and the pressure is calculated.

The code shows good agreement with a variety of published and proprietary data on fission gas release, fuel temperatures and clad deflections (Reference 17). These data include variations in power, time, fuel density, and geometry.

a. Fuel/Cladding Mechanical Interaction

One factor in fuel element duty is potential mechanical interaction of fuel and clad. This fuel/clad interaction produces cyclic stresses and strains in the clad, and these in turn consume clad fatigue life. The reduction of fuel/clad interaction is therefore a goal of design. The technology of using prepressurized fuel rods has been developed to further this objective.

The gap between the fuel and clad is sufficient to prevent hard contact between the two. However, during power operation, a gradual compressive creep of the clad onto the fuel pellet occurs due to the external pressure exerted on the rod by the coolant. Clad compressive creep eventually results in the fuel/clad contact. Once fuel/clad contact occurs, changes in power level result in changes in clad stresses and strains. By using prepressurized fuel rods to partially offset the effect of the coolant external pressure, the rate of clad creep toward the surface of the fuel is reduced. Fuel rod prepressurization delays the time at which fuel/clad contact occurs and hence significantly reduces the extent of cyclic stresses and strains experienced by the clad both before and after fuel/clad contact. These factors result in an increase in the fatigue life margin of the clad and lead to greater clad reliability. If gaps should form in the fuel stacks, clad flattening will be prevented by the rod prepressurization so that the flattening time will be greater than the fuel life time.

A two-dimensional (r, θ) finite element model has been developed to investigate the effects of radial pellet cracks on stress concentrations in the clad. Stress concentration is defined here as the difference between the maximum clad stress in the θ direction and the mean clad stress. The first case has the fuel and clad in mechanical equilibrium, and as a result the stress in the clad is close to zero. In subsequent cases, the pellet power is increased in steps and the resultant fuel thermal expansion imposes tensile stress in the clad. In addition to uniform clad stresses, stress concentrations develop in the clad adjacent to radial cracks in the pellet. These radial cracks have a tendency to open during a power increase but the frictional forces between fuel and clad oppose the opening of these cracks and result in localized increases in clad stress. As the power is further increased, large tensile stresses exceed the ultimate tensile strength of UO₂, and additional cracks develop in the fuel thus limiting the magnitude of the stress concentration in the clad.

due to the buildup of zirconium oxide and other substances. Secondary failures which have been observed in defective rods are attributed to hydrogen embrittlement of the cladding. Post-irradiation examinations point to the hydriding failure mechanism rather than a waterlogging mechanism; the secondary failures occur as axial cracks or blisters in the cladding and are similar regardless of the primary failure mechanism. Such cracks do not result in flow blockage, or increase the effects of any postulated transients. More information is provided in Reference 19.

e. Potentially Damaging Temperature Effects During Transients

The fuel rod experiences many operational transients (intentional maneuvers) during its residence in the core. A number of thermal effects must be considered when analyzing the fuel rod performance.

The clad can be in contact with the fuel pellet at some time in the fuel lifetime. Clad/pellet interaction occurs if the fuel pellet temperature is increased after the clad is in contact with the pellet. Clad/pellet interaction is discussed in Subsection 4.2.3.3a.

The potential effects of operation with waterlogged fuel are discussed in Subsection 4.2.3.3d, which concluded that waterlogging is not a concern during operational transients.

Clad flattening, as shown in Reference 6, has been observed in some operating Westinghouse supplied power reactors. Thermal expansion (axial) of the fuel rod stack against a flattened section of clad could cause failure of the clad. This is no longer a concern because clad flattening is precluded by design during the fuel residence in the core (see Subsection 4.2.3.1).

Potential differential thermal expansion between the fuel rods and the guide thimbles during a transient is considered in the design. Excessive bowing of the fuel rods is precluded because the grid assemblies allow axial movement of the fuel rods relative to the grids. Specifically, thermal expansion of the fuel rods is considered in the grid design so that axial loads imposed on the fuel rods during a thermal transient will not result in excessively bowed fuel rods.

f. Fuel Element Burnout and Potential Energy Release

As discussed in Subsection 4.4.2.2, the core is protected from DNB over the full range of possible operating conditions. In the extremely unlikely event that DNB should occur, the clad temperature will rise due to degradation in heat transfer caused by steam blanketing at the rod surface. During this time, some chemical reaction between the cladding and the coolant will occur. However,

because of the relatively good film boiling heat transfer following DNB, and the short time of the transient, the energy release resulting from this reaction is insignificant compared to the power produced by the fuel.

g. Coolant Flow Blockage Effects on Fuel Rods

This evaluation is presented in Subsection 4.4.4.7.

4.2.3.4 Spacer Grids

The coolant flow channels are established and maintained by the structure composed of grids and guide thimbles. The lateral spacing between fuel rods is provided and controlled by the support dimples of adjacent grid cells. Contact of the fuel rods on the dimples is maintained by the clamping force of the grid springs. Lateral motion of the fuel rods is opposed by the spring force and the internal moments generated between the spring and the support dimples. Grid testing is discussed in Reference 13.

As shown in Reference 13, grid crushing tests and seismic and loss-of-coolant accident evaluations show that the grids will maintain a geometry that is capable of being cooled under the worst-case accident Condition IV event.

4.2.3.5 Fuel Assembly

a. Stresses and Deflections

The fuel assembly component stress levels are limited by the design. For example, stresses in the fuel rod due to axial thermal expansion and zirconium alloy irradiation growth are limited by the relative motion of the rod as it slips over the grid spring and dimple surfaces. Clearances between the fuel rod ends and nozzles are provided so that zircaloy irradiation growth does not result in rod end interferences. Stresses in the fuel assembly caused by tripping of the Rod Cluster Control Assembly have little influence on fatigue because of the small number of events during the life of an assembly. Assembly components and prototype fuel assemblies made from production parts have been subjected to structural tests to verify that the design bases requirements are met.

The fuel assembly design loads for shipping and handling have been established at 4g axial and 6g lateral. Accelerometers are permanently placed into the shipping cask to monitor and detect fuel assembly accelerations that would exceed the criteria. Past history and experience have indicated that loads which exceed the allowable limits rarely occur. Exceeding the limits requires reinspection of the fuel assembly for damage. Tests on various fuel assembly components such as the grid assembly, sleeves, inserts and structure joints have been performed to assure that the shipping design limits

- g. Survey of radiation and contamination levels of new fuel assembly.

Surveillance of fuel and reactor performance is routinely conducted. Power distribution is monitored using excore fixed and incore detectors. Coolant activity and chemistry are followed to permit early detection of any fuel clad defects.

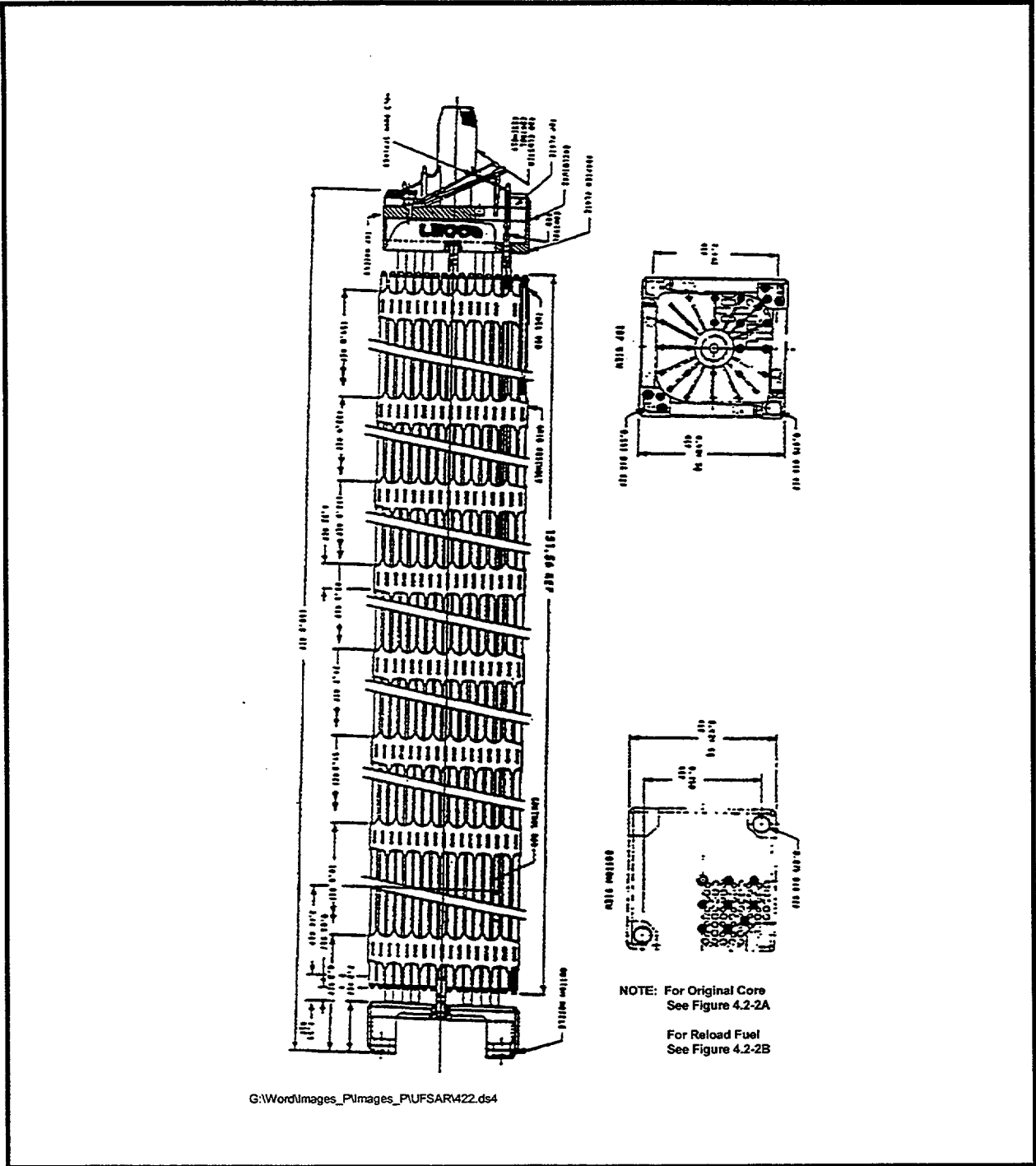
Visual irradiated fuel inspections will be conducted as necessary during each refueling. Selected fuel assemblies may be inspected for fuel rod failure, structural integrity, crud deposition, rod bow and other irregularities. Fuel assemblies will be selected for inspection based upon performance history and recommendations made by the fuel supplier.

The fuel inspection program will be expanded to include more fuel assemblies or greater detail of examination if high coolant activity is experienced during operation, irregularities are noted in fuel performance, irregularities are noted during routine inspections, or if a new fuel design is incorporated.

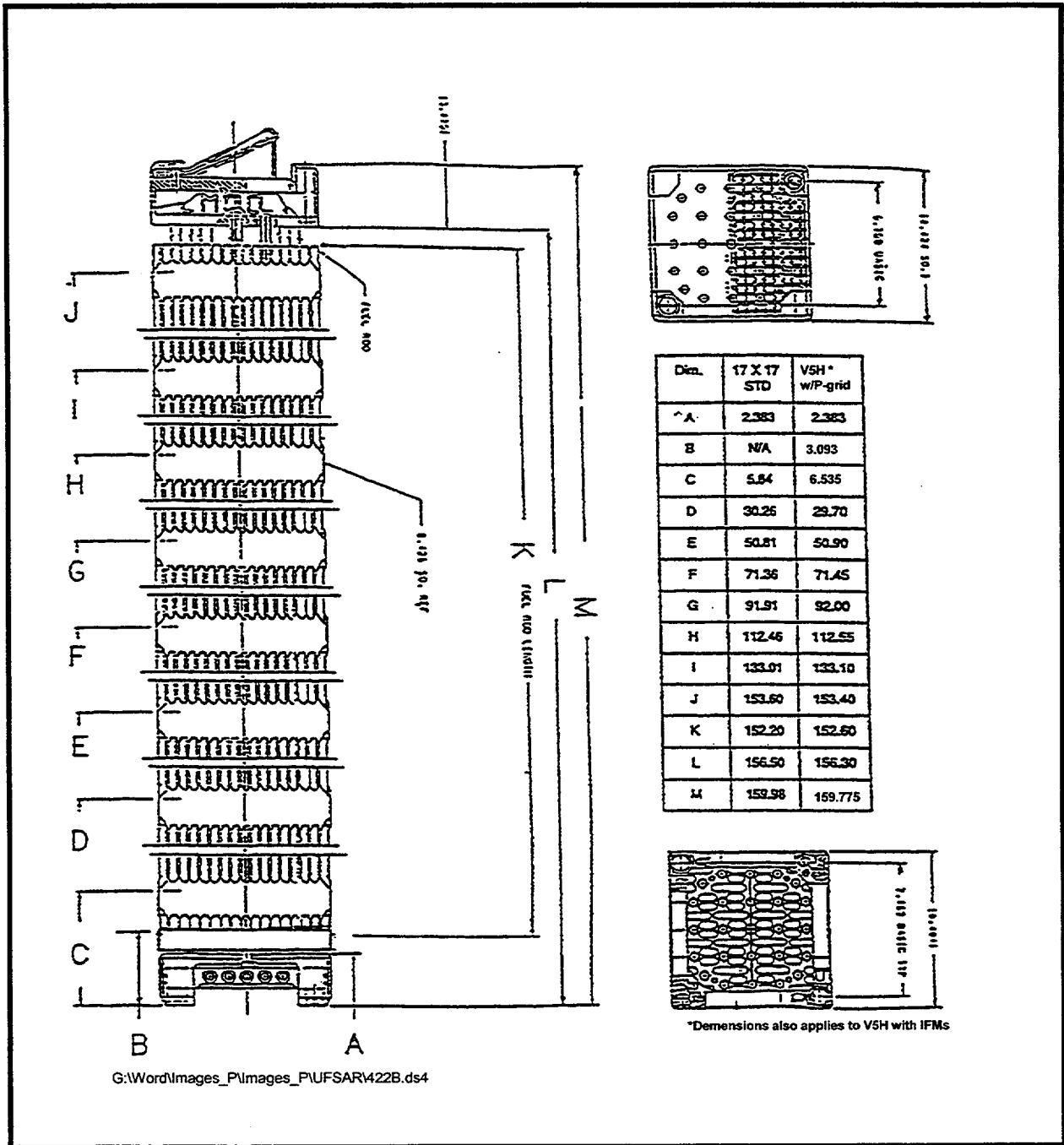
4.2.5 References

1. Slagle, W. H., "Operational Experience with Westinghouse Cores," WCAP-8183, (latest revision).
2. Beaumont, M. D., and Iorii, J. A., "Properties of Fuel and Core Component Materials," WCAP-9179, Revision 1 (Proprietary), July 1978.
3. Not used
4. Hellman, J. M. (Ed.), "Fuel Densification Experimental Results and Model for Reactor Application," WCAP-8218-P-A (Proprietary) and WCAP-8219-A (Nonproprietary), March 1975.
5. Not used
6. George, R. A., Lee, Y. C. and Eng. G. H., "Revised Clad Flattening Model," WCAP-8377 (Proprietary) and WCAP-8381 (Nonproprietary), July 1974.
7. Risher, D. H., et al., "Safety Analysis for the Revised Fuel Rod Internal Pressure Design Basis," WCAP-8963 (Proprietary), November 1976 and WCAP-8964 (Nonproprietary), August 1977.
8. Cohen, J., "Development and Properties of Silver Base Alloys as Control Rod Materials for Pressurized Water Reactors," WAPD-214, December 1959.

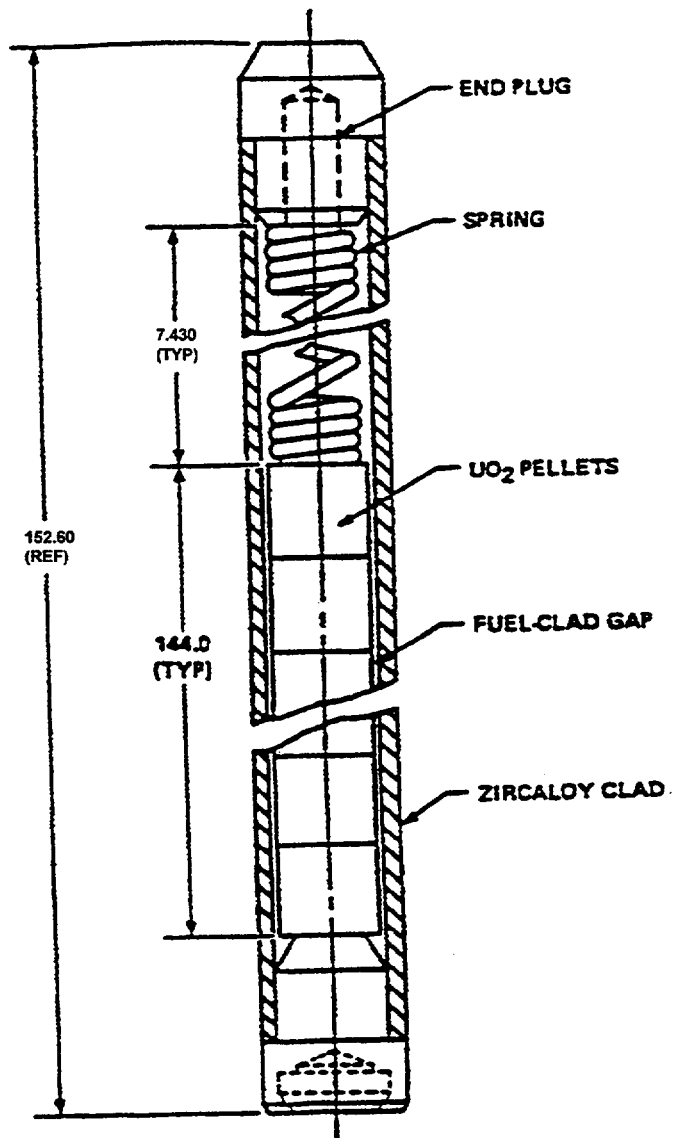
9. Eggleston, F. T., "Safety-Related Research and Development for Westinghouse Pressurized Water Reactors, Program Summaries-Winter 1977-Summer 1978," WCAP-8768, Revision 2, October 1978.
10. Demario, E. E., "Hydraulic Flow Test of the 17x17 Fuel Assembly," WCAP-8278 (Proprietary) and WCAP-8279 (Nonproprietary), February 1974.
11. Skaritka, J., et al., "Fuel Rod Bow Evaluation," WCAP-8691, Revision 1 (Proprietary) and WCAP-8692, Revision 1 (Nonproprietary), July 1979.
12. O'Donnell, W. J. and Langer, B. F., "Fatigue Design Basis for Zircaloy Components," Nuclear Science and Engineering 20 1-12, 1964.
13. Gesinski, L., and Chiang, D., "Safety Analysis of the 17x17 Fuel Assembly for Combined Seismic and Loss-of-Coolant Accident," WCAP8236 (Proprietary) and WCAP-8288 (Nonproprietary) December 1973.
14. Davidson, S. L. (Ed.), et. al., "VANTAGE-5 Fuel Assembly, Reference Core Report," WCAP-10444-P-A, Westinghouse Electric Corporation, September 1985.
15. Davidson, S. L. (Ed.), et. al., "VANTAGE-5H Fuel Assembly," WCAP-10444-P-A Addendum 2-A, Westinghouse Electric Corporation, April 1988.
16. Davidson, S. L. and Ryan, T.L., "VANTAGE+ Fuel Assembly Reference Core Report," WCAP-12610-P-A and Appendices A through D, Westinghouse Electric Corporation, April 1995.
17. Weiner, R. A., et al., "Improved Fuel Performance Models for Westinghouse Fuel Rod Design and Safety Evaluations," WCAP-10851-P-A (Proprietary) and WCAP-11873-A (Non-Proprietary), August 1988.
18. Kersting, P. J., et al., "Assessment of Clad Flattening and Densification Power Spike Factor Elimination in Westinghouse Nuclear Fuel," WCAP-13589-A, March 1995.
19. Stephan, L. A., "The Effects of Cladding Material and Heat Treatment on the Response of Water Logged UO₂ Fuel Rods to Power Bursts," IN-ITR 1970.
20. Davidson, S. L., "Westinghouse Fuel Criteria Evaluation Process," WCAP-12488-A, October 1994.



SEABROOK STATION UPDATED FINAL SAFETY ANALYSIS REPORT	Fuel Assembly Outline - 17 x 17	
	REV. 07	FIGURE 4.2-2



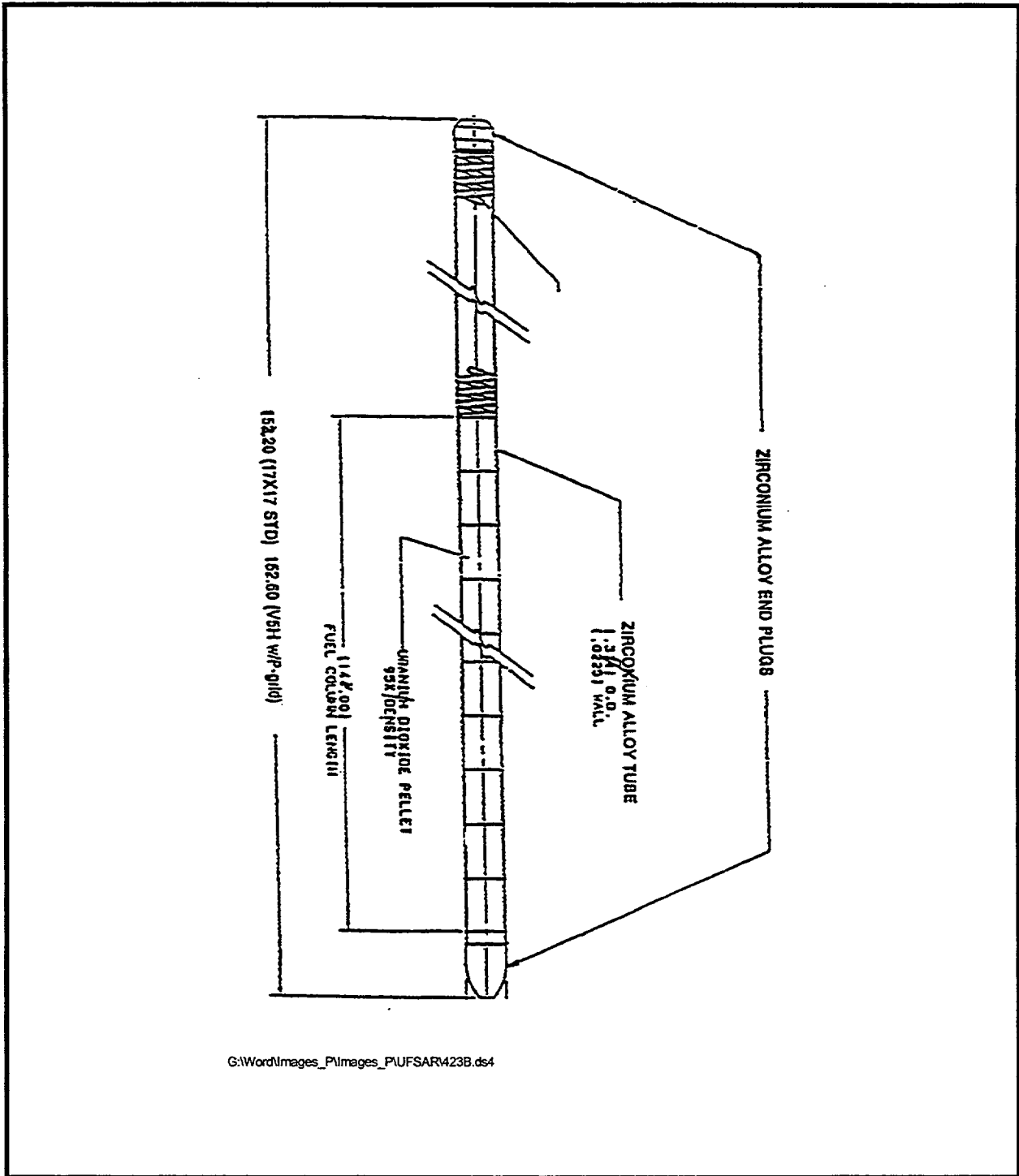
SEABROOK STATION UPDATED FINAL SAFETY ANALYSIS REPORT	Fuel Assembly Outline 17 x 17 Reload Fuel	
	REV. 07	FIGURE 4.2-2B



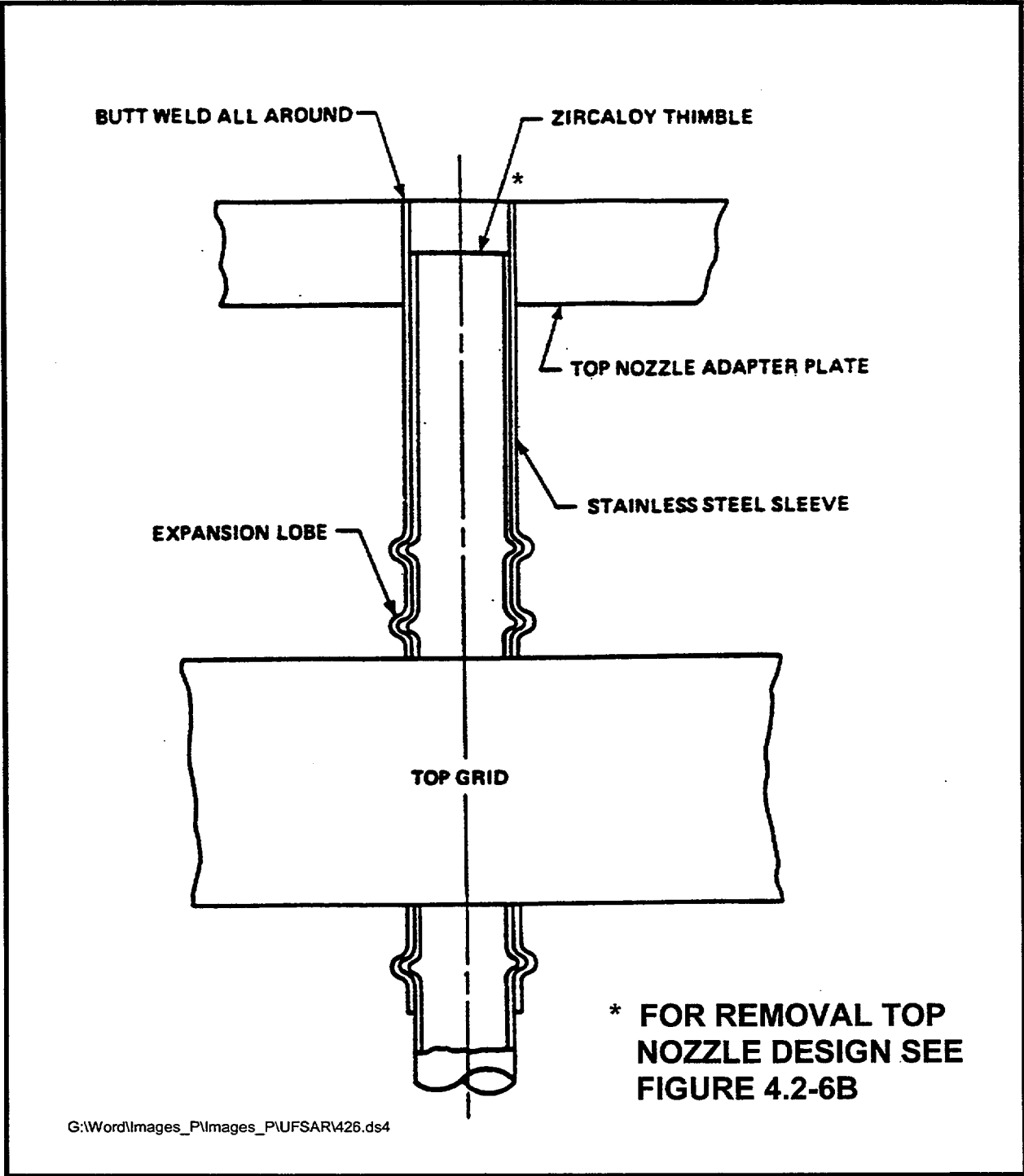
SPECIFIC DIMENSIONS DEPEND ON DESIGN VARIABLES SUCH AS
PRE-PRESSURIZATION, POWER HISTORY, AND DISCHARGE BURNUP

G:\Word\Images_P\Images_P\UFSAR\423.ds4

SEABROOK STATION UPDATED FINAL SAFETY ANALYSIS REPORT	Fuel Rod Schematic	
	REV. 07	FIGURE 4.2-3



SEABROOK STATION UPDATED FINAL SAFETY ANALYSIS REPORT	Fuel Rod Schematic Reload Fuel	
JB 6/22/01	REV. 07	FIGURE 4.2-3B

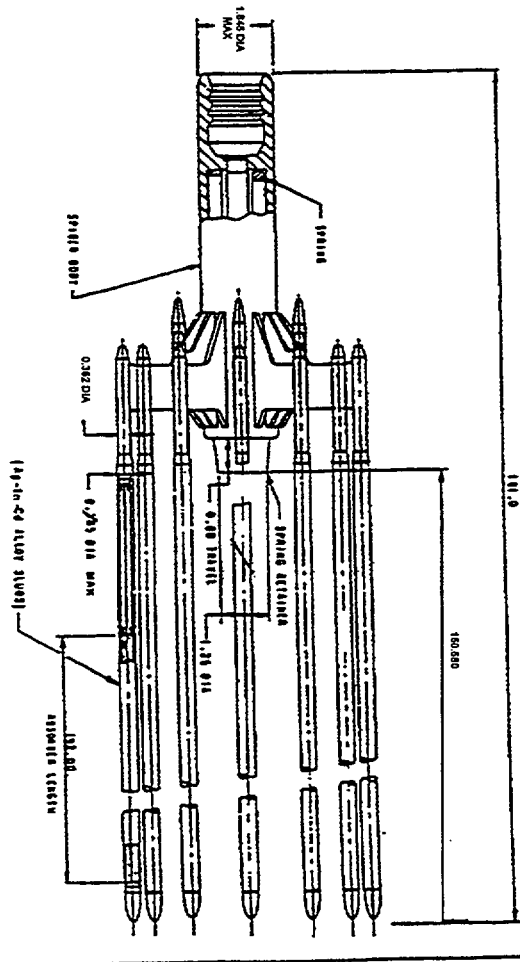
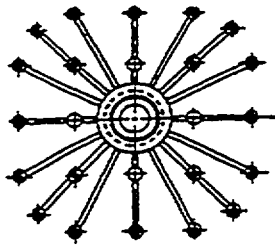


SEABROOK STATION UPDATED
FINAL SAFETY ANALYSIS REPORT

Top Grid to Nozzle Attachment

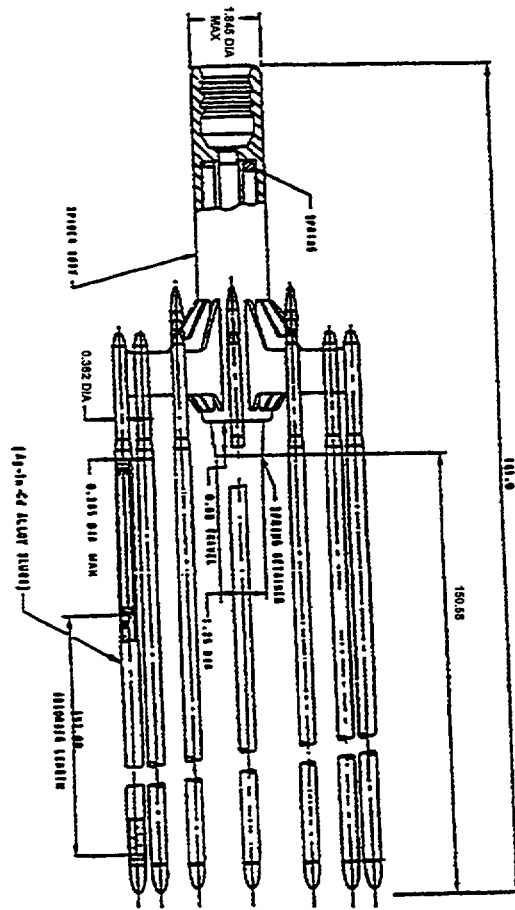
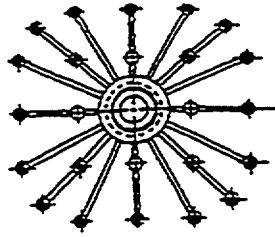
REV. 07

FIGURE 4.2-6



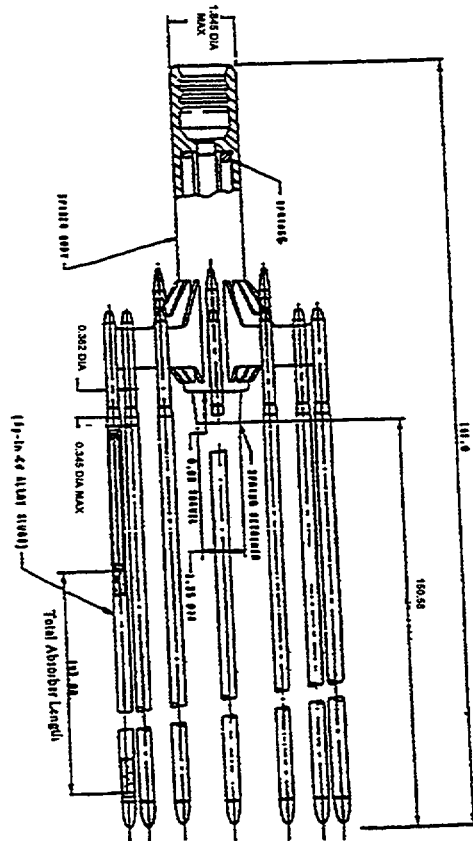
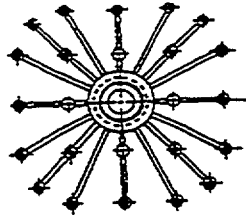
G:\Word\Images_P\Images_P\UFSAR\429.ds4

SEABROOK STATION UPDATED FINAL SAFETY ANALYSIS REPORT	Rod Cluster Control Assembly Outline	
	REV. 07	FIGURE 4.2-9



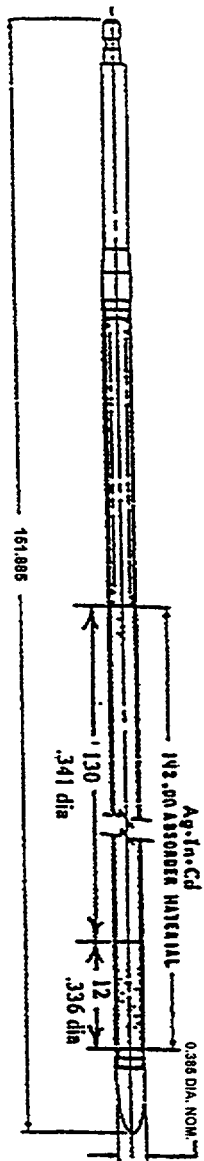
G:\Word\Images_P\Images_P\UFSAR\429A.ds4

SEABROOK STATION UPDATED FINAL SAFETY ANALYSIS REPORT	Rod Cluster Control Assembly Outline Original RCCAs	
	REV. 07	FIGURE 4.2-9A



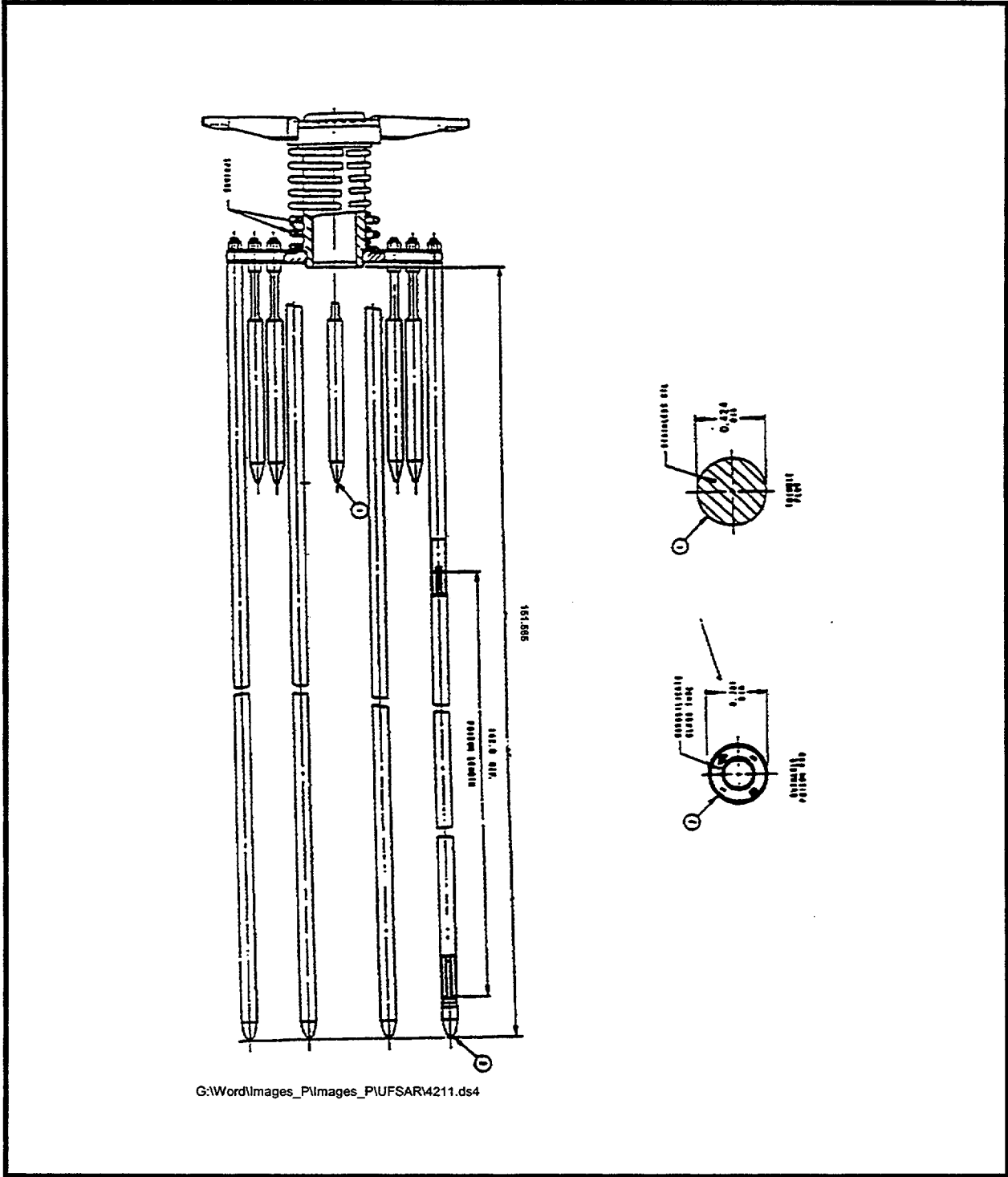
G:\Word\Images_P\Images_P\UFSAR\429B.ds4

SEABROOK STATION UPDATED FINAL SAFETY ANALYSIS REPORT	Rod Cluster Control Assembly Outline Replacement RCCAs	
	REV. 07	FIGURE 4.2-9B

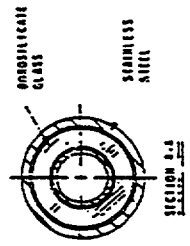
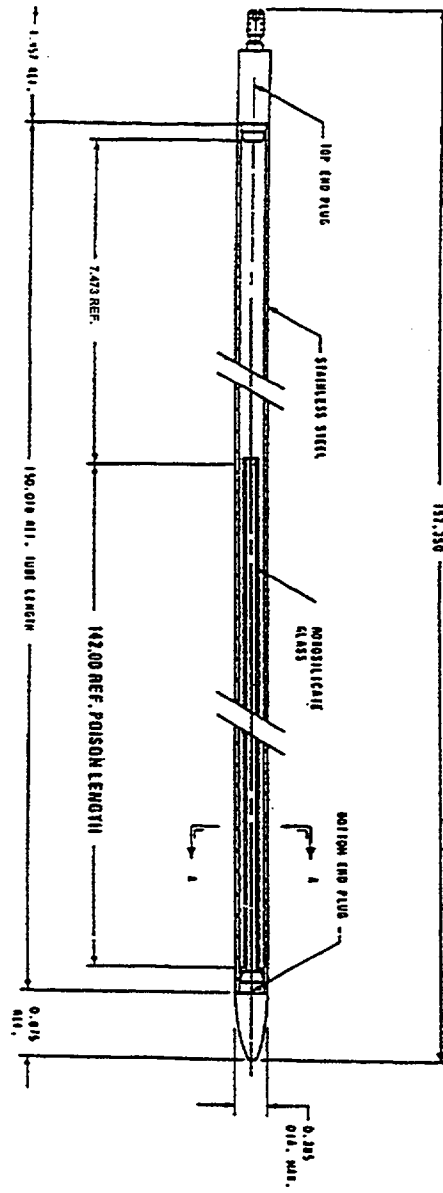


G:\Word\Images_P\Images_PUFSAR\4210B.ds4

SEABROOK STATION UPDATED FINAL SAFETY ANALYSIS REPORT	Ag-In-Cd Absorber Rod Replacement RCCAs	
	REV. 07	FIGURE 4.2.10B

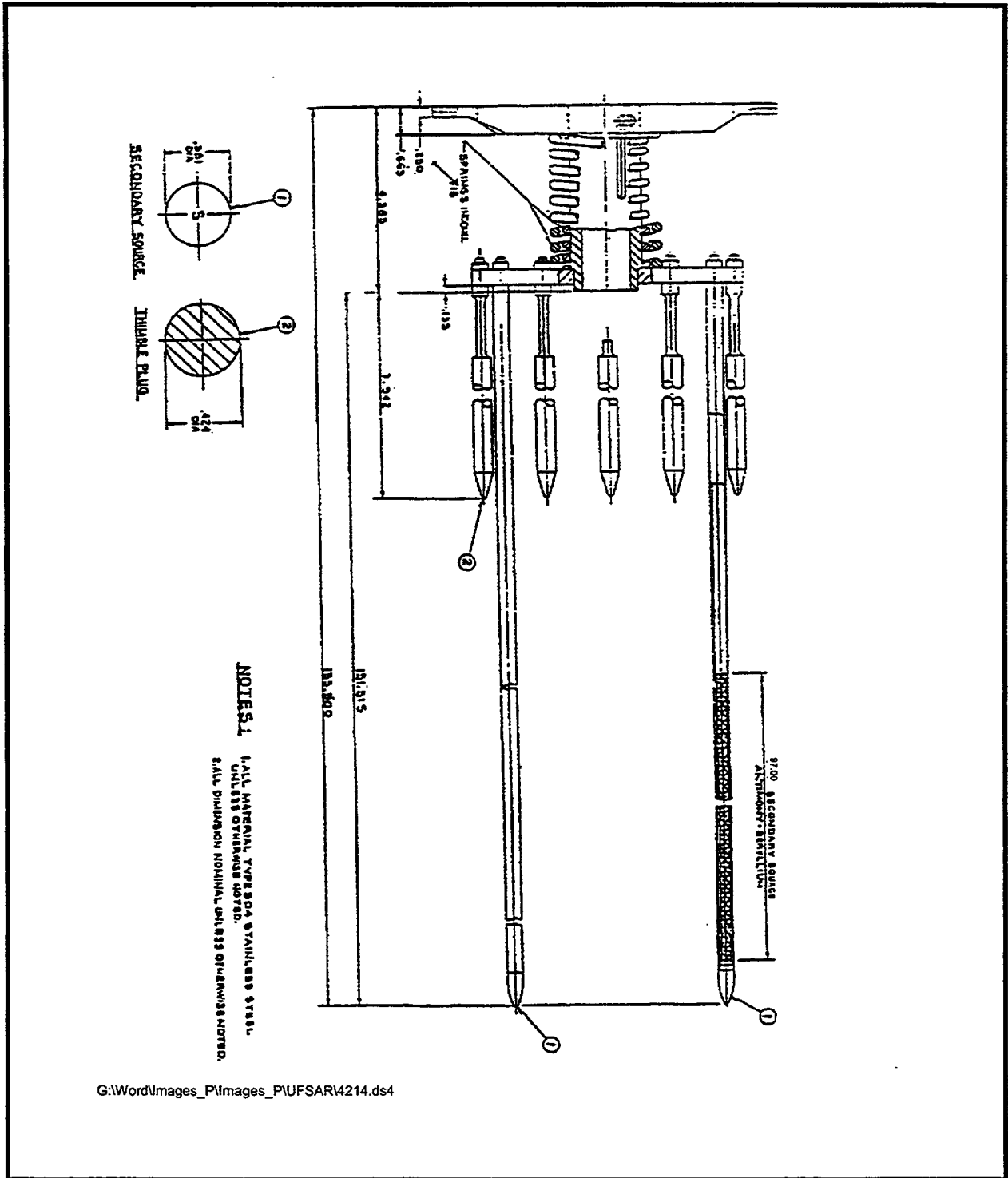


SEABROOK STATION UPDATED FINAL SAFETY ANALYSIS REPORT	Burnable Poison Assembly	
	REV. 07	FIGURE 4.2-11



G:\Word\images_P\images_P\UFSAR\4212.ds4

SEABROOK STATION UPDATED FINAL SAFETY ANALYSIS REPORT	Burnable Poison Rod Cross Section	
	REV. 07	FIGURE 4.2-12



G:\Word\Images_P\Images_P\UFSAR4214.ds4

SEABROOK STATION UPDATED FINAL SAFETY ANALYSIS REPORT	Secondary Source Assembly	
	REV. 07	FIGURE 4.2-14

4.3-2 are chosen to encompass the best estimate reactivity coefficients, including the uncertainties given in Subsection 4.3.3.3 over appropriate operating conditions calculated for this cycle and the expected values for the subsequent cycles. The most positive as well as the most negative values are selected to form the design basis range used in the transient analysis. A direct comparison of the best estimate and design limit values shown in Table 4.3-2 can be misleading since in many instances, the most conservative combination of reactivity coefficients is used in the transient analysis even though the extreme coefficients assumed may not simultaneously occur at the condition of lifetime, power level, temperature and boron concentration assumed in the analysis. The need for re-evaluation of any accident in a subsequent cycle is contingent upon whether or not the coefficients for that cycle fall within the identified range used in the analysis presented in Chapter 15 with due allowance for the calculational uncertainties given in Subsection 4.3.3.3. Control rod requirements are given in Table 4.3-3 for the core described and for a hypothetical equilibrium cycle since these are markedly different. These latter numbers are provided for information only and their validity in a particular cycle would be an unexpected coincidence.

4.3.2.4 Control Requirements

To ensure the shutdown margin stated in the Technical Specifications and the Core Operating Limits Report under conditions where a cooldown to ambient temperature is required, concentrated soluble boron is added to the coolant. Boron concentrations for several core conditions are listed in Table 4.3-2. For all core conditions including refueling, the boron concentration is well below the solubility limit. The Rod Cluster Control Assemblies are employed to bring the reactor to the hot shutdown condition. The minimum required shutdown margin is given in the Technical Specifications.

The ability to accomplish the shutdown for hot conditions is demonstrated in Table 4.3-3 by comparing the difference between the Rod Cluster Control Assembly reactivity available with an allowance for the worst stuck rod with that required for control and protection purposes. The shutdown margin includes an allowance of 10 percent for analytic uncertainties (see Subsection 4.3.2.4i). The largest reactivity control requirement appears at the EOL when the moderator temperature coefficient reaches its peak negative value as reflected in the larger power defect.

The control rods are required to provide sufficient reactivity to account for the power defect from full power to zero power and to provide the required shutdown margin. The reactivity addition resulting from power reduction consists of contributions from Doppler, variable average moderator temperature, flux redistribution, and reduction in void content as discussed below.

a. Doppler

The Doppler effect arises from the broadening of U-238 and Pu-240 resonance peaks with an increase in effective pellet temperature. This effect is most noticeable over the range of zero power to full power due to the large pellet temperature increase with power generation.

b. Variable Average Moderator Temperature

When the core is shutdown to the hot, zero power condition, the average moderator temperature changes from the equilibrium full load value determined by the steam generator and turbine characteristics (steam pressure, heat transfer, tube fouling, etc.) to the equilibrium no load value, which is based on the steam generator shell side design pressure. The design change in temperature is conservatively increased by 7.6°F to account for the control dead band and measurement errors.

c. Redistribution

During full power operation, the coolant density decreases with core height, and this, together with partial insertion of control rods, results in less fuel depletion near the top of the core. Under steady state conditions, the relative power distribution will be slightly asymmetric towards the bottom of the core. On the other hand, at Hot Zero Power conditions, the coolant density is uniform up the core, and there is no flattening due to the Doppler. The result will be a flux distribution which at zero power can be skewed toward the top of the core. The reactivity insertion due to the skewed distribution is calculated with an allowance for effects of xenon distribution.

d. Void Content

A small void content in the core is due to nucleate boiling at full power. The void collapse coincident with power reduction makes a small reactivity contribution.

e. Rod Insertion Allowance

At full power, the control bank is operated within a prescribed band of travel to compensate for small periodic changes in boron concentration, changes in temperature and very small changes in the xenon concentration not compensated for by a change in boron concentration. When the control bank reaches either limit of this band, a change in boron concentration is required to compensate for additional reactivity changes. Since the insertion limit is set by

2. Radial Power Distribution

The core described herein is calculated to be stable against X-Y xenon induced oscillations at all times in life.

The X-Y stability of large PWRs has been further verified as part of the startup physics test program for cores with 193 fuel assemblies. The measured X-Y stability of the cores with 157 and 193 assemblies was in good agreement with the calculated stability as discussed in Subsections 4.3.2.7d and 4.3.2.7e. In the unlikely event that X-Y oscillations occur, backup actions are possible and would be implemented if necessary, to increase the natural stability of the core as discussed in the Technical Specifications. This is based on the fact that several actions could be taken to make the moderator temperature coefficient more negative, which will increase the stability of the core in the X-Y plane.

Provisions for protection against nonsymmetric perturbations in the X-Y power distribution that could result from equipment malfunctions are made in the protection system design. This includes control rod drop, rod misalignment and asymmetric loss of coolant flow.

4.3.2.8 Vessel Irradiation

A brief review of the methods and analyses used in the determination of neutron and gamma ray flux attenuation between the core and the pressure vessel is given below. A more complete discussion on the pressure vessel irradiation and surveillance program is given in Section 5.3.

The materials that serve to attenuate neutrons originating in the core and gamma rays from both the core and structural components consist of the core baffle, core barrel, neutron pads and associated water annuli, all of which are within the region between the core and the pressure vessel.

In general, few group neutron diffusion theory codes are used to determine fission power density distributions within the active core, and the accuracy of these analyses is verified by incore measurements on operating reactors. Region and rodwise power sharing information from the core calculations is then used as source information in two-dimensional S_n transport calculations which compute the flux distributions throughout the reactor.

The neutron flux distribution and spectrum in the various structural components varies significantly from the core to the pressure vessel. Representative values of the neutron flux distribution and spectrum are presented in Table 4.3-5. The values listed are based on time averaged equilibrium cycle reactor core parameters and power distributions; and, thus, are suitable for long-term nvt projections and for correlation with radiation damage estimates.

As discussed in Section 5.3, the irradiation surveillance program utilizes actual test samples to verify the accuracy of the calculated fluxes at the vessel.

4.3.3 Analytical Methods

Calculations required in nuclear design consist of three distinct types, which are performed in sequence:

1. Determination of effective fuel temperatures
2. Generation of macroscopic few-group parameters
3. Space-dependent, few-group diffusion calculations.

These calculations are carried out by computer codes which can be executed individually; however, most of the codes required have been linked to form an automated design sequence which minimizes design time, avoids errors in transcription of data, and standardizes the design methods.

4.3.3.1 Fuel Temperature (Doppler) Calculations

Temperatures vary radially within the fuel rod, depending on the heat generation rate in the pellet, the conductivity of the materials in the pellet, gap, and clad, and the temperature of the coolant.

The fuel temperatures for use in nuclear design Doppler calculations are obtained from the fuel rod design model described in Subsection 4.2.1.3 which considers the effect of radial variation of pellet conductivity, expansion-coefficient and heat generation rate, elastic deflection of the clad, and a gap conductance which depends on the initial fill gap, the hot open gap dimension, fuel swelling, fission gas release, and plastic clad deformation. Further gap closure occurs with burnup and accounts for the decrease in Doppler defect with burnup.

4.3.3.2 Macroscopic Group Constants

Macroscopic few-group constants and analogous microscopic cross sections (needed for feedback and microscopic depletion calculations) are generated for fuel cells by a recent version of the CASMO or PHOENIX-P (References 1 and 11) code, which provide burnup dependent cross sections. Fast and thermal cross section library tapes contain microscopic cross sections taken from the ENDF/B-VI library, with a few exceptions where other data provided good agreement with critical experiments, isotopic measurements, and plant critical boron values. The effect on the unit fuel cell of nonlattice components in the fuel assembly is obtained by supplying an appropriate volume fraction of these materials in an extra region which is homogenized with the unit cell in the fast and thermal flux

calculations. In the thermal calculation, the fuel rod, clad, and moderator are homogenized by energy-dependent disadvantage factors derived from an analytical fit to integral transport theory results.

Group constants for control rods, IFBA rods, guide thimbles, instrument thimbles and interassembly gaps are generated in a manner analogous to the fuel cell calculation. Baffle and reflector group constants are taken from two dimensional PHOENIX-P models of the core and baffle/reflector internals.

Nodal group constants are obtained by a flux-volume homogenization of the fuel cells, burnable poison cells, guide thimbles, instrumentation thimbles, interassembly gaps, and control rod cells from one mesh internal per cell X-Y unit fuel assembly diffusion calculations.

Validation of the cross section method is based on analysis of isotopic data, plant critical boron (C_B) values at HZP, BOL and at HFP as a function of burnup as shown in Reference 11. Control rod worth measurements are also shown in Reference 11.

Confirmatory critical experiments on burnable poisons are described in Reference 1.

4.3.3.3 Spatial Three Dimensional Calculations

Spatial three dimensional calculations consist primarily of two-group advanced nodal calculations using a version of ANC (Reference 12) or SIMULATE (Reference 2). Full three dimensional calculations are performed using four radial nodes per assembly and twenty four axial nodes. Pin power reconstruction is performed within the code to determine discrete pin powers and detailed detector reaction rates. The code also contains means to follow the core spectral history to compensate for depletion of nodes not at the general conditions used in generating the cross sections.

Validation of ANC and SIMULATE calculations is associated with the validation of the group constants themselves, as discussed in Subsection 4.3.3.2. Validation of the Doppler calculations is associated with the fuel temperature validation discussed in Subsection 4.3.3.1. Validation of the moderator coefficient calculations is obtained by comparison with plant measurements at Hot Zero Power conditions.

Validation of the spatial codes for calculating power distributions involves the use of incore and excore detectors and is discussed in Subsection 4.3.2.2g.

4.3.4 References

1. A.S. DiGiovine, K.B. Spinney, D.G. Napolitano, J. Pappas, "CASMO-3G Validation", YAEC-1363, April, 1988.
2. A.S. DiGiovine, J.P. Gorski, M.A. Tremblay, "SIMULATE-3 Validation and Verification", YAEC-1659, September, 1998.
3. "Westinghouse Anticipated Transients Without Reactor Trip Analysis", WCAP-8330, August 1974.
4. ATWS Final Rule - Code of Federal Regulations 10 CFR 50.62 and Supplementary Information Package, "Reduction of Risk from Anticipated Transient without Scram (ATWS) Events for Light Water-Cooled Nuclear Power Plants."
5. Oelrich, R. L. and Kersting, P. J., "Assessment of Clad Flattening and Densification Power Spike Factor Elimination in Westinghouse Nuclear Fuel," WCAP-13589, January 1993.
6. Meyer, R.O., "The Analysis of Fuel Densification," Division of Systems Safety, USNRC, NUREG-0085, July 1976.
7. Guimond, P. J., et al., "Core Thermal Limit Protection Function Setpoint Methodology for Seabrook Station", YAEC-1854-P-A, October 1992.
8. J.P. Gorski, "Seabrook Station Unit 1 Fixed Incore Detector System Analysis", YAEC-1855-P-A, October 1992.
9. Cermek, J. O., et al., "Pressurized Water Reactor pH - Reactivity Effect Final Report," WCAP-3696-8 (EURAE-2074), October 1968.
10. Moore, J. S., Power Distribution Control of Westinghouse Pressurized Water Reactors," WCAP-7811, December 1971.
11. Nguyen, T. Q., et. al. "Qualification of the PHOENIX-P/ANC Nuclear Design System for Pressurized Water Reactor Cores", WCAP-11596-P-A, June 1998 (Westinghouse Proprietary)
12. Liu, Y. S, Meliksetion, A, Rathkopt, J. A., Little D. C., Nakano, F., Poploski, M. J., "ANC-A Westinghouse Advanced Nodal Computer Code", WCAP-10965-P-A, September, 1986 (Westinghouse Proprietary)

13. Poncelet, C. G. and Christie, A. M., "Xenon-Induced Spatial Instabilities in Large PWRs," WCAP-3680-20, (EURAECE-1974) March 1968.
14. Skogen, F. B. and McFarlane, A. F., "Control Procedures for Xenon-Induced X-Y Instabilities in Large PWRs," WCAP-3680-21, (EURAECE-2111), February 1969.
15. Skogen, F. B. and McFarlane, A. F., "Xenon-Induced Spatial Instabilities in Three-Dimensions," WCAP-3680-22 (EURAECE-2116), September 1969.
16. Lee, J. C., et al., "Axial Xenon Transient Tests at the Rochester Gas and Electric Reactor," WCAP-7964, June 1971.

TABLE 4.3-2
(Sheet 1 of 2)

NUCLEAR DESIGN PARAMETERS
(Typical Low Leakage Cycle Design)

<u>Core Average Linear Power, kW/ft. including densification effects</u>	5.44	
<u>Total Heat Flux Hot Channel Factor, F_Q</u>	2.50	
<u>Nuclear Enthalpy Rise Hot Channel Factor, $F_{\Delta H}^N$</u>	1.65	
<u>Reactivity Coefficients⁺</u>	Design Limits	Best Estimate
Doppler-only Power, Lower Curve Coefficients, pcm/% power ⁺⁺	-19.4 to -12.6	-15 to -11
(See Figure 15.1-3, Sh. 1), Upper Curve	-9.55 to -6.05	-14 to -8.5
Doppler Temperature Coefficient pcm/ $^{\circ}F^{++}$	-2.9 to -1.2	-2.0 to -1.3
Moderator Temperature Coefficient, pcm/ $^{\circ}F^{++}$	+5. to -47	+2. to -39.
Boron Coefficient, pcm/ppm ⁺⁺	-16 to -7	-14.5 to -7.3
Rodded Moderator Density, pcm/gm/cc ⁺⁺	$\leq 0.50 \times 10^5$	$\leq 0.28 \times 10^5$
<u>Delayed Neutron Fraction and Lifetime</u>		
β_{eff} BOL, (EOL)	0.0075, (0.0044)	
<u>Control Rods</u>		
Rod Requirements	See Table 4.3-3	
Maximum Bank Worth, pcm	< 2000	
Maximum Ejected Rod Worth	See Chapter 15	

+ Uncertainties are given in Subsection 4.3.3.3

++Note: 1 pcm = (percent mille) $10^{-5} \Delta\rho$ where $\Delta\rho$ is calculated from two statepoint values of k_{eff} by $\ln(K_2/K_1)$.

TABLE 4.3-2
(Sheet 2 of 2)

NUCLEAR DESIGN PARAMETERS
(Typical Low Leakage Cycle Design)

Radial Factor Peak Pin FΔh (BOL to EOL)

Unrodded	1.44 to 1.40
D bank	1.44 to 1.40
D + C	1.55 to 1.44

Boron Concentrations

Zero Power, $k_{\text{eff}} = 0.99$, Cold Rod Cluster Control Assemblies Out	1745
Zero Power, $k_{\text{eff}} = 0.99$, Hot Rod Cluster Control Assemblies Out	1873
Design Basis Refueling Boron Concentration	2000
Zero Power, $k_{\text{eff}} \leq 0.95$, Cold Rod Cluster Control Assemblies In	1424
Zero Power, $k_{\text{eff}} = 1.00$, Hot Rod Cluster Control Assemblies Out	1739
Full Power, No Xenon, $k_{\text{eff}} = 1.0$, Hot Rod Cluster Control Assemblies Out	1564
Full Power, Equilibrium Xenon, $k_{\text{eff}} = 1.0$, Hot Rod Cluster Control Assemblies Out	1179
Reduction with Fuel Burnup Cycle ppm/GWd/Mtu ⁺⁺⁺	See Figure 4.3-3

⁺⁺⁺ Gigawatt Day (GWd) = 1000 Megawatt Day (1000 MWd).

TABLE 4.3-3REACTIVITY REQUIREMENTS FOR ROD CLUSTER CONTROL ASSEMBLIES

Reactivity Effects, <u>Percent</u>	<u>Beginning-of-Life (First Cycle)</u>	<u>End-of-Life (First Cycle)</u>	<u>End-of-Life (Typical Low Leakage Cycle)</u>
1. Control requirements			
Fuel temperature, Doppler ($\% \Delta \rho$)	1.36	1.12	1.53
Moderator temperature** ($\% \Delta \rho$)	0.15	1.22	1.20
Redistribution ($\% \Delta \rho$)	0.50	0.85	***
Rod insertion allowance ($\% \Delta \rho$)	0.50	0.50	0.45
2. Total control ($\% \Delta \rho$)	2.51	3.69	3.18
3. Estimated Rod Cluster Control Assembly worth (57 rods, Ag-In-Cd)			
a. All full length assemblies inserted ($\% \Delta \rho$)	8.73	8.83	7.42
b. All but one (highest worth) assemblies inserted ($\% \Delta \rho$)	7.69	7.76	6.58
4. Estimated Rod Cluster Control Assembly credit with 10 percent adjustment to accommodate uncertainties, 3b - 10 percent ($\% \Delta \rho$)	6.92	6.98	5.93
5. Shutdown margin available, 4-2 ($\% \Delta \rho$)	4.41	3.29	2.75****

** Includes void effects

*** Redistribution included in Doppler portion

**** The design basis minimum shutdown is 1.3%.

TABLE 4.3-4

AXIAL STABILITY INDEX PRESSURIZED WATER
REACTOR CORE WITH A 12 FOOT HEIGHT

<u>Burnup</u> <u>(MWd/Mtu)</u>	<u>F_z</u>	<u>C_B</u> <u>(ppm)</u>	<u>Stability Index (hr⁻¹)</u>	
			<u>Exp</u>	<u>Calc</u>
1550	1.34	1065	-0.041	-0.032
7700	1.27	700	-0.014	-0.006
		Difference:	+0.027	+0.026

4.4 THERMAL AND HYDRAULIC DESIGN

4.4.1 Design Bases

The overall objective of the thermal and hydraulic design of the reactor core is to provide adequate heat transfer which is compatible with the heat generation distribution in the core such that heat removal by the Reactor Coolant System or the Emergency Core Cooling System (when applicable) assures that the following performances and safety criteria requirements are met:

- a. Fuel damage (defined as penetration of the fission product barrier, i.e., the fuel rod clad) is not expected during normal operation and operational transients (Condition I) or any transient conditions arising from faults of moderate frequency (Condition II). It is not possible, however, to preclude a very small number of rod failures. These will be within the capability of the plant cleanup system, and are consistent with the plant design bases.
- b. The reactor can be brought to a safe state following a Condition III event with only a small fraction of fuel rods damaged (see above definition) although sufficient fuel damage might occur to preclude resumption of operation without considerable outage time.
- c. The reactor can be brought to a safe state and the core can be kept subcritical with acceptable heat transfer geometry following transients arising from Condition IV events.

In order to satisfy the above criteria, the following design bases have been established for the thermal and hydraulic design of the reactor core.

4.4.1.1 Departure From Nucleate Boiling Design Basis

a. Basis

There will be at least 95 percent probability that departure from nucleate boiling (DNB) will not occur on the limiting fuel rods during normal operation and operational transients and any transient conditions arising from faults of moderate frequency (Conditions I and II events), at 95 percent confidence level.

For this application, the Design Limit DNBR values for 17 x 17 V5H +(w/o IFMs) are 1.27 for typical cells and 1.26 for thimble cells. The design limit DNBR values for V5H + (w/IFMs) are 1.26 for typical cells and 1.24 for thimble cells. For use in the DNB safety analyses, the limit DNBR is conservatively increased to provide DNB margin to offset the effect of rod bow, transition core, RCS flow a normally and any other DNB penalties that may occur, and to provide flexibility in design and operation of the plant. For V5H + (w/o IFMs) fuel, Safety Analysis Limit DNBR values of 1.40 for both typical and thimble cells are employed in the analysis. For V5H +

(w/IFMs) fuel, Safety Analysis Limit DNBR value of 1.91 for both typical and thimble cells are employed in the analysis.

b. Discussion

By preventing DNB, adequate heat transfer is assured between the fuel clad and the reactor coolant, thereby preventing clad damage as a result of inadequate cooling. Maximum fuel rod surface temperature is not a design basis, as it will be within a few degrees of coolant temperature during operation in the nucleate boiling region.

Limits provided by the nuclear control and protection systems are such that this design basis will be met for transients associated with Condition II events including overpower transients. There is an additional large DNBR margin at rated power operation and during normal operating transients.

The thermal-hydraulic analysis of the 17 x 17 V5H + (w/o IFMs) and V5H (w/IFMs) fuel used in Seabrook Station incorporates the use of the VIPRE-01 computer code and the Revised Thermal Design Procedure (RTDP). The WRB-1 DNB correlation is used for the V5H (w/o IFMs) and the WRE-2 DNB correlation is used for the V5H (w/IFMs). The W-3 correlation is still used when conditions are outside the range of the WRB-1 or WRB-2 correlations and applicability of the RTDP.

The WRB-1 DNB correlation is based entirely on rod bundle data and takes credit for the significant improvement in the accuracy of the critical heat flux predictions over previous DNB correlations. The approval of the NRC that a 95/95 limit DNBR of 1.17 is appropriate for the V5H (w/o IFMs) and 17 x 17 standard fuel assemblies has been documented.

The WRB-2 DNB correlation is a modification of the WRB-1 DNB correlation, based on rod bundle data, that takes advantage of the DNB benefit of reduced grid spacings associated with IFMs. The approval of the NRC that a 95 x 95 limit DNBR of 1.17 is appropriate in the V5H (w IFMs) has been documented.

The W-3 correlation with a 95/95 limit DNBR of 1.30 is used below the fuel assembly first mixing vane grid. The W-3 correlation with a 95/95 limit DNBR of 1.45 is used in the pressure range of 500 to 1000 psia.

With RTDP methodology, variations in plant operating parameters, nuclear and thermal parameters, fuel fabrication parameters, and DNB correlation predictions are considered statistically to obtain the overall DNBR uncertainty factor which is used to define the design limit DNBR that satisfies the DNB design criterion. The

criterion is that the probability that DNB will not occur on the most limiting fuel rod is at least 95 percent (at 95 percent confidence level) for any Condition I or II event. Conservative uncertainty values used to calculate the design limit DNBR are based on Reference 9. Since the uncertainties are all included in the uncertainty factor, the accident analysis is done with input parameters at their nominal or best-estimate values. RTDP analyses use a new flow parameter, minimum measured flow (MMF), equal to thermal design flow (TDF) plus a flow uncertainty. Analyses by standard methods continue to use TDF.

4.4.1.2 Fuel Temperature Design Basis

a. Basis

During modes of operation associated with Condition I and Condition II events, there is at least a 95 percent probability that the peak kW/ft fuel rods will not exceed the UO_2 melting temperature at the 95 percent confidence level. The nominal melting temperature of UO_2 is taken as 5080°F (Reference 1), unirradiated, decreasing 58°F per 10,000 MWd/Mtu exposure.

b. Discussion

By precluding UO_2 melting, the fuel geometry is preserved and possible adverse effects of molten UO_2 on the cladding are eliminated. Cycle-specific values for the peak linear heat generation rate precluding centerline melt are determined as a function of fuel rod average exposure. The determination of these values includes allowance of sufficient margin to accommodate the uncertainties in the thermal evaluations described in Subsection 4.4.2.9a. To preclude fuel centerline melting, these values are observed as an overpower limit for Condition I and II events, and employed as a basis for overpower protection system setpoints. Fuel rod thermal evaluations are performed at various burnups to assure that this design basis as well as the fuel integrity design bases given in Section 4.2 is met.

4.4.1.3 Core Flow Design Basis

a. Basis

A minimum of 93.7 percent of the thermal flow rate will pass through the fuel rod region of the core and be effective for fuel rod cooling. Coolant flow through the thimble tubes, as well as the leakage from the core barrel-baffle region into the core, are not considered effective for heat removal.

b. Discussion

As noted in section 4.4.1.1, in core cooling evaluations the flow rate entering the reactor vessel is assumed to be the minimum measured flow rate (MMF), when the WRB-1 or WRB-2 correlation and RTDP are applicable, and the thermal design flow rate (TDF) otherwise. A maximum of 4.8 percent of the MMF value is allotted as bypass flow. Similarly, a maximum of 6.3 percent of the TDF value is allotted as bypass flow. These values include rod cluster control guide thimble cooling flow for the case of all thimble plug assemblies inserted, head cooling flow, baffle leakage, and leakage to the vessel outlet nozzle.

4.4.1.4 Hydrodynamic Stability Design Basis

Modes of operation associated with Conditions I and II events shall not lead to hydrodynamic instability.

4.4.1.5 Other Considerations

The above design bases, together with the fuel clad and fuel assembly design bases given in Subsection 4.2.1, are sufficiently comprehensive so additional limits are not required.

Fuel rod diametral gap characteristics, moderator-coolant flow velocity and distribution, and moderator void are not inherently limiting. Each of these parameters is incorporated into the thermal and hydraulic models used to ensure the above-mentioned design criteria are met. For instance, the fuel rod diametral gap characteristics change with time (see Subsection 4.2.3.3) and the fuel rod integrity is evaluated on that basis. The effect of the moderator flow velocity and distribution (see Subsection 4.4.2.2) and moderator void distribution (see Subsection 4.4.2.4) are included in the core thermal (VIPRE-01) evaluation and thus affect the design bases.

Meeting the fuel clad integrity criteria covers possible effects of clad temperature limitations. As noted in Subsection 4.2.3.3, the fuel rod conditions change with time. A single clad temperature limit for Condition I or Condition II events is not appropriate since, of necessity, it would be overly conservative. A clad temperature limit is applied to the loss-of-coolant accident (Subsection 15.6.5), control rod ejection accident, and locked rotor accident.

4.4.2 Description

4.4.2.1 Summary Comparison

The design of the four-loop standard plant, Seabrook Unit 1 as described in

this report, has similar thermal and hydraulic parameters as the W. B. McGuire Nuclear Station, Units 1 and 2, reactor design.

Values of pertinent parameters, along with critical heat flux ratios, fuel temperatures and linear heat generation rates, are presented in Table 4.4-1 for all coolant loops in service. It is also noted, that in this power capability evaluation there has not been any change in the design criteria. The reactor is still designed to meet the DNB design criterion of Section 4.4.1.1, as well as no fuel centerline melting during normal operation, operational transients and faults of moderate frequency.

All DNB analyses were performed such that the DNBR margins are available for offsetting rod bow penalties and for flexibility in design.

Fuel densification has been considered in the DNB and fuel temperature evaluations.

4.4.2.2 Critical Heat Flux Ratio or Departure from Nucleate Boiling Ratio and Mixing Technology

The minimum DNBRs for the rated power, design overpower and anticipated transient conditions are given in Table 4.4-1. The minimum DNBR in the limiting flow channel is usually downstream of the peak heat flux location (hot spot) due to the increased downstream enthalpy rise.

DNBRs are calculated by using the correlation and definitions described in the following Subsections 4.4.2.2a and 4.4.2.2b. The VIPRE-01 computer code (discussed in Subsection 4.4.4.5a) is used to determine the flow distribution in the core and the local conditions in the hot channel for use in the DNB correlation. The use of hot channel factors is discussed in Subsection 4.4.4.3a (nuclear hot channel factors) and in Subsection 4.4.2.2d (hot channel factors).

a. Departure from Nucleate Boiling Technology

The WRB-1 and WRB-2 DNB correlations are used to evaluate critical heat flux in the fuel assemblies. The W-3 correlation with a 95/95 limit DNBR of 1.30 is used below the fuel assembly first mixing vane grid. The W-3 correlation with a 95/95 limit DNBR of 1.45 is used in the pressure range of 500 to 1000 psia. These correlations are tested against measured heat flux data in order to establish correlation limits which satisfy the DNB design basis stated in Section 4.4.1.1. The WRB-1 correlation takes advantage of the improvement in the accuracy of critical heat flux predictions over previous DNBR correlations to establish a lower correlation limit of 1.17. The WRB-2 correlation taken advantage of the DNB benefit of reduced grid specifics associated with IFMs.

b. Definition of Departure from Nucleate Boiling Ratio (DNBR)

The DNBR heat flux ratio (DNBR) as applied to this design when all flow cell walls are heated, is:

$$\text{DNBR} = \frac{q''_{\text{DNB},N}}{q''_{\text{loc}}} \quad (4.4-1)$$

where:

$$q''_{\text{DNB},N} = \frac{q''_{\text{DNB},EU}}{F} \quad (4.4-2)$$

$q''_{\text{DNB},EU}$ is the uniform DNB heat flux as predicted by the WRB-1 (Reference 7), WRB-2 (Reference 80), or W-3 (Reference 8) DNB correlation.

F is the flux shape factor to account for nonuniform axial heat flux distributions (Reference 8) with the "C" term modified as in Reference 3.

q''_{loc} is the actual local heat flux.

A multiplier of 0.88 is applied for all DNB analyses using the W-3 correlation.

The DNBR when a cold wall is present is the same as equation 4.4-1 above when the WRB-1 or WRB-2 correlations are applied. When the W-3 correlation is applied, the DNBR is:

$$\text{DNBR} = \frac{q''_{\text{DNB},N,CW}}{q''_{\text{loc}}} \quad (4.4-4)$$

where:

$$q''_{\text{DNB},N,CW} = \frac{q''_{\text{DNB},EU,Dh} \times \text{CWF}}{F} \quad (4.4-5)$$

$q''_{\text{DNB},EU,Dh}$ is the uniform DNB heat flux as predicted by the W-3 cold wall DNB correlation (Reference 3) when not all flow cell walls are heated (thimble cold wall cell).

$$\text{CWF} = 1.0 - Ru \left[13.76 - 1.37e^{1.78x} - 4.732 \left\{ \frac{G}{10^6} \right\}^{-0.0535} \right] \quad (4.4-6)$$

$$-0.0619 \left(\frac{P}{1000} \right)^{0.14} - 8.50 Dh^{0.107} \quad]$$

and $Ru = 1 - De/Dh$.

Values of minimum DNB provided in Tables 4.4-1 and 4.4-2 are the limiting values obtained by applying the above two definitions of DNBR to the appropriate cell (typical cell with all walls heated, or a thimble cold wall cell with a partial heated wall condition).

c. Mixing Technology

1. Flow Mixing

The subchannel mixing model incorporated in the VIPRE-01 Code and used in reactor design is based on experimental data (Reference 17). The mixing vanes incorporated in the spacer grid design induce additional flow mixing between the various flow channels in a fuel assembly as well as between adjacent assemblies. This mixing reduces the enthalpy rise in the hot channel resulting from local power peaking or unfavorable mechanical tolerances.

2. Thermal Diffusion

The rate of heat exchange by mixing between flow channels is proportional to the difference in the local mean fluid enthalpy of the respective channels of the local fluid density and flow velocity. The proportionality is expressed by the dimensionless thermal diffusion coefficient (TDC) which is defined as:

$$TDC = \frac{w'}{\rho Va} \quad (4.4-7)$$

where:

- w' = flow exchange rate per unit length, (lb_m/ft-sec)
- ρ = fluid density, lb_m/ft³
- V = fluid velocity, ft/sec
- a = lateral flow area between channels per unit length, ft²/ft

The application of the TDC in the VIPRE-01 analysis for determining the overall mixing effect or heat exchange rate is presented in Reference 81.

As a part of an ongoing research and development program, Westinghouse has sponsored and directed mixing tests at Columbia University (Reference 12). These series of tests,

using the "R" mixing vane grid design on 13, 26 and 32 inch grid spacing, were conducted in pressurized water loops at Reynolds numbers similar to that of PWR core under the following single and two phase (subcooled boiling) flow conditions:

Pressure	1500 to 2400 psia
Inlet temperature	332 to 642°F
Mass velocity	1.0 to 3.5×10^6 lb _m /hr-ft ²
Reynolds number	1.34 to 7.45×10^5
Bulk outlet quality	-52.1 to 13.5%

TDC is determined by comparing code predictions with the measured subchannel exit temperatures. Data for 26 inch axial grid spacing are presented in Figure 4.4-1 where the thermal diffusion coefficient is plotted versus the Reynolds number. TDC is found to be independent of Reynolds number, mass velocity, pressure and quality over the ranges tested. The two phase data (local, subcooled boiling) fell within the scatter of the single phase data. The effect of two-phase flow on the value of TDC has been demonstrated by Cadek (Reference 12), Rowe and Angle (References 13 and 14), and Gonzalez-Santalo and Griffith (Reference 15). In the subcooled boiling region, the values of TDC were indistinguishable from the single phase values. In the quality region, Rowe and Angle show that in the case with rod spacing similar to that in PWR reactor core geometry, the value of TDC increased with quality to a point and then decreased, but never below the single phase value. Gonzalez-Santalo and Griffith showed that the mixing coefficient increased as the void fraction increased.

The data from these tests on the "R" grid showed that a design TDC value of 0.038 (for 26 inch grid spacing) can be used in determining the effect of coolant mixing.

A mixing test program similar to the one described above was conducted at Columbia University for the 17x17 geometry and mixing vane grids on 26 inch spacing (Reference 16). The mean value of TDC obtained from these tests was 0.059, and all data was well above the current design value of 0.038.

Since the actual reactor grid spacing is approximately 20 inches, additional margin is available for this design, as the value of TDC increases as grid spacing decreases (Reference 12).

The inclusion of three intermediate flow mixer grids in the upper span of the V5H (w IFMs) fuel assembly results in a grid spacing of approximately 10 inches. Per Reference 80, a TDC value of 0.038 was chosen as a conservatively low value for use in V5H (w IFMs) to determine the effect of constant mixing

in the core thermal performance analysis.

3. Inlet Flow Maldistribution

A conservatively low total core inlet flow is used in VIPRE-01 subchannel analysis. The applicable core inlet flow is reduced by a cycle-specific factor accounting for the effect of inlet flow maldistribution on core thermal performance. Determination of the flow reduction factor is discussed in Subsection 4.4.4.2b.

4. Flow Redistribution

Redistribution of flow in the hot channel resulting from the high flow resistance in the channel due to local or bulk boiling and the effect of the nonuniform power distribution is inherently considered in the VIPRE-01 analysis for every operating condition which is evaluated.

d. Hot Channel Factors

The total hot channel factors for heat flux and enthalpy rise are defined as the maximum-to-core average ratios of these quantities. The heat flux hot channel factor considers the local maximum linear heat generation rate at a point (the hot spot), and the enthalpy rise hot channel factor involves the maximum integrated value along a channel (the hot channel).

Each of the total hot channel factors considers a nuclear hot channel factor (see Subsection 4.4.4.3) describing the neutron power distribution and an engineering hot channel factor which allows for fabrication tolerances.

1. Heat Flux Engineering Hot Channel Factor, F_Q^E

The heat flux engineering hot channel factor is used to evaluate the maximum heat flux. This subfactor has a value of 1.03 and is determined by statistically combining the tolerances for the fuel pellet diameter, density, enrichment, eccentricity, and the fuel rod diameter. Measured manufacturing data on Westinghouse 17x17 fuel were used to verify that this value was not exceeded for 95 percent of the limiting fuel rods at a 95 percent confidence level. Thus, it is expected that a statistical sampling of the fuel assemblies of this plant will yield a value no larger than 1.03.

2. Enthalpy Rise Engineering Hot Channel Factor, $F_{\Delta H}^E$

The effect of fabrication tolerances on the hot channel enthalpy rise is also considered in the core thermal subchannel analysis. The development of the WRB-1 and WRB-2 DNBR design limits used with the RTDP included consideration of the fabrication tolerances for pellet diameter, density and enrichment, fuel rod diameter, pitch and bowing.

Values employed in the analysis related to the above fabrication variations are based on applicable limiting tolerances, such that design values are met for 95 percent of the limiting channels at a 95 percent confidence level. Measured manufacturing data on Westinghouse 17x17 fuel show the tolerances used are conservative. In addition, each fuel assembly is checked to assure the channel spacing design criteria are met.

When the W-3 correlation is employed the effect of fabrication variations is applied in the VIPRE-01 analysis as a direct multiplier on the hot channel enthalpy rise.

e. Effects of Rod Bow on DNBR

The phenomenon of fuel rod bowing, as described in Reference 83, must be accounted for in the DNBR safety analysis of Condition I and Condition II events for each plant application. Applicable generic credits for margin resulting from retained conservatism in the evaluation of DNBR are used to offset the effect of rod bow.

For the safety analysis of Seabrook Unit I, sufficient DNBR margin was maintained to accommodate full and low flow rod bow DNBR penalties identified in Reference 4. The referenced penalties are applicable to the analyses using the WRB-1 DNB and the WRB-2 DNB correlations.

The maximum rod bow penalty (1.3 percent DNBR) accounted for in the design safety analysis is based on an assembly average burnup of 24,000 MWd/Mtu. At burnups greater than 24,000 MWd/Mtu, credit is taken for the effect of $F_{\Delta H}^N$ burndown, due to the decrease in fissionable isotopes and the buildup of fission product inventory, and no additional rod bow penalty is required (Reference 85).

In the upper spans of the V5H + (w IFMs) fuel assembly, additional restraint is provided with the intermediate flow mixer grids such that the grid-to-grid spacing in those spans with IFM grids is approximately 10 inches compared to approximately 20 inches in the other spans. Using the NRC approved scaling factor results in predicted channel closure in the limiting 10-inch spans of less

than 50-percent closure. Therefore, no rod bow DNBR penalty is required in the 10-inch spans in V5H (w IFMs) safety analyses.

f. Transition Core DNB Methodology

The V5H (w/o IFMs) and V5H (w IFMs) designs have been shown to be hydraulically compatible in Reference 85.

The Westinghouse transition core DNB methodology is given in References 86, 87, and 88. Using this methodology, transition cores are analyzed as if the entire core consisted of one assembly type (full V5H (w/o IFMs) or full V5H (w IFMs)). The resultant DNBRs are then reduced by the appropriate transition core penalty.

The V5H (w IFMs) fuel assembly has a higher mixing vane grid loss coefficient relative to the V5H (w/o IFMs) mixing vane grid loss coefficient. In addition, the V5H (w IFMs) fuel assembly has IFM grids located in spans between mixing vane grids, where no grid exists in the V5H (w/o IFMs) assembly. The higher loss coefficients and the additional grids introduce localized flow redistribution from the V5H (w IFMs) fuel assembly into the V5H (w/o IFMs) assembly at the axial zones near the mixing vane grid and the IFM grid position in a transition core. Between the grids, the tendency for velocity equalization in parallel open channels causes flow to return to the V5H (w IFMs) fuel assembly. The localized flow redistribution described above actually benefits the V5H (w/o IFMs) assembly. This benefit more than offsets the slight mass flow bias due to velocity equalization at nongrid locations. Thus, the analysis for a full core of V5H (w/o IFMs) is appropriate for that fuel type in a transition core. There is no transition core DNBR penalty for the V5H (w/o IFMs) fuel.

The transition core DNBR penalty for V5H (w IFMs) fuel is discussed in References 89 and 90. The transition core penalty is a function of the number of V5H (w IFMs) fuel assemblies in the core, Reference 91. Sufficient DNBR margin is maintained in the V5H (w IFMs) safety analysis to completely offset this transition core penalty.

4.4.2.3 Linear Heat Generation Rate

The core average and maximum LHGRs are given in Table 4.4-1. The method of determining the maximum LHGR is given in Subsection 4.3.2.2.

4.4.2.4 Void Fraction Distribution

The calculated core average and the hot subchannel maximum and average void fractions are presented in Table 4.4-2 for operation at full power with the original design hot channel factors. The void fraction distribution in the core at various radial and axial locations is presented in Reference 18. The void models used in the VIPRE-01 computer code are described in Subsection

4.4.2.7c. Typical normalized core flow and enthalpy rise distributions are shown in Figures 4.4-2 through 4.4-4 for the Cycle 1 core design. The distributions are also typical of those which would be found in later operating cycles.

4.4.2.5 Core Coolant Flow Distribution

Assembly average coolant mass velocity and enthalpy at various radial and axial core locations are given below. Typical coolant enthalpy rise and flow distributions are shown for the 4 foot elevation (1/3 of core height) in Figure 4.4-2, and 8 foot elevation (2/3 of core height) in Figure 4.4-3 and at the core exit in Figure 4.4-4. These distributions are for the full power conditions as given in Table 4.4-1 and for the radial power density distribution shown in Figure 4.3-7, which correspond to the Cycle 1 core design. The values are also typical for later operating cycles. The analysis for this case utilized a uniform core inlet enthalpy and inlet flow distribution. No orificing is employed in the reactor design.

4.4.2.6 Core Pressure Drops and Hydraulic Loads

a. Core Pressure Drops

The analytical model and experimental data used to calculate the pressure drops shown in Table 4.4-1 are described in Subsection 4.4.2.7. The core pressure drop includes the fuel assembly, lower core plate, and upper core plate pressure drops. The full power operation pressure drop values shown in Table 4.4-1 are the unrecoverable pressure drops across the vessel, including the inlet and outlet nozzles, and across the core. These pressure drops are based on a measured flow of 404,000 GPM total for actual plant operating conditions as described in Section 5.1.

Uncertainties associated with the core pressure drop values are discussed in Subsection 4.4.2.9b.

b. Hydraulic Loads

The fuel assembly hold down springs, Figure 4.2-2, are designed to keep the fuel assemblies in contact with the lower core plate under all Condition I and II events, with the exception of the turbine overspeed transient associated with a loss of external load. The hold down springs are designed to tolerate the possibility of an over deflection associated with fuel assembly liftoff for this case, and provide contact between the fuel assembly and the lower core plate following this transient. More adverse flow conditions occur during a loss-of-coolant accident. These conditions are presented in Subsection 15.6.5.

Hydraulic loads at normal operating conditions are calculated considering the mechanical design flow which is described in Section

5.1 and accounting for the minimum core bypass flow based on manufacturing tolerances. Core hydraulic loads at cold plant startup conditions are based on the cold mechanical design flow, but are adjusted to account for the coolant density difference. Conservative core hydraulic loads for a pump overspeed transient, which could possibly create flow rates 18 percent greater than the best estimate flow, are evaluated to be approximately twice the fuel assembly weight.

4.4.2.7 Correlation and Physical Data

a. Surface Heat Transfer Coefficients

Forced convection heat transfer coefficients are obtained from the familiar Dittus-Boelter correlation (Reference 20), with the properties evaluated at bulk fluid conditions:

$$\frac{hD_e}{K} = 0.023 \left[\frac{D_e G}{\mu} \right]^{0.8} \left[\frac{C_p \mu}{K} \right]^{0.4} \quad (4.4-8)$$

where:

- h = heat transfer coefficient, (Btu/hr-ft²-°F)
- D_e = equivalent diameter, (ft)
- K = thermal conductivity, (Btu/hr-ft-°F)
- G = mass velocity, (lb_m/hr-ft²)
- μ = dynamic viscosity, (lb_m/ft-hr)
- C_p = heat capacity, (Btu/lb_m-°F)

This correlation has been shown to be conservative (Reference 21) for rod bundle geometries with pitch-to-diameter ratios in the range used by PWRs.

The onset of nucleate boiling occurs when the clad wall temperature reaches the amount of superheat predicted by Thom's correlation, Reference 22. After this occurrence the outer clad wall temperature is determined by:

$$\Delta T_{sat} = (0.072 \exp(-P/1260)) (q'')^{0.5} \quad (4.4-9)$$

where:

- ΔT_{sat} = wall superheat, T_w - T_{sat}, (°F)
- q'' = wall heat flux, (Btu/hr-ft²)
- P = pressure, (psia)
- T_w = outer clad wall temperature, (°F)
- T_{sat} = saturation temperature of coolant at P, (°F)

b. Total Core and Vessel Pressure Drop

Unrecoverable pressure losses occur as a result of viscous drag (friction) and/or geometry changes (form) in the fluid flow path. The flow field is assumed to be incompressible, turbulent, single-phase water. These assumptions apply to the core and vessel pressure drop calculations for the purpose of establishing the primary loop flow rate. Two-phase considerations are neglected in the vessel pressure drop evaluation because the core average void is negligible (see Table 4.4-2). Two-phase flow considerations in the core thermal subchannel analyses are considered and the models are discussed in Subsection 4.4.4.2c. Core and vessel pressure losses are calculated by equations of the form:

$$P_L = \left[K + \frac{F L}{D_e} \right] \frac{\rho V^2}{2 g_c} \quad (4.4-10) \quad (144)$$

Where:

P_L = unrecoverable pressure drop, (lb_f/in^2)

ρ = fluid density, (lb_m/ft^3)

L = length, (ft)

D_e = equivalent diameter, (ft)

V = fluid velocity, (ft/sec)

$$g_c = 32.174 \frac{\text{lb}_m \cdot \text{ft}}{\text{lb}_f \cdot \text{sec}^2}$$

K = form loss coefficient, dimensionless

F = friction loss coefficient, dimensionless

Fluid density is assumed to be constant at the appropriate value for each component in the core and vessel. Because of the complex core and vessel flow geometry, precise analytical values for the form and friction loss coefficients are not available. Therefore, experimental values for these coefficients are obtained from geometrically similar models.

Values are quoted in Table 4.4-1 for unrecoverable pressure loss across the reactor vessel, including the inlet and outlet nozzles and across the core. The results of full-scale tests of core components and fuel assemblies were utilized in developing the core pressure loss characteristic. The pressure drop for the vessel was obtained by combining the core loss with correlation of 1/7th scale model hydraulic test data on a number of vessels (References 23 and 24) and form loss relationships (Reference 25). Moody curves (Reference 26) were used to obtain the single phase friction factors.

c. Void Fraction Correlation

Empirical correlations are used in VIPRE to model the void fraction in two phase flow. The subcooled void correlation used to model the non equilibrium transition from single phase to nucleate boiling is given in Reference 81. The bulk (saturated) void model relates flow quality with void fraction which can account for phase slip.

4.4.2.8 Thermal Effects of Operational Transients

DNB core safety limits are generated as a function of coolant temperature, pressure, core power and axial power imbalance. Steady state operation within these safety limits insures that the minimum DNBR is not less than the safety analysis limit. Figure 15.0-1 shows the safety analysis limit lines and the resulting Overtemperature ΔT trip lines (which become part of the Technical Specifications or Core Operating Limits Report), plotted as ΔT , versus T_{avg} for various pressures. This system provides adequate protection against anticipated operational transients that are slow with respect to fluid transport delays in the primary system. In addition, for fast transients, e.g., uncontrolled rod bank withdrawal at power incident (Subsection 15.4.2), specific protection functions are provided as described in Section 7.2 and the use of these protection functions is described in Chapter 15.

4.4.2.9 Uncertainties in Estimates

a. Uncertainties in Fuel and Clad Temperatures

As discussed in paragraph 4.4.2.11, the fuel temperature is a function of crud, oxide, clad, pellet-clad gap, and pellet conductances. Uncertainties in the fuel temperature calculation are essentially of two types: fabrication uncertainties, such as variations in the pellet and clad dimensions and the pellet density; and model uncertainties, such as variations in the pellet conductivity and the gap conductance. These uncertainties have been quantified by comparison of the thermal model to the inpile thermocouple measurements, (References 40 - 46) by out-of-pile measurements of the fuel and clad properties, (References 47 - 58) and by measurements of the fuel and clad dimensions during fabrication. The resulting uncertainties are then used in all evaluations involving the fuel temperature. The effect of densification on fuel temperature uncertainties is also included in the calculation of the total uncertainty.

In addition to the temperature uncertainty described above, the measurement uncertainty in determining the local power and the effect of density and enrichment variations on the local power are considered in establishing the heat flux hot channel factor. These uncertainties are described in paragraph 4.3.2.2.1.

Reactor trip setpoints, as specified in the Technical Specifications, include allowance for instrument and measurement uncertainties such as calorimetric error, instrument drift and channel reproducibility, temperature measurement uncertainties, noise, and heat capacity variations.

Uncertainty in determining the cladding temperature results from uncertainties in the crud and oxide thicknesses. Because of the excellent heat transfer between the surface of the rod and the coolant, the film temperature drop does not appreciably contribute to the uncertainty.

b. Uncertainties in Pressure Drops

Core and vessel pressure drops based on a measured flow, as described in Section 5.1, are quoted in Table 4.4-1. The uncertainties quoted are based on the uncertainties in both the test results and the analytical extension of these values to the reactor application.

A major use of the core and vessel pressure drops was to determine the primary system coolant flow rates as discussed in Section 5.1. As discussed in Subsection 4.4.5.1, tests on the primary system prior to initial criticality were made to verify that conservative primary system coolant flow has been used in the mechanical design and safety analyses of the plant.

c. Uncertainties Due to Inlet Flow Maldistribution

The effects of uncertainties in the inlet flow maldistribution criteria used in the core thermal analyses are discussed in Subsection 4.4.4.2b.

d. Uncertainty in DNB Correlation

The uncertainty in the DNB correlation (Subsection 4.4.2.2) can be written as a statement on the probability of not being in DNB based on the statistics of the DNB data. This is discussed in Subsection 4.4.2.2b.

e. Uncertainties in DNBR Calculations

The uncertainties in the DNBRs calculated by VIPRE-01 analysis (see Subsection 4.4.4.5a) due to uncertainties in the nuclear peaking factors are accounted for by applying conservatively high values of the nuclear peaking factors and considering measurement error allowances in the determination of the WRB-1 and WRB-2 DNBR limits employed with the RTDP. In addition, conservative values for the engineering hot channel factors are used as discussed in Subsection 4.4.2.2d. The results of a sensitivity study (Reference 18) show

that the minimum DNBR in the hot channel is relatively insensitive to variations in the core-wide-radial power distribution (for the same value of $F_{\Delta H}^N$).

The ability of the VIPRE-01 computer code to accurately predict flow and enthalpy distributions in rod bundles is discussed in Subsection 4.4.4.5a and in References 80 and 81.

f. Uncertainties in Flow Rates

The uncertainties associated with loop flow rates are discussed in Section 5.1. For core thermal performance evaluations, a minimum loop flow is used which is less than the best estimate loop flow. In addition, up to 6.3 percent of the thermal design flow is assumed to be ineffective for core heat removal capability because it bypasses the core through the various available vessel flow paths described in Subsection 4.4.4.2a.

g. Uncertainties in Hydraulic Loads

As discussed in Subsection 4.4.2.6b, hydraulic loads on the fuel assembly are evaluated for a pump overspeed transient which creates flow rates 18 percent greater than the mechanical design flow. The mechanical design flow as stated in Section 5.1 is greater than the best estimate or most likely flow rate value for the actual plant operating condition.

h. Uncertainty in Mixing Coefficient

The value of the mixing coefficient, TDC, used in VIPRE-01 analyses for this application is 0.038. The mean value of TDC obtained in the "R" grid mixing tests described in Subsection 4.4.2.2a was 0.042 (for 26 inch grid spacing). The value 0.038 is one standard deviation below the mean value; approximately 90 percent of the data give values of TDC greater than 0.038 (Reference 12).

The results of the mixing tests done on 17x17 geometry, as discussed in Subsection 4.4.2.2c, had a mean value of TDC of 0.059 and standard deviation of $\sigma = 0.007$. Hence the current design value of TDC is almost 3 standard deviations below the mean for 26 inch grid spacing.

4.4.2.10 Flux Tilt-Considerations

Significant quadrant power tilts are not anticipated during normal operation since this phenomenon is caused by some asymmetric perturbation. A dropped or misaligned Rod Cluster Control Assembly could cause changes in hot channel factors. However, these events are analyzed separately in Chapter 15.

Other possible causes for quadrant power tilts include X-Y xenon transients,

inlet temperature mismatches, enrichment variations within tolerances and so forth.

In addition to unanticipated quadrant power tilts as described above, other readily explainable asymmetries may be observed during calibration of the excore detector quadrant power tilt alarm. During operation, incore maps are taken at least once per month and, periodically, additional maps are obtained for calibration purposes. Each of these maps is reviewed for deviations from the expected power distributions. Asymmetry in the core, from quadrant to quadrant, is frequently a consequence of the design when assembly and/or component shuffling and rotation requirements do not allow exact symmetry preservation. In each case, the acceptability of an observed asymmetry, planned or otherwise, depends solely on meeting the required accident analyses assumptions.

In practice, once acceptability has been established by review of the incore maps, the quadrant power tilt alarms and related instrumentation are adjusted to indicate zero Quadrant Power Tilt Ratio as the final step in the calibration process. This action ensures that the instrumentation is correctly calibrated to alarm in the event an unexplained or unanticipated change occurs in the quadrant to quadrant relationships between calibration intervals. Proper functioning of the quadrant power tilt alarm is significant because no allowances, beyond accounting for the maximum tilt allowed by Technical Specifications, are made in the design for increased hot channel factors due to unexpected developing flux tilts, since all likely causes are prevented by design or procedures, or are specifically analyzed. Finally, in the event that unexplained flux tilts do occur, the Technical Specifications (Subsection 3/4.2.4) provide appropriate corrective actions to ensure continued safe operation of the reactor.

4.4.2.11 Fuel and Cladding Temperatures

Consistent with the thermal-hydraulic design bases described in Subsection 4.4.1, the following discussion pertains mainly to fuel pellet temperature evaluation. A discussion of fuel clad integrity is presented in Subsection 4.2.3.1.

The thermal-hydraulic design assures that the maximum fuel temperature is below the melting point of UO_2 (melting point of $5080^\circ F$ (Reference 1) unirradiated and decreasing by $58^\circ F$ per 10,000 MWd/Mtu). To preclude center melting, and as a basis for overpower protection system setpoints, cycle-specific values for the peak linear heat generation rate precluding centerline melt are determined as a function of fuel rod average exposure. These are observed as an overpower limit for Condition I and II events. They provide sufficient margin for uncertainties in the thermal evaluations described in Subsection 4.4.2.9a. The temperature distribution within the fuel pellet is predominantly a function of the local power density and the UO_2 thermal conductivity. However, the computation of radial fuel temperature distributions combines crud, oxide, clad gap and pellet conductances. The factors which influence these conductances, such as gap size (or contact

pressure), internal gas pressure, gas composition, pellet density, and radial power distribution within the pellet, etc., have been combined into a Westinghouse semi-empirical thermal model (see Subsection 4.2.3.3) with the model modifications for time dependent fuel densification given in Reference 2. This thermal model enables the determination of these factors and their net effects on temperature profiles. The temperature predictions have been compared to inpile fuel temperature measurements (References 40-46 and 59) and melt radius data (References 60 and 61).

As described in Reference 2, fuel rod thermal evaluations (fuel centerline, average and surface temperatures) are determined throughout the fuel rod lifetime with consideration of time dependent densification. To determine the maximum fuel temperatures, various burnup rods, including the highest burnup rod, are analyzed over the rod linear power range of interest.

The principal factors which are employed in the determination of the fuel temperature are discussed below.

a. UO₂ Thermal Conductivity

The thermal conductivity of uranium dioxide was evaluated from data reported from a number of measurements.

At the higher temperatures, thermal conductivity is best obtained by utilizing the integral conductivity to melt which can be determined with more certainty. From an examination of the data, it has been concluded that the best estimate for the value of 2800°C Kdt is 93 watts/cm.

The design curve is in excellent agreement with the recommendation of the IAEA panel (Reference 36).

b. Radial Power Distribution in UO₂ Fuel Rods

An accurate description of the radial power distribution as a function of burnup is needed for determining the power level for incipient fuel melting and other important performance parameters such as pellet thermal expansion, fuel swelling and fission gas release rates.

Radial power distribution in UO₂ fuel rods is determined with the neutron transport code LASER. The LASER code has been validated by comparing the code predictions on radial burnup and isotopic distributions with measured radial microdrill data (References 62 and 63). A "radial power depression factor," f , is determined using radial power distributions predicted by LASER. The factor, f , enters into the determination of the pellet centerline temperature, T_c , relative to the pellet surface temperature, T_s , through the expression:

$$\int_{T_s}^{T_c} K(T) \, dT = \frac{q' f}{4 \pi} \quad (4.4-11)$$

where:

$K(T)$ = the thermal conductivity for UO_2 with a uniform density distribution

q' = the linear power generation rate.

c. Gap Conductance

The temperature drop across the pellet-clad gap is a function of the gap size and the thermal conductivity of the gas in the gap. The gap conductance model is selected such that when combined with the UO_2 thermal conductivity model, the calculated fuel centerline temperatures reflect the inpile temperature measurements. A more detailed discussion of the gap conductance model is presented in Reference 64.

d. Surface Heat Transfer Coefficients

The fuel rod surface heat transfer coefficients during subcooled forced convection and nucleate boiling are presented in Subsection 4.4.2.7a.

e. Fuel Clad Temperatures

The outer surface of the fuel rod at the hot spot operates at a temperature of approximately 660°F for steady operation at rated power throughout core life due to the onset of nucleate boiling. Initially (beginning-of-life), this temperature is that of the clad metal outer surface.

During operation over the life of the core, the buildup of oxides and crud on the fuel rod surface causes the clad surface temperature to increase. Allowance is made in the fuel center melt evaluation for this temperature rise. Since the thermal-hydraulic design basis limits DNB, adequate heat transfer is provided between the fuel clad and the reactor coolant so that the core thermal output is not limited by considerations of clad temperature.

f. Treatment of Peaking Factors

The total heat flux hot channel factor, F_Q , is defined by the ratio of the maximum to core average heat flux. As presented in Table 4.3-2 and discussed in Subsection 4.3.2.2f, the design value of F_Q for normal operation is 2.50. This results in a peak linear power of 13.6 kW/ft at full power conditions.

The centerline temperature must be below the UO_2 melt temperature over the lifetime of the rod, including allowances for uncertainties. The fuel temperature design basis is discussed in Subsection 4.4.1.2. The centerline temperature resulting from overpower transients/operator errors is below that required to produce melting.

4.4.3 Description of the Thermal and Hydraulic Design of the Reactor Coolant System

4.4.3.1 Plant Configuration Data

Plant configuration data for the thermal hydraulic and fluid systems external to the core are provided in the appropriate Chapters 5, 6, and 9. Implementation of the Emergency Core Cooling System (ECCS) is discussed in Chapter 15. Some specific areas of interest are the following:

- a. Total coolant flow rates for the Reactor Coolant System (RCS) and each loop are provided in Table 5.1-1. Flow rates employed in the evaluation of the core are presented in Section 4.4.
- b. Total RCS volume including pressurizer and surge line, RCS liquid volume including pressurizer water at steady state power conditions are given in Table 5.1-1.
- c. The flow path length through each volume may be calculated from physical data provided in the above referenced tables.
- d. The height of fluid in each component of the RCS may be determined from the physical data presented in Section 5.4. The components of the RCS are water filled during power operation with the pressurizer being approximately 60 percent water filled.
- e. Components of the ECCS are to be located so as to meet the criteria for net positive suction head described in Section 6.3.
- f. Line lengths and sizes for the Safety Injection System are determined so as to guarantee a total system resistance which will provide, as a minimum, the fluid delivery rates assumed in the safety analyses described in Chapter 15.

- g. The parameters for components of the RCS are presented in Section 5.4, component and subsystem design.
- h. The steady state pressure drops and temperature distributions through the RCS are presented in Table 5.1-1.

4.4.3.2 Operating Restrictions on Pumps

The minimum net positive action head (NPSH) and minimum seal injection flow rate must be established before operating the reactor coolant pumps. With the minimum 6 gpm labyrinth seal injection flow rate established, the operator will have to verify that the system pressure satisfies NPSH requirements.

4.4.3.3 Power-Flow Operating Map (BWR)

Not applicable to pressurized water reactors.

4.4.3.4 Temperature-Power Operating Map

The relationship between Reactor Coolant System temperature and power is shown in Figure 4.4-6.

The effects of reduced core flow due to inoperative pumps is discussed in Subsections 5.4.1, 15.3.1, and 15.3.2. Natural circulation capability of the system is demonstrated in Subsection 15.2.6.

4.4.3.5 Load Following Characteristics

The Reactor Coolant System is designed on the basis of steady state operation at full power heat load. The reactor coolant pumps utilize constant speed drives. The reactor coolant pump assembly is described in Section 5.4. Reactor power is controlled to maintain average coolant temperature at a value which is a linear function of load, as described in Section 7.7.

4.4.3.6 Thermal and Hydraulic Characteristics Summary Table

The thermal and hydraulic characteristics are given in Tables 4.3-1 and 4.4-1.

4.4.4 Evaluation

4.4.4.1 Critical Heat Flux

The critical heat flux correlation utilized in the core thermal analysis is explained in detail in Subsection 4.4.2.

4.4.4.2 Core Hydraulics

a. Flow Paths Considered in Core Pressure Drop and Thermal Design

The following flow paths for core bypass flow are considered:

1. Flow through the spray nozzles into the upper head for head cooling purposes.
2. Flow entering into the RCC guide thimbles to cool the control rods.
3. Leakage flow from the vessel inlet nozzle directly to the vessel outlet nozzle through the gap between the vessel and the barrel.
4. Flow introduced between the baffle and the barrel for the purpose of cooling these components and which is not considered available for core cooling.
5. Flow in the gaps between the fuel assemblies on the core periphery and the adjacent baffle wall.

The above contributions are evaluated to confirm that the design value of the core bypass flow is met. The design value of core bypass flow for Seabrook Station is equal to 6.3 percent of the total vessel flow when all thimble plugs are resident.

Of the total allowance, 2.0 percent is associated with the core, item 2 above, and the remainder is associated with the internals (items 1, 3, 4 and 5 above). Calculations have been performed using drawing tolerances on a worst case basis and accounting for uncertainties in pressure losses. Based on these calculations, the core bypass flow for the plant is < 6.3 percent when all thimble plugs are resident.

b. Inlet Flow Distributions

Data have been considered from several 1/7th scale hydraulic reactor model tests (References 23, 24, and 37) in arriving at the core inlet flow maldistribution criteria to be used in the VIPRE-01 analyses (see Subsection 4.4.4.5a).

The effect of the total flow rate on the inlet velocity distribution was studied in the experiments of Reference 23. As was expected, on the basis of the theoretical analysis, no significant variation could be found in inlet velocity distribution with reduced flow rate.

c. Empirical Friction Factor Correlations

Two empirical friction factor correlations are used in the VIPRE-01 computer code (described in Subsection 4.4.4.5a).

The friction factor in the axial direction, parallel to the fuel rod axis, is evaluated using the correlations described in Reference 81).

The flow in the lateral directions, normal to the fuel rod axis, views the reactor core as a large tube bank. Thus, the lateral friction factor proposed by Idel'chik (Reference 25) is applicable. This correlation is of the form:

$$F_L = A Re_L^{-0.2} \quad (4.4-12)$$

where:

A is a function of the rod pitch and diameter as given in Reference 25.

Re_L is the lateral Reynolds number based on the rod diameter.

4.4.4.3 Influence of Power Distribution

The core power distribution, which is largely established at beginning-of-life by fuel enrichment, loading pattern, and core power level is also a function of variables such as control rod worth and position, and fuel depletion throughout lifetime. Radial power distributions in various planes of the core are often illustrated for general interest; however, the core radial enthalpy rise distribution as determined by the integral of power up each channel is of greater importance for DNB analyses. These radial power distributions, characterized by $F_{\Delta H}^N$ (defined in paragraph 4.3.2.2.1), as well as axial heat flux profiles are discussed in the following two paragraphs.

4.4.4.3.1 Nuclear Enthalpy Rise Hot Channel Factor, $F_{\Delta H}^N$

Given the local power density q' (kW/ft) at a point x, y, z in a core with N fuel rods and height H ,

$$F_{\Delta H}^N = \frac{\text{hot rod power}}{\text{average rod power}} = \frac{\text{MAX} \int_0^H q'(x_0, y_0, z_0) dz}{\frac{1}{N} \sum_{\text{all rods}} \int_0^H q'(x, y, z) dz}$$

The way in which $F_{\Delta H}^N$ is used in the DNB calculation is important. The location of minimum DNBR depends on the axial profile, and the value of DNBR depends on the enthalpy rise to that point. Basically, the maximum value of the rod integral is used to identify the most likely rod for minimum DNBR. An axial power profile is obtained which, when normalized to the design value of $F_{\Delta H}^N$, recreates the axial heat flux along the limiting rod. The surrounding rods are assumed to have the same axial profile with rod average powers which are typical distributions found in hot assemblies. In this manner, worst-case axial profiles can be combined with worst-case radial distributions for reference DNB calculations.

It should be noted again that $F_{\Delta H}^N$ is an integral and is used as such in DNB calculations. Local heat fluxes are obtained by using hot channel and adjacent channel explicit power shapes which take into account variations in horizontal power shapes throughout the core.

For operation at a fraction of full power, the design $F_{\Delta H}^N$ used is given by:

$$F_{\Delta H}^N = F_{\Delta H}^{RTD} [1 + PF_{\Delta H} (1 - P)]$$

$F_{\Delta H}^{RTD}$ is the limit at rated thermal power (RTP) specified in the core Operating Limits Report (COLR).

$PF_{\Delta H}$ is the power factor multiplier for $F_{\Delta H}^N$ specified in the COLR.

P is the fraction of rated thermal power.

The permitted relaxation of $F_{\Delta H}^N$ is included in the DNB protection setpoints and allows radial power shape changes with rod insertion to the insertion limits, (Reference 84) thus allowing greater flexibility in the nuclear design.

4.4.4.3.2 Axial Heat Flux Distributions

As discussed in paragraph 4.3.2.2, the axial heat flux distribution can vary as a result of rod motion or power change or as a result of a spatial xenon transient which may occur in the axial direction. Consequently, it is necessary to measure the axial power imbalance by means of the excore nuclear detectors (as discussed in paragraph 4.3.2.2.7) and to protect the core from excessive axial power imbalance. The reference axial shape used in establishing core DNB limits (that is, overtemperature ΔT protection system setpoints) is a chopped cosine with a peak-to-average value of 1.55. The reactor trip system provides automatic reduction of the trip setpoints on excessive axial power imbalance. To determine the magnitude of the setpoint reduction, the reference shape is supplemented by other axial shapes skewed to the bottom and top of the core.

The course of those accidents in which DNB is a concern is analyzed in chapter 15 assuming that the protection setpoints have been set on the basis of these shapes. In many cases, the axial power distribution in the hot channel

changes throughout the course of the accident due to rod motion, coolant temperature, and power level changes.

The initial conditions for the accidents for which DNB protection is required are assumed to be those permissible within the specified axial offset control limits described in paragraph 4.3.2.2. In the case of the loss-of-flow accident, the hot channel heat flux profile is very similar to the power density profile in normal operation preceding the accident.

4.4.4.4 Core Thermal Response

A general summary of the steady state thermal-hydraulic design parameters including thermal output, flow rates, etc., is provided in Table 4.4-1 for all loops in operation.

As stated in Subsection 4.4.1, the design bases of the application are to prevent DNB and to prevent fuel melting for Condition I and II events. The protective systems described in Chapter 7 are designed to meet these bases. The response of the core to Condition II transients is given in Chapter 15.

4.4.4.5 Analytical Techniques

a. Core Analysis

The objective of reactor core thermal design is to determine the maximum heat-removal capability in all flow subchannels and to show that the core safety limits are not exceeded using the most conservative power distribution. The thermal design takes into account local variations in dimensions, power generation, flow redistribution, and mixing. VIPRE-01 is a realistic three-dimensional matrix model which has been developed to account for hydraulic and nuclear effects on the enthalpy rise in the core. (References 81 and 82) The behavior of the hot assembly is determined by superimposing the power distribution among the assemblies upon the inlet flow distribution while allowing for flow mixing and flow distribution between assemblies. The local variations in power, fuel rod and pellet fabrication, and mixing within the hottest assembly are superimposed on the average conditions of the hottest assembly in order to determine the conditions in the hot channel.

b. Steady State Analysis

The VIPRE-01 computer program and subchannel analysis methodology, as approved by the NRC (References 81 and 82) is used to determine coolant density, mass velocity, enthalpy, vapor void, static pressure, and DNBR distributions within the reactor core hot subchannel under all expected operating conditions. The VIPRE-01 code is described in detail in Reference 81, including models and correlations used.

c. Experimental Verification

Experimental verification of VIPRE-01 is presented in References 11 and 81.

The VIPRE-01 analysis methodology is based on a knowledge and understanding of the heat transfer and hydrodynamic behavior of the coolant flow and the mechanical characteristics of the fuel elements. VIPRE-01 analysis provides a realistic evaluation of the core performance and is used in the thermal analyses as described above.

d. Transient Analysis

The approved VIPRE-01 methodology (References 81 and 82) was shown to be conservative for transient thermal-hydraulic analysis.

4.4.4.6 Hydrodynamic and Flow Power Coupled Instability

Boiling flows may be susceptible to thermohydrodynamic instabilities, (Reference 69). These instabilities are undesirable in reactors since they may cause a change in thermohydraulic conditions that may lead to a reduction in the DNB heat flux relative to that observed during a steady flow condition or to undesired forced vibrations of core components. Therefore, a thermohydraulic design criterion was developed which states that modes of operation under Conditions I and II events shall not lead to thermohydrodynamic instabilities.

Two specific types of flow instabilities are considered for Westinghouse PWR operation. These are the Ledinegg or flow excursion type of static instability and the density wave type of dynamic instability.

A Ledinegg instability involves a sudden change in flow rate from one steady state to another. This instability occurs (Reference 69) when the slope of the reactor coolant system pressure drop-flow rate curve ($\delta\Delta P/\delta G$ internal) becomes algebraically smaller than the loop supply (pump head) pressure drop-flow rate curve ($\delta\Delta P/\delta G$ external). The criterion for stability is thus ($\delta\Delta P/\delta G$ internal $>$ $\delta\Delta P/\delta G$ external). The Westinghouse pump head curve has a negative slope ($\delta\Delta P/\delta G_{\text{external}} < 0$) whereas the reactor coolant system pressure drop-flow rate curve has a positive slope ($\delta\Delta P/\delta G$ internal $>$ 0) over the Condition I and Condition II operational ranges. Thus, the Ledinegg instability will not occur.

The mechanism of density wave oscillations in a heated channel has been described by Lahey and Moody (Reference 70). Briefly, an inlet flow fluctuation produces an enthalpy perturbation. This perturbs the length and the pressure drop of the single phase region and causes quality or void perturbations in the two phase regions which travel up the channel with the flow. The quality and length perturbations in the two-phase region create

two-phase pressure drop perturbations. However, since the total pressure drop across the core is maintained by the characteristics of the fluid system external to the core, then the two-phase pressure drop perturbation feeds back to the single phase region. These resulting perturbations can be either attenuated or self-sustained.

A simple method has been developed by Ishii (Reference 71) for parallel closed channel systems to evaluate whether a given condition is stable with respect to the density wave type of dynamic instability. This method has been used to assess the stability of typical Westinghouse reactor designs (References 72, 73, 74), under Conditions I and II operation. The results indicate that a large margin to density wave instability exists, e.g., increases on the order of 150 to 200 percent of rated reactor power would be required for the predicted inception of this type of instability.

The application of the method of Ishii, Reference 71, to Westinghouse reactor designs is conservative due to the parallel open channel feature of Westinghouse PWR cores. For such cores, there is little resistance to lateral flow leaving the flow channels of high power density. There is also energy transfer from channels of high power density to lower power density channels. This coupling with cooler channels has led to the opinion that an open channel configuration is more stable than the above closed channel analysis under the same boundary conditions. Flow stability tests (Reference 75) have been conducted where the closed channel systems were shown to be less stable than when the same channels were cross connected at several locations. The cross connections were such that the resistance to channel-to-channel cross flow and enthalpy perturbations would be greater than that which would exist in a PWR core which has a relatively low resistance to cross flow.

Flow instabilities which have been observed have occurred almost exclusively in closed channel systems operating at low pressures relative to the Westinghouse PWR operating pressures. Kao, Morgan and Parker (Reference 76) analyze parallel closed channel stability experiments simulating a reactor core flow. These experiments were conducted at pressures up to 2200 psia. The results showed that for flow and power levels typical of power reactor conditions, no flow oscillations could be induced above 1200 psia.

Additional evidence that flow instabilities do not adversely affect thermal margin is provided by the data from the rod bundle DNB tests. Many Westinghouse rod bundles have been tested over wide ranges of operating conditions with no evidence of premature DNB or of inconsistent data which might be indicative of flow instabilities in the rod bundle.

In summary, it is concluded that thermohydrodynamic instabilities will not occur under Condition I and II modes of operation for Westinghouse PWR reactor designs. A large power margin, greater than doubling rated power, exists to predicted inception of such instabilities. Analysis has been performed which shows that minor plant to plant differences in Westinghouse reactor design such as fuel assembly arrays, core power to flow ratios, fuel assembly length, etc., will not result in gross deterioration of the above power margins.

4.4.4.7 Fuel Rod Behavior Effects from Coolant Flow Blockage

Coolant flow blockages can occur within the coolant channels of a fuel assembly or external to the reactor core. The effects of fuel assembly blockage within the assembly on fuel rod behavior is more pronounced than external blockages of the same magnitude. In both cases, the flow blockages cause local reductions in coolant flow. The amount of local flow reduction, where it occurs in the reactor, and how far along the flow stream the reduction persists are considerations which will influence the fuel rod behavior. The effects of coolant flow blockages in terms of maintaining rated core performance are determined both by analytical and experimental methods. The experimental data are usually used to augment analytical tools such as computer programs. Inspection of the DNB correlation (Subsection 4.4.2.2 and Reference 8) shows that the predicted DNBR is dependent upon the local values of quality and mass velocity.

Thermal-hydraulic codes are capable of predicting the effects of local flow blockages on DNBR within the fuel assembly on a subchannel basis, regardless of where the flow blockage occurs. In Reference 19, it is shown that for a fuel assembly similar to the Westinghouse design, the flow distribution within the fuel assembly when the inlet nozzle is completely blocked can be accurately predicted. Full recovery of the flow was found to occur about 30 inches downstream of the blockage. With the reference reactor operating at the nominal full power conditions specified in Table 4.4-1, the effects of an increase in enthalpy and decrease in mass velocity in the lower portion of the fuel assembly would not result in the reactor reaching a minimum DNBR below the safety analysis limit.

From a review of the open literature it is concluded that flow blockage in "open lattice cores" similar to the Westinghouse cores cause flow perturbations which are local to the blockage. For instance, A. Ohtsubol, et al. (Reference 77), show that the mean bundle velocity is approached asymptotically about 4 inches downstream from a flow blockage in a single flow cell. Similar results were also found for 2 and 3 cells completely blocked. P. Basmer, et al. (Reference 78) tested an open lattice fuel assembly in which 41 percent of the subchannels were completely blocked in the center of the test bundle between spacer grids. Their results show the stagnant zone behind the flow blockage essentially disappears after 1.65 L/De or about 5 inches for their test bundle. They also found that leakage flow through the blockage tended to shorten the stagnant zone or, in essence the complete recovery length. Thus, local flow blockages within a fuel assembly have little effect on subchannel enthalpy rise. The reduction in local mass velocity is the main parameter which affects the DNBR. Westinghouse analysis results presented in the original Seabrook FSAR demonstrated that if the plant was operating at full power and nominal steady state conditions as specified in Table 4.4-1, a substantial reduction in local mass velocity would be required to reduce the DNBR close to the DNBR Safety Analysis Limits. The above mass velocity effect on the DNB correlation was based on the assumption of fully developed flow along the full channel length. In reality, a local flow blockage is expected

to promote turbulence and thus would likely not effect DNBR at all.

Coolant flow blockages induce local crossflows as well as promote turbulence. Fuel rod behavior is changed under the influence of a sufficiently high crossflow component. Fuel rod vibration could occur, caused by this crossflow component, through vortex shedding or turbulent mechanisms. If the crossflow velocity exceeds the limit established for fluid elastic stability, large amplitude whirling results. The limits for a controlled vibration mechanism are established from studies of vortex shedding and turbulent pressure fluctuations. The crossflow velocity required to exceed fluid elastic stability limits is dependent on the axial location of the blockage and the characterization of the crossflow (jet flow or not). These limits are greater than those for vibratory fuel rod wear. Crossflow velocity above the established limits can lead to mechanical wear of the fuel rods at the grid support locations. Fuel rod wear due to flow induced vibration is considered in the fuel rod fretting evaluation (Section 4.2).

4.4.5 Testing and Verification

4.4.5.1 Tests Prior to Initial Criticality

A reactor coolant flow test was performed following fuel loading but prior to initial criticality. Elbow tap pressure drop data obtained in this test allowed determination of the coolant flow rates at reactor operating conditions. This test verified that conservative coolant flow rates have been used in the core thermal and hydraulic analysis.

4.4.5.2 Initial Power and Plant Operation

Core power distribution measurements are made at several core power levels (see Chapter 14). These tests are used to insure that conservative peaking factors are used in the core thermal and hydraulic analysis.

4.4.5.3 Component and Fuel Inspections

Inspections performed on the manufactured fuel are delineated in Subsection 4.2.4. Fabrication measurements critical to thermal and hydraulic analysis are obtained to verify that the engineering hot channel factors in the design analyses (Subsection 4.4.2.2d) are met.

4.4.6 Instrumentation Requirements

4.4.6.1 Incore Instrumentation

Instrumentation is located in the core so that radial, axial, and azimuthal core characteristics may be obtained for all core quadrants.

The incore instrumentation thimbles enter the core from the bottom and are positioned in the full length instrumentation guide tubes that are located in the center of the fuel assemblies. Figure 4.4-7 shows the location of the 58 instrumented assemblies in the core. Each thimble consists of the calibration tube for the moveable incore detectors, five fixed platinum detectors at various core heights, and a core-exit thermocouple at the tip of the thimble. The platinum detectors measure the gamma and neutron flux and are processed to determine the local power distribution. Each thermocouple measures the temperature of the fluid in the guide tube that is heated by conduction from the bulk core fluid and by gamma heating of the components in the guide tube.

The core-exit thermocouples provide a backup to the flux monitoring instrumentation for monitoring power distribution. The routine, systematic collection of thermocouple readings by the main plant computer system provides a data base. From this data base, abnormally high or abnormally low readings, quadrant temperature tilts, or systematic departures from a prior reference map can be deduced.

The Incore Detector System would be used for more detailed mapping if the thermocouple system were to indicate an abnormality. These two complementary systems are more useful when taken together than either system alone would be. The Incore Instrumentation System is described in more detail in Subsection 7.7.1.9.

The incore instrumentation is provided to obtain data from which fission power density distribution in the core, coolant enthalpy distribution in the core, and fuel burnup distribution may be determined.

4.4.6.2 Overtemperature and Overpower ΔT Instrumentation

The Overtemperature ΔT trip protects the core against low DNBR. The Overpower ΔT trip protects against excessive power (fuel rod rating protection).

As discussed in Subsection 7.2.1.1b, factors included in establishing the Overtemperature ΔT and Overpower ΔT trip setpoints include the reactor coolant temperature in each loop and the axial distribution of core power through the use of the two section excore neutron detectors.

4.4.6.3 Instrumentation to Limit Maximum Power Output

The output of the three ranges (source, intermediate, and power) of detectors, with the electronics of the nuclear instruments, is used to limit the maximum power output of the reactor within their respective ranges.

There are six radial locations containing a total of eight neutron flux detectors installed around the reactor in the primary shield, two proportional counters for the source range installed on opposite "flat" portions of the core containing the primary startup sources at an elevation approximately one quarter of the core height. Two compensated ionization chambers for the

intermediate range, located in the same instrument wells and detector assemblies as the source range detectors, are positioned at an elevation corresponding to one half of the core height; four dual section uncompensated ionization chamber assemblies for the power range installed vertically at the four corners of the core and located equidistant from the reactor vessel at all points and, to minimize neutron flux pattern distortions, within one foot of the reactor vessel. Each power range detector provides two signals corresponding to the neutron flux in the upper and in the lower sections of a core quadrant. The three ranges of detectors are used as inputs to monitor neutron flux from a completely shutdown condition to 120 percent of full power with the capability of recording overpower excursions up to 200 percent of full power.

The output of the power range channels is used for:

- a. The rod speed control function
- b. To alert the operator to an excessive power unbalance between the quadrants
- c. To protect the core against rod ejection accidents
- d. To protect the core against adverse power distributions resulting from dropped rods.

Details of the neutron detectors and nuclear instrumentation design and the control and trip logic are given in Chapter 7. The limits on neutron flux operation and trip setpoints are given in the Technical Specifications and Core Operating Limits Report.

4.4.6.4 Loose Parts Monitoring System (LPMS)

The LPMS is a system provided for the detection of loose metallic parts in the primary system during preoperational testing, startup and power operation modes. The LPMS, together with the associated programmatic and reporting procedures, comprise the Loose Part Detection Program described in Regulatory Guide 1.133, Rev. 1.

A detailed comparison of the LPMS with each of the specific positions of Section C of Regulatory Guide 1.133 is presented below.

Reg. Guide Position

Discussion

- | | |
|-------|---|
| C.1.a | A total of sixteen loose part sensors are provided to detect loose part impacts with a kinetic energy of 0.5 ft-lb. of parts weighing between .25 lb. and 30 lbs. in the vicinity of six natural collection regions in the nuclear steam supply system. |
| C.1.b | |

Reg. Guide
PositionDiscussion

- a) Two sensors on the exterior of the reactor vessel in the vicinity of the lower plenum and two sensors on the reactor vessel head lifting lugs.
- b) Three sensors on the exterior of each steam generator in the vicinity of the reactor coolant inlet plenum. Two sensors are normally active and one is normally passive. The normally passive sensor may be switched into the system to replace a normally active sensor or to aid in the localization of a loose part in a steam generator.

C.1.c

Two or more independently monitored sensors are provided at each natural collection region. Each of these channels is physically separated from each other at the sensors up to and including the charge converters. From there, sensor signals are routed by individual shielded cables through seismically qualified conduit and tray associated with safety-related Train A up to penetration EDE-MM-126. Outside containment, all signal cabling is routed in seismically qualified tray associated with safety-related Train A up to the control room electronics.

C.1.d

C.4.e

The Automatic Data Acquisition System of the LPMS will be actuated (all active channels simultaneously) by the system electronics when the measured magnitude of the acoustic signal from any one channel exceeds the predetermined alert level for that channel. An audible alarm will alert control room personnel of any excursion above the predetermined alert level.

To ensure that the data provided at the output of the system electronics is recorded to allow accurate offline analysis, the recorder is wide-band with respect to the bandwidth of the filtered data. The analog recorder provided will use the direct (as opposed to FM) recording mode. Two selectable tape speeds are provided, allowing selection of recording bandwidth.

The Automatic Data Acquisition System has a manual override.

Reg. Guide
PositionDiscussion

- C.1.e
C.2
C.3
- c.4.b
- a) Minimization of false alarms due to flow or other disturbances not indicative of metallic loose part impacts.
- b) Maintenance of sensitivity to metallic loose part impacts under conditions of varying background noise.
- c) The signal filtering process attenuates the signals due to operational disturbances outside the filter system's bandwidth.
- d) The alert logic is capable of functioning satisfactorily in varying background noise levels.
- e) To differentiate between valid impacts and plant noise associated with one-time transient events (as opposed to steady state noise), the alert module common to each group of six electronic channels of the LPMS incorporates a variable timer circuit. The alert module will not perform its functions (alarm actuation and automatic recorder actuation) unless a predetermined number of impacts (excursions above the alert level) occur within a predetermined time period. This time circuit may be disabled, by use of a selector switch, so that any single excursion above the alert level will cause the alarm module to perform its functions.
- f) To vary the alert level from one sensor to the other to compensate for various background noises at each sensor location.

The alert level for each channel is a function of the steady state background noises measured by that channel, according to the relation:

$$AL = (1 + K) BN$$

Where AL is the alert level, BN is the background noise level, and K is the fraction of the background noise level by which an impact must exceed the background in order to be detected.

Reg. Guide
PositionDiscussion

The K value was individually determined for each channel following initial system calibration. The K value for each channel was initially determined within two constraints:

- a) The value $(1 + K) BN$ shall be greater than the largest signal presented to the impact detection module when noise of magnitude BN is applied to the input terminals of the system electronics, as determined by factory acceptance testing of the LPMS and in situ monitoring of the signals presented to each impact detector.
- b) The value $(1 + K) BN$ (for the largest expected BN level) shall be less than the magnitude of the signal associated with the specified detectable loose part impact, as determined during initial LPMS calibration.
- c) The minimum value of K consistent with the above criterion (a) was chosen and the satisfaction of criterion (b) was then verified. Satisfaction of these criteria will be periodically verified during operation in accordance with Regulatory Position 3.e of Regulatory Guide 1.133.

The alert level for power operation was submitted to the commission (in the startup report) following completion of the startup test program.

If the alert level is exceeded, diagnostic steps will be taken within 72 hours to determine if a loose part is present. The safety significance of any identified loose part will be determined.

During initial startup, power operation and refueling, channel checks, monitoring audio channels, channel functional tests, background noise measurements, and channel calibrations will be performed as prescribed in the regulatory guide. A channel calibration includes the adjustments recommended by the vendor and an assessment of the overall channel response by observing the response to a known mechanical input or by comparing the background noise spectra to baseline background noise spectra.

Calibration equipment and procedures are available for review at Seabrook Station.

Reg. Guide
PositionDiscussion

- C.1.f The LPMS has the capability for periodic on-line channel checks and channel functional tests in addition to on-line and off-line channel calibration.
- C.1.g The LPMS is designed to operate under normal environmental conditions.
C.4.k
- The LPMS (excluding the recording equipment) has been seismically qualified to IEEE 344-75 to be functional up to and including the Operating Basis Earthquake (OBE). The LPMS sensor, charge converter, and system cabinet are seismically supported.
- C.1.h The LPMS will be included in the Seabrook surveillance and maintenance program. Any components that are not qualified for 40 years will be replaced prior to the end of their service life. Maintenance actions will be performed in accordance with approved procedures. The documented maintenance history results will be maintained and evaluated over the life of the plant.
- C.1.i Recognition of a faulty channel is easily identified by a blinking LED condition. All Control Room electronics are rack-mounted, designed for the ease of replacement or repair in the event of a malfunctioning channel.
- C.4.a The loose parts monitoring sensors are piezoelectric accelerometers designed for use in high temperature and high radiation environments.
- Two accelerometers are mounted on the reactor vessel head. These accelerometers are mounted into two of the vessel head lifting lugs. Two accelerometers are threaded into clamps on the bottom-mounted instrumentation tubes. These locations allow monitoring of the reactor vessel upper and lower plenums and facilitated the mounting of the sensors.
- There are three accelerometers on each steam generator, two which are normally active and the third normally passive. The two normally active sensors are located in a vertical line approximately 16 inches above and below the centerline of the tube sheet, oriented 20° on the hot leg side of the tube lane centerline. The normally passive accelerometer is located on the tube sheet centerline 90° from the other sensors but still on the hot leg side of the tube lane centerline. These accelerometers are mounted on the side of the steam generator. All steam generator sensors are capable of monitoring the

Reg. Guide
Position

Discussion

- steam generator reactor coolant inlet plenum. They are dispersed to assist in localization of a loose part.
- C.4.c Anticipated major sources of external and internal noises are pump starts, reactor trip, and control rod stepping.
- C.4.d By meeting the criteria as defined in position C.3, the acquisition of quality data is ensured.
- C.4.f Operability and surveillance requirements for the LPMS are
C.5 included in Technical Requirements Manual.
- C.4.g Seabrook procedures provide a diagnostic program using information from other plant systems and operating history to confirm the presence of a loose part.
- C.4.h The procedures for performing channel check, channel functional test, and background noise measurements are available at Seabrook Station.
- C.4.i Radiation protection procedures have been developed to provide guidance and direction to station personnel for minimizing radiation exposure during maintenance, calibration, and diagnostic work activities. The overall radiation protection program is described in the Updated FSAR Chapter 12.
- C.4.j Seabrook's non-licensed training program provides pertinent training for plant personnel involved with system operation, and maintenance. Loose part diagnosis is performed by an organization qualified to interpret loose part data.
- C.6 If the presence of a loose part is confirmed and is evaluated to have safety significance, it will be reported to the NRC in accordance with 10 CFR 50.72.

4.4.6.5 Instrumentation for Detection of Inadequate Core Cooling

The Inadequate Core Cooling Monitoring System installed at Seabrook Station includes the following:

- Core Exit Thermocouple Monitoring
- Core Subcooling Margin Monitor
- Reactor Vessel Level Monitoring

The inadequate core cooling monitor provides improved information presentation and display to the plant operators on the status of core heat removal capability. The system monitors core exit thermocouples and wide-range reactor pressure and calculates core subcooling margin utilizing redundant

channels of instrumentation and control room displays.

The monitoring system displays several levels of information including: (a) bulk average core exit thermocouple trending (b) a spatial map exhibiting the thermocouple temperature at its respective location in the core (c) a core map showing minimum, average, and maximum quadrant temperatures (d) subcooling margin (e) a detailed data list exhibiting thermocouple location, tag designation, temperature; and (f) hot channel core exit temperature.

The Reactor Vessel Level Instrumentation System (RVLIS) consists of two redundant independent trains that monitor the reactor vessel water levels. Each train provides two vessel level indications: full range and dynamic head. The full range RVLIS reading provides an indication of reactor vessel water level from the bottom of the vessel to the top of the vessel during natural circulation conditions. The dynamic head reading provides an indication of reactor core, internals, and outlet nozzle pressure drop for any combination of operating reactor coolant pumps. Comparison of the measured pressure drop with the normal, single phase pressure drop provides an approximate indication of the relative void content of the circulating fluid.

4.4.6.6 Instrumentation for Mid-loop Operation

Generic Letter 88-17, "Loss of Decay Heat Removal," recommended that licensees implement certain actions prior to operation in a reduced Reactor Coolant System (RCS) inventory condition with irradiated fuel in the core. The concern stated in the Generic Letter is the potential consequences involved in preventing and recovering from loss of shutdown cooling while operating in a reduced inventory condition. The NRC recommended expeditious action and programmed enhancements to maintain sufficient equipment in an operable or available status so as to mitigate a loss of shutdown cooling or RCS inventory should they occur. Reduced inventory is defined by the NRC to be an RCS level lower than three feet below the reactor vessel flange.

In response to the NRC recommendations, the design includes (1) reliable indications of parameters that describe the state of the RCS and the performance of systems normally used to cool the RCS for both normal and accident conditions, (2) procedures to cover reduced inventory operation and (3) provisions for alternate sources of inventory for addition if necessary. The following is a brief description of the plant equipment, instrumentation and procedures that are used to comply with the recommendations of Generic Letter 88-17:

Reactor Coolant System Level Monitoring: At least two diverse RCS level indications are operational during reduced inventory conditions with irradiated fuel in the core. Continuous level indications are monitored in the Control Room and audible alarms sound on inadvertent transition in RCS level from the existing operating condition. The RCS level instrumentation consists of an RCS sight glass, wide range level indication provided by differential pressure measurement and three diverse narrow range level indicators provided by ultrasonic measurements (2) and differential pressure measurement (1). With exception of the sight glass, the RCS level

instrumentation provides diverse indication, trend and low-level alarm capability in the control room via the Main Plant Computer System (MPCS) during all phases of operation under reduced inventory.

Reactor Coolant System Temperature Monitoring: When the reactor vessel head is located on the reactor vessel, two independent core exit temperature measurements are demonstrated to be operable prior to draining the RCS down to reduced inventory. The core exit temperature measurements are provided using the core exit thermocouple portion of the redundant Class 1E safety-related Inadequate Core Cooling Monitor.

Thermocouple readings are displayed on the Main Control Board and input into the MPCS. Mid-loop high temperature alarms are provided by the MPCS based on selection of the maximum reliable thermocouple temperature.

Residual Heat Removal System Performance: Continuous monitoring and trend capability of Residual Heat Removal System performance is provided in the Control Room by the MPCS. The RHR system parameters that are monitored include RHR loop flow, RHR heat exchanger inlet and outlet temperatures, RHR pump suction pressures and RHR pump motor current indications.

Administrative Controls: Controls are in place to implement specific actions to be taken when draining the RCS with irradiated fuel in the core. Required actions are based on the Westinghouse Owners Group reduced inventory project guidance and plant specific analyses. Plant procedures include the necessary information to determine equipment and/or operational requirements and limitations, including:

1. Prior to entry into a reduced inventory condition, controls are established to provide reasonable assurance that containment closure can be achieved before core is uncovered as a result of loss of decay heat removal. With the exception of penetrations that are in use or undergoing maintenance which are administratively controlled, at least one boundary of each containment penetration is maintained intact during reduced inventory operation. In the event of a loss of decay heat removal, administratively controlled penetrations are closed.
2. Prior to entering a reduced inventory condition, communication is established between the control room and a local nuclear systems operator in containment.
3. When operating at reduced inventory with steam generator nozzle dams in place, one centrifugal charging pump and one safety injection pump are available with a specified flow path to the reactor core. A gravity flow path from the Reactor Water Storage Tank (RWST) to the RCS is also made available as a secondary source. An adequate vent is provided to preclude RCS pressurization that could prevent gravity feed from the RWST and/or damage to the steam generator nozzle dams. Administrative controls assure availability of the

redundant centrifugal charging and safety injection pumps upon unavailability of the operable pump.

4. When operating at reduced inventory with nozzle dams removed and the RCS vent closed for evacuation and fill, one centrifugal charging pump and one safety injection pump are available with specified flow paths to the reactor core. A gravity feed flow path from the RWST is also available for inventory addition as a secondary source. Administrative controls assure availability of the redundant centrifugal charging and safety injection pumps upon unavailability of the operable pump.

4.4.7 References

1. Christensen, J. A., Allio, R. J. and Biancheria, A., "Melting Point of Irradiated UO₂," WCAP-6065, February 1965.
2. Hellman, J. M. (Ed.), "Fuel Densification Experimental Results and Model for Reactor Application," WCAP-8218-P-A (Proprietary), March 1975 and WCAP-8219-A, March 1975.
3. Tong, L. S., "Boiling Crisis and Critical Heat Flux," AEC Critical Review Series, TID-25887, 1972.
4. "Evaluation of Westinghouse Request for Generic Approval", ENCLOSURE to letter from Carl Berlinger (NRC) to E. P. Rahe, Jr., (Westinghouse), "Request for Reduction in Fuel Assembly Burnup Limit for Calculation of Maximum Rod Bow Penalty", dated June 18, 1986.
5. Not used
6. Not Used
7. WCAP-8762-P-A, "New Westinghouse Correlation WRB-1 for Predicting Critical Heat Flux in Rod Bundles With Mixing Vane Grids", Westinghouse Electric Corporation, F. E. Motley, July 1984.
8. Tong, L. S., "Prediction of Departure from Nucleate Boiling for an Axially Non-Uniform Heat Flux Distribution," J. Nucl. Energy, 21, 241-248 (1967).
9. Tuley, C. R., Williams, T. P.; and Reagan, J. R., "Westinghouse Revised Thermal Design Procedure Instrument Uncertainty Methodology for North Atlantic Energy Service Corp. Seabrook Nuclear Power Station Unit 1, 24 month fuel cycle evaluation WCAP-14829," June 1998
10. Not used

11. NP-2511-CCM Volumes 1-5, "VIPRE-01: A Thermal-Hydraulic Code for Reactor Cores", Electric Power Research Institute.
12. Cadek, F. F., Motley, F. E. and Dominicis, D. P., "Effect of Axial Spacing on Interchannel Thermal Mixing with the R Mixing Vane Grid," WCAP-7941-P-A (Proprietary), January 1975 and WCAP-7959-A, January 1975.
13. Rowe, D. S., Angle, C. W., "Crossflow Mixing Between Parallel Flow Channels During Boiling, Part II Measurements of Flow and Enthalpy in Two Parallel Channels," BNWL-371, part 2, December 1967.
14. Rowe, D. S., Angle, C. W., "Crossflow Mixing Between Parallel Flow Channels During Boiling, Part III Effect of Spacers on Mixing Between Two Channels," BNWL-371, part 3, January 1969.
15. Gonzalez-Santalo, J. M. and Griffith, P., "Two-Phase Flow Mixing in Rod Bundle Subchannels," ASME Paper 72-WA/NE-19.
16. Motley, F. E., Wenzel A. H., Cadek, F. F., "The Effect of 17x17 Fuel Assembly Geometry on Interchannel Thermal Mixing," WCAP-8298-P-A (Proprietary), January 1975 and WCAP-8299-A, January 1975.
17. Cadek, F. F., "Interchannel Thermal Mixing Vane Grids," WCAP-7667-P-A (Proprietary), January 1975 and WCAP-7755-A, January 1975.
18. Hochreiter, L. F., "Application of the THINC-IV Program to PWR Design," WCAP-8054 (Proprietary), October 1973, and WCAP-8195, October 1973.
19. Hochreiter, L. E., Chelemer, H. and Chu, P. T., "THINC-IV An Improved Program for Thermal-Hydraulic Analysis of Rod Bundle Cores," WCAP-7956, June 1973.
20. Dittus, F. W., and Boelter, L. M. K., "Heat Transfer in Automobile Radiators of the Tubular Type," Calif. Univ. Publication In Eng., 2, No. 13, 443461 (1930).
21. Weisman, J., "Heat Transfer to Water Flowing Parallel to Tube Bundles," Nucl. Sci. Eng., 6, 78-79 (1959).
22. Thom, J. R. S., Walker, W. M., Fallon, T. A. and Reising, G. F. S., "Boiling in Sub-Cooled Water During Flow up Heated Tubes or Annuli," Proc. Instn. Mech. Engrs., 180, Pt. C, 226-46 (1955-66).
23. Hetsroni, G., "Hydraulic Tests of the San Onofre Reactor Model," WCAP-3269-8, June 1964.
24. Hetsroni, G., "Studies of the Connecticut-Yankee Hydraulic Model," NYO-3250-2, June 1965.

25. Idel'chik, I. E., "Handbook of Hydraulic Resistance," AEC-TR-6630, 1960.
26. Moody, L. F., "Friction Factors for Pipe Flow," Transaction of the American Society of Mechanical Engineers, 66, 671-684 (1944).
27. Maurer, G. W., "A Method of Predicting Steady State Boiling Vapor Fractions in Reactor Coolant Channels," WAPD-BT-19, pp. 59-70. June 1960.
28. Griffith, P., Clark, J. A. and Rohsenow W. M., "Void Volumes in Subcooled Boiling Systems," ASME Paper No. 58-HT-19.
29. Bowring, R. W., "Physical Model, Based on Bubble Detachment, and Calculation of Steam Voidage in the Subcooled Region of a Heated Channel," HPR-10, December 1962.
30. Not used
31. Not used
32. Not used
33. Not used
34. Not used
35. Not used
36. International Atomic Energy Agency, "Thermal Conductivity of Uranium Dioxide," Report of the Panel held in Vienna, April 1965, IAEA Technical Reports Series, No. 59, Vienna, The Agency, 1966.
37. Carter, F. D., "Inlet Orificing of Open PWR Cores," WCAP-9004, January 1969 (Proprietary) and WCAP-7836, January 1972 (Nonproprietary).
38. Novendstern, E. H. and Sandberg, R. O., "Single Phase Local Boiling and Bulk Boiling Pressure Drop Correlations," WCAP-2850 (Proprietary), April 1966 and WCAP-7916, June 1972.
39. Not used
40. Kjaerheim, G., and Rolstad, E., "In-Pile Determination of UO₂ Thermal Conductivity, Density Effects, and Gap conductance," HPR-80, December 1967.

41. Kjaerheim, G., In-Pile Measurements of Center Fuel Temperatures and Thermal Conductivity Determination of Oxide Fuels, Paper IFA-175 Presented at the European Atomic Energy Society Symposium on Performance Experience of Water-Cooled Power Reactor Fuel, Stockholm, Sweden, October 1969.
42. Cohen, I., Lustman, B., and Eichenberg, D., "Measurement of the Thermal Conductivity of Metal-Clad Uranium Oxide Rods During Irradiation," WAPD-228, 1960.
43. Clough, D. J., and Sayers, J. B., "The Measurement of the Thermal Conductivity of UO_2 under Irradiation in the Temperature Range 150° to $1600^\circ C$," AERE-R-4690, UKAEA Research Group, Harwell, December 1964.
44. Stora, J. P., et al., "Thermal Conductivity of Sintered Uranium Oxide under In-Pile Conditions," EURAE-1095, 1964.
45. Devold, I., "A Study of the Temperature Distribution in UO_2 Reactor Fuel Elements," AE-318, Aktiebolaget Atomenergi, Stockholm, Sweden, 1968.
46. Balfour, M. G., Christensen, J. A., and Ferrari, H. M., "In-Pile Measurement of UO_2 Thermal Conductivity," WCAP-2923, 1966.
47. Howard, V. C., and Gulvin, T. G., "Thermal Conductivity Determinations on Uranium Dioxide by a Radial Flow Method," UKAEA IG-Report 51, November 1960.
48. Lucks, C. F., and Deem, H. W., "Thermal Conductivity and Electrical Conductivity of UO_2 ," in Progress Reports Relating to Civilian Applications, BMI-1448 (Revised) for June 1960, BNI-1489 (Revised) for December 1960, and BMI-1518 (Revised) for May 1961.
49. Daniel, J. L., Matolich, J., Jr., and Deem, H. W., "Thermal Conductivity of UO_2 " HW-69945, September 1962.
50. Feith, A. D., "Thermal Conductivity of UO_2 by a Radial Heat Flow Method," TID-21668, 1962.
51. Vogt, J., Grandell, L., and Runfors, U., "Determination of the Thermal Conductivity of Unirradiated Uranium Dioxide," AB Atomenergi Report RMB-527, 1964, Quoted by IAEA Technical Report Series No. 59, "Thermal Conductivity of Uranium Dioxide."
52. Nishijima, T., Kawada, T., and Ishihata, A., "Thermal Conductivity of Sintered UO_2 and Al_2O_3 at High Temperatures," Journal of the American Ceramic Society 48, pp 31-34, 1965.

53. Ainscough, J. B., and Wheeler, M. J., "Thermal Diffusivity and Thermal Conductivity of Sintered Uranium Dioxide, "Proceedings of the Seventh Conference of Thermal Conductivity, National Institute of Standards and Technology, Washington, p 467, 1968.
 54. Godfrey, T. G., et al., "Thermal Conductivity of Uranium Dioxide and Armco Iron by an Improved Radial Heat Flow Technique," ORNL-3556, June 1964.
 55. Stora, J. P., et al., "Thermal Conductivity of Sintered Uranium Oxide Under In-Pile Conditions," EURAE-1095, August 1964.
 56. Bush, A. J., "Apparatus for Measuring Thermal Conductivity to 2500°C," Report 64-1P6-401-43 (Proprietary), Westinghouse Research Laboratories, February 1965.
 57. Asamoto, R. R., Anselin, F. L., and Conti, A. E., "The Effect of Density on the Thermal Conductivity of Uranium Dioxide," GEAP-5493, April 1968.
 58. Kruger, O. L., Heat Transfer Properties of Uranium and Plutonium Dioxide, Paper 11-N-68F, Presented at the Fall Meeting of Nuclear Division of American Ceramic Society, Pittsburgh, September 1968.
 59. Leech, W. J., et al., "Revised PAD Code Thermal Safety Model, WCAP-8720, Addendum 2, October 1982.
 60. Duncan, R. N., "Rabbit Capsule Irradiation of U₂," CVTR Project, CVNA-142, June 1962.
 61. Nelson, R. C., et al., "Fission Gas Release from UO₂ Fuel Rods with Gross Central Melting," GEAP-4572, July 1964.
 62. Poncelet, C. G., "Burnup Physics of Heterogeneous Reactor Lattices," WCAP-6069, June 1965.
 63. Nodvick, R. J., "Saxton Core II Fuel Performance Evaluation," WCAP-3385-56, Part II, "Evaluation of Mass Spectrometric and Radiochemical Analyses of Irradiated Saxton Plutonium Fuel," July 1970.
 64. Weiner, R. A., et al., "Improved Fuel Performance Models for Westinghouse Fuel Rod Design and Safety Evaluation," WCAP-10851-P-A, August 1988.
- References 65 through 68 are not used.
69. J. A. Boure, A. E. Bergles, and L. S. Tong, "Review of Two-Phase Flow Instability," Nucl. Engr. Design 25 (1973) p. 165-192.

70. R. T. Lahey and F. J. Moody, "The Thermal Hydraulics of a Boiling Water Reactor," American Nuclear Society, 1977.
71. P. Saha, M. Ishii, and N. Zuber, "An Experimental Investigation of the Thermally Induced Flow Oscillations in Two-Phase Systems," J. of Heat Transfer, Nov. 1976, pp. 616-662.
72. Virgil C. Summer FSAR, Docket #50-395.
73. Byron/Braidwood FSAR, Docket #50-456.
74. South Texas FSAR, Docket #50-498.
75. S. Kakac, T. N. Veziroglu, K. Akyuzlu, O. Berkol, "Sustained and Transient Boiling Flow Instabilities in a Cross-Connected Four-Parallel-Channel Upflow System," Proc. of 5th International Heat Transfer Conference, Tokyo, Sept. 3-7, 1974.
76. H. S. Kao, C. D. Morgan, and W. B. Parker, "Prediction of Flow Oscillation in Reactor Core Channel," Trans. ANS, Vol. 16, 1973, pp. 212-213.
77. Ohtsubo A., and Uruwashi, S., "Stagnant Fluid due to Local Flow Blockage," J. Nucl. Sci. Technol., 9, No. 7, 433-434, (1972).
78. Basmer, P., Kirsh, D. and Schultheiss, G. F., "Investigation of the Flow Pattern in the Recirculation Zone Downstream of Local Coolant Blockages in Pin Bundles," Atomwirtschaft, 17, No. 8, 416-417, (1972). (In German).
79. Not used
80. Davidson, S. L. (Editor), "Reference Core Report - VANTAGE 5 Fuel Assembly," WCAP-10444-P-A, September 1985, "VANTAGE 5H Fuel Assembly," WCAP-10444-P-A, Addendum 2-A, April 1988.
81. WCAP-14565, "VIPRE-01 Modeling and Qualification for Pressurized Water Reactor Non-LOCA Thermal-Hydraulic Safety Analysis," Y X Sung, et al., April 1997.
82. Letter from T. H. Essig (NRC) to H. Sepp (Westinghouse), "Acceptance for Referencing of Licensing Topical Report WCAP-14565, "VIPRE-01 Modeling and Qualification for Pressurized Water Reactor Non-LOCA Thermal/Hydraulic Safety Analysis (TAC No. M98666)," January 19, 1999.
83. Skaritka, J., ed, "Fuel Rod Bow Evaluation," WCAP-8691, Revision 1, July 1979.

84. McFarlane, A. F., "Power Peaking Factors," WCAP-7912-P-A (Proprietary) and WCAP-7912-A (Nonproprietary), January 1975.
85. Letter From C. Berlinger (NRC) to E. P. Rahe Jr. (W), Subject: "Request for Reduction in Fuel Assembly Burnup Limit for Calculation of Maximum Rod Bow Penalty," June 18, 1986.
86. Davidson, S. L. and Iorii, J. A., "Reference Fore Report 17 x 17 Optimized Fuel Assembly," WCAP-9500-A, May 1982.
87. Letter from E. P. Rahe (W) to Miller (NRC), NS-EPR-2573, Subject: "WCAP-9500 and WCAPS-9401/9402 NRC SER Mixed Core Compatibility Items," March 19, 1982.
88. Letter from C. O. Thomas (NRC) to Rahe (W), Subject: "Supplemental Acceptance No. 2 for Referencing Topical Report WCAP-9500," January 1983.
89. Letter from W. J. Johnson (Westinghouse) to M. W. Hodges (NRC), NS-NRC-87-3268, Subject: "VANTAGE 5 DNB Transition Core Effects," October 2, 1987.
90. Letter from M. W. Hodges (NRC) to W. J. Johnson (W), "NRC SER on VANTAGE 5 Transition Core Effects," February 24, 1988.
91. Schueren, P. and McAtee, K. R., "Extension of Methodology for Calculating Transition Core DNBR Penalties," WCAP-11837-P-A, January 1990.
92. Generic Letter 88-17, "Loss of Decay Heat Removal," dated October 17, 1988.
93. NAESCO letter NYN-93154 from T. C. Feigenbaum (NAESCO) to USNRC, "Revised Commitment Related to Generic Letter 88-17," November 5, 1993.
94. PSNH letter NYN-89001 from G. S. Thomas (PSNH) to USNRC, "Response to Generic Letter 88-17," January 3, 1989.
95. PSNH letter NYN-89012 from G. S. Thomas (PSNH) to USNRC, "Response to Generic Letter 88-17," February 3, 1989.

TABLE 4.4-1
(Sheet 1 of 2)

THERMAL AND HYDRAULIC COMPARISON TABLE

<u>Design Parameters</u>	<u>Seabrook Original Design</u>	<u>Seabrook Current Design^a</u>
Reactor core heat output (MWt)	3411	3411
Reactor core heat output (10^6 Btu/hr)	11,641	11,641
Heat generated in fuel (%)	97.4	97.4
System pressure, nominal (psia)	2250	2250
System pressure, minimum steady state (psia)	2220	2200
DNB Correlation	"R" (W-3 with Modified Spacer Factor)	WRB-1 ^b V+(w/o IFMs) WRB-2 ^b V+(w IFMs)
Correlation Limit Value, WRB-1 or WRB-2	1.3	1.17 ^b
Design Limit Value		
Typical flow channel	1.3	1.27 V+(w/o IFMs) 1.26 V+(w IFMs)
Thimble (cold wall) flow channel	1.3	1.26 V+(w/o IFMs) 1.24 V+(w IFMs)
Safety Analysis Limit Value		
Typical flow channel	1.3	1.40 V+(w/o IFMs) 1.91 V+(w IFMs)
Thimble (cold wall) flow channel	1.3	1.40 V+(w/o IFMs) 1.91 V+(w/ IFMs)
Minimum DNBR at nominal conditions		
Typical flow channel	2.06	2.41 ^c V+(w/o IFMs)
Thimble (cold wall) flow channel	1.72	3.02 ^c V+(w/ IFMs) 2.32 ^c V+(w/o IFMs) 2.88 ^c V+(w/ IFMs)
<u>Coolant Flow</u>		
Total thermal flow rate (10^6 lb _m /hr)	142.1	145.7 ^d
Effective flow rate for heat transfer (10^6 lb _m /hr)	133.9	138.7 ^d
Effective flow area for heat transfer (ft ²)	51.1	51.3
Average velocity along fuel rods (ft/sec)	16.7	17.1 ^d
Average mass velocity (10^6 lb _m /hr-ft ²)	2.62	2.71 ^d
<u>Coolant Temperature</u>		
Nominal inlet (°F)	558.8	559.5 ^d
Average rise in vessel (°F)	59.4	58.0 ^d
Average rise in core (°F)	62.6	60.6 ^d
Average in core (°F)	591.8	591.4 ^d
Average in vessel (°F)	588.5	588.5

TABLE 4.4-1
(Sheet 2 of 2)

THERMAL AND HYDRAULIC COMPARISON TABLE

<u>Design Parameters</u>	<u>Seabrook Original Design</u>	<u>Seabrook Current Design</u>
<u>Heat Transfer</u>		
Active heat transfer, surface area (ft ²)	59,700	59,700
Average heat flux (Btu/hr-ft ²)	189,800	189,800
Maximum heat flux for normal operation (Btu/hr-ft ²)	440,300 ^e	474,500 ^f
Average linear power (Kw/ft)	5.44	5.445
Peak linear power for normal operation (Kw/ft)	12.6 ^e	13.6 ^f
<u>Pressure Drop</u>		
Across core (psi)	25.7±2.6 ^g	28.5±2.85 ^h
Across vessel, including nozzle (psi)	48.2±7.2 ^g	48.7±7.3 ^h

^a V+ (w/IFMs) means V5H (with IFMs)

V+ (w/o IFMs) means V5H (without IFMs)

^b For conditions outside the range of applicability of WRB-1 or WRB-2, the W-3 correlation is used with a correlation limit of 1.45 in the pressure range of 500 to 1000 psia and 1.30 for pressures above 1000 psia.

^c This value is associated with the current design power distribution at 100 % rated power: a 1.65/1.04=1.586 $F_{\text{delta-h}}$ value for V+ (w/o IFMs), a 1.60/1.04=1.54 $F_{\text{delta-h}}$ Value for V+(w/IFMs) and a 1.55 chopped cosine axial power shape.

^d At minimum measured flow conditions.

^e This limit is associated with the original design value of $F_Q = 2.32$.

^f This limit is associated with the current design value of $F_Q = 2.50$.

^g Based on the original best estimate reactor flow rate as discussed in Section 5.1, and with thimble plug assemblies inserted.

^h For V5H (w/IFMs) based on a measured flow of 404,000gpm with thimble plug assemblies inserted.

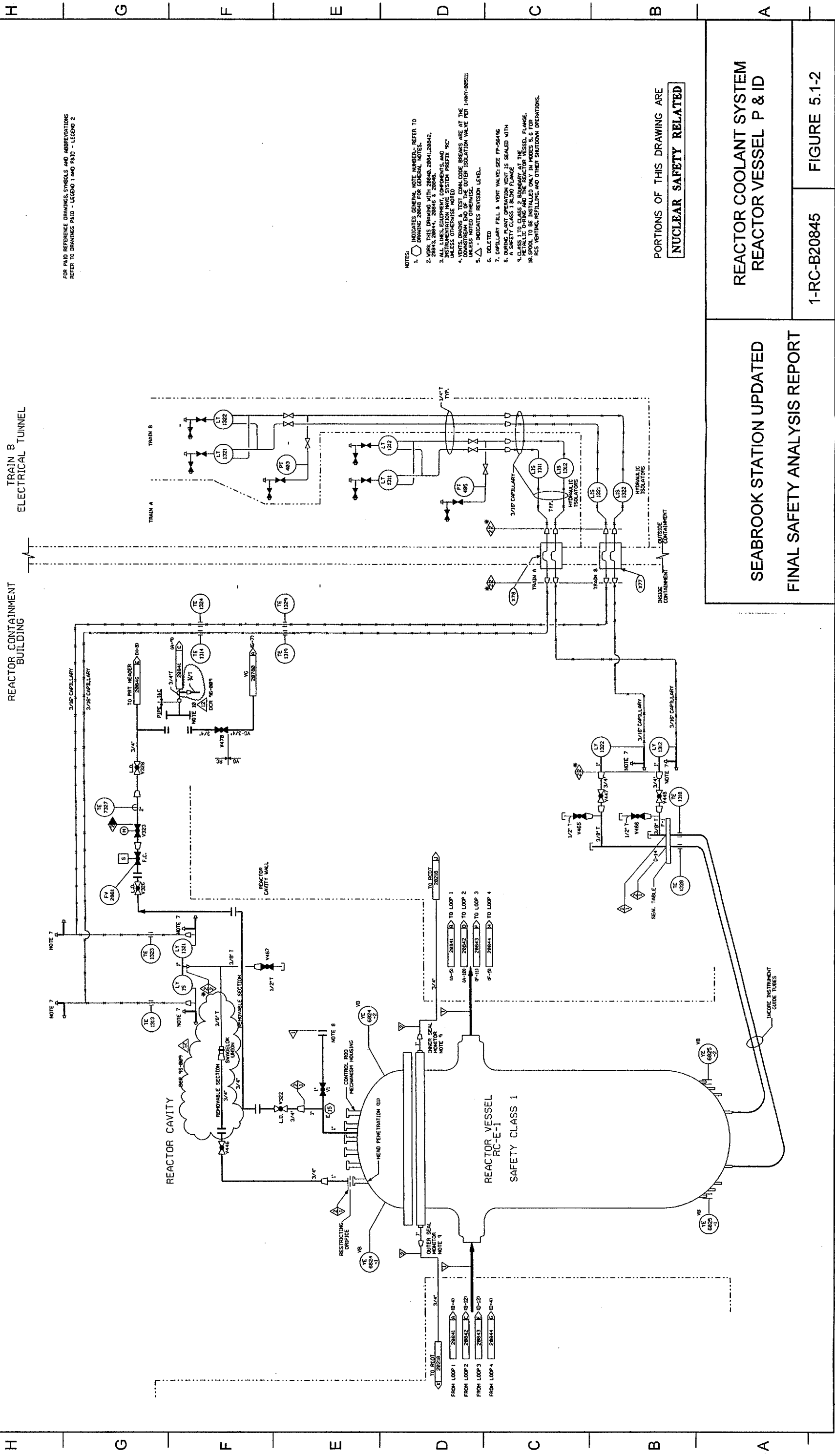
TABLE 4.4-2VOID FRACTIONS AT NOMINAL REACTOR CONDITIONS^a

		<u>Average</u>	<u>Maximum</u>
Core	(V5H w/o IFMs)	0.0	-
	(V5H w/IFMs)	0.0	-
Hot Subchannel	(V5H w/o IFMs)	0.07	0.58
	(V5H w/IFMs)	0.00	0.00

^a. The values are associated with the current design power distribution at 100% rated power, a $1.65/1.04 = 1.586$ $F_{\text{delta-h}}$ value for V+(w/o IFMs), a $1.60/1.04 = 1.54$ $F_{\text{delta-h}}$ value for V5H (w/IFMs) and a 1.55 chopped cosine power shape.

FIGURE 4.4-5

(DELETED)



FOR P&ID REFERENCE DRAWINGS, SYMBOLS AND ABBREVIATIONS REFER TO DRAWINGS P&ID - LEGEND 1 AND P&ID - LEGEND 2

- NOTES:
1. ○ INDICATES GENERAL NOTE NUMBER. REFER TO DRAWING 28848 FOR GENERAL NOTES.
 2. WORK THIS DRAWING WITH 28840, 28841, 28842, 28843, 28844, 28846 & 28848.
 3. INSTRUMENTATION MAY BE OBTAINED FROM THE INSTRUMENTATION WORK SYSTEM PREPARED BY UNLESS OTHERWISE NOTED.
 4. VENTS, DRAINING & TEST POINTS ARE AT THE CLASS 1 TO CLASS 2 BOUNDARY AT THE METALLIC DRUM AND THE REACTOR VESSEL FLANGE. INSTRUMENTATION MAY BE OBTAINED FROM THE INSTRUMENTATION WORK SYSTEM PREPARED BY UNLESS OTHERWISE NOTED.
 5. △ INDICATES REVISION LEVEL.
 6. DELETED
 7. CAPILLARY FILL & VENT VALVES SEE P&ID 28846.
 8. BORING & WAX OPERATIONS SHOULD BE SEaled WITH A SAFETY CLASS 1 BULKY FLANGE.
 9. CLASS 1 TO CLASS 2 BOUNDARY AT THE METALLIC DRUM AND THE REACTOR VESSEL FLANGE.
 10. INSTRUMENTATION MAY BE OBTAINED FROM THE INSTRUMENTATION WORK SYSTEM PREPARED BY UNLESS OTHERWISE NOTED.

PORTIONS OF THIS DRAWING ARE
NUCLEAR SAFETY RELATED

REACTOR COOLANT SYSTEM
REACTOR VESSEL P & ID

1-RC-B20845

FIGURE 5.1-2

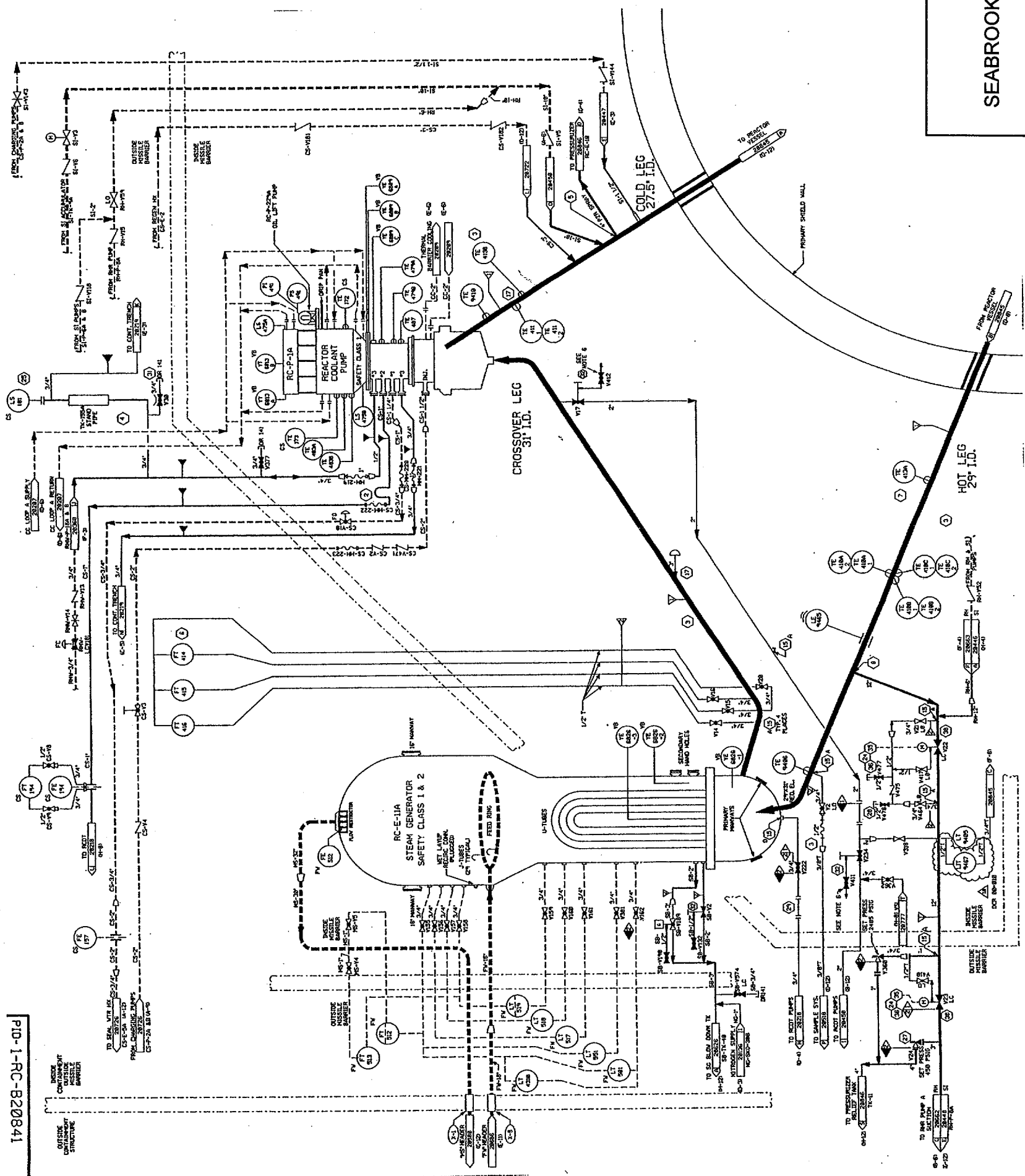
SEABROOK STATION UPDATED
FINAL SAFETY ANALYSIS REPORT

FOR PAID REFERENCE DRAWINGS, SYMBOLS AND ABBREVIATIONS REFER TO DRAWINGS PAID - LEGEND 1 AND PAID - LEGEND 2

- NOTES:
1. INDICATES GENERAL NOTE NUMBER - REFER TO DRAWING 28618 FOR GENERAL NOTES.
 2. WORK THIS DRAWING WITH DRAWINGS 28618, 28619, 28620, 28621, 28622, 28623, 28624, 28625, 28626, 28627, 28628, 28629, 28630, 28631, 28632, 28633, 28634, 28635, 28636, 28637, 28638, 28639, 28640, 28641, 28642, 28643, 28644, 28645, 28646, 28647, 28648, 28649, 28650, 28651, 28652, 28653, 28654, 28655, 28656, 28657, 28658, 28659, 28660, 28661, 28662, 28663, 28664, 28665, 28666, 28667, 28668, 28669, 28670, 28671, 28672, 28673, 28674, 28675, 28676, 28677, 28678, 28679, 28680, 28681, 28682, 28683, 28684, 28685, 28686, 28687, 28688, 28689, 28690, 28691, 28692, 28693, 28694, 28695, 28696, 28697, 28698, 28699, 28700, 28701, 28702, 28703, 28704, 28705, 28706, 28707, 28708, 28709, 28710, 28711, 28712, 28713, 28714, 28715, 28716, 28717, 28718, 28719, 28720, 28721, 28722, 28723, 28724, 28725, 28726, 28727, 28728, 28729, 28730, 28731, 28732, 28733, 28734, 28735, 28736, 28737, 28738, 28739, 28740, 28741, 28742, 28743, 28744, 28745, 28746, 28747, 28748, 28749, 28750, 28751, 28752, 28753, 28754, 28755, 28756, 28757, 28758, 28759, 28760, 28761, 28762, 28763, 28764, 28765, 28766, 28767, 28768, 28769, 28770, 28771, 28772, 28773, 28774, 28775, 28776, 28777, 28778, 28779, 28780, 28781, 28782, 28783, 28784, 28785, 28786, 28787, 28788, 28789, 28790, 28791, 28792, 28793, 28794, 28795, 28796, 28797, 28798, 28799, 28800.
 3. ALL LINES AND COMPONENTS, UNLESS OTHERWISE NOTED, HAVE SYSTEM PRESSURE UNLESS OTHERWISE NOTED.
 4. VENT, DRAIN, A TEST CONNECTIONS, AND INSTRUMENTATION BREAKS ARE AT THE DOWNSTREAM END OF THE OUTER ISOLATION VALVE PER THE RESULTS UNLESS NOTED OTHERWISE.
 5. INDICATES REVISION LEVEL.
 6. VALVE STOPS MAINTAINED CLOSED UNLESS VALVE IS VAI2 AND ARE TO BE MAINTAINED CLOSED UNLESS VALVE STOP LEAK-OFF TO BE CONSIDERED INOPERABLE.

PORTIONS OF THIS DRAWING ARE NUCLEAR SAFETY RELATED

REF. DRAWING NO.	TITLE
9783-F-080811	18 CHEMICAL VOLUME CONTROL SYS. PURIFICATION PAID
9783-F-080818	17 SAFETY INJECTION SYS. HIGH HEAD PAID
9783-F-080819	12 SAFETY INJECTION SYS. ACCUMULATIONS PAID
9783-F-080828	15 RESIDUAL HEAT REMOVAL SYS. PAID
9783-F-080829	13 REACTOR COOLANT SYS. PRESSURIZER PAID
9783-F-080830	14 REACTOR COOLANT SYS. LOOP NO. 1 PAID
9783-F-080832	12 REACTOR COOLANT SYS. REACTOR VESSEL PAID



REACTOR COOLANT SYSTEM LOOP NO. 1

SEABROOK STATION UPDATED FINAL SAFETY ANALYSIS REPORT

1-RC-B20841

FIGURE 5.1-3 SH 1

PID-1-RC-B20841

SEABROOK UPDATED FSAR

3. If all reactor coolant pumps have stopped for more than 5 minutes during plant heatup, and the reactor coolant temperature is greater than the charging and seal injection water temperature, no attempt shall be made to restart a pump unless a steam bubble is formed in the pressurizer. This precaution will minimize the pressure transient when the pump will be started and the cold water previously injected by the charging pumps will be circulated through the warmer reactor coolant components. The steam bubble will accommodate the resultant expansion as the cold water is rapidly warmed.
4. If all reactor coolant pumps are stopped and the RCS is being cooled down by the residual heat exchangers, a nonuniform temperature distribution may occur in the reactor coolant loops and the secondary side of the steam generators. No attempt shall be made to restart a reactor coolant pump unless (1) a steam bubble is formed in the pressurizer or (2) the secondary water temperature of each steam generator is less than 50°F above each of the RCS cold leg temperatures when the cold leg temperatures are less than or equal to 350°F.
5. During plant cooldown, all steam generators shall be connected to the steam header to assure a uniform cooldown of the reactor coolant loops.
6. At least one reactor coolant pump shall be maintained in service until the reactor coolant temperature is reduced to 160°F.

These special precautions back up the normal operational mode of maximizing periods of steam bubble operation so that cold overpressure transient prevention is continued during periods of transitional operations.

The specific plant configurations of emergency core cooling system testing and alignment will also highlight procedures required to prevent developing cold overpressurization transients. During these limited periods of plant operation, the following procedures shall be followed:

1. To preclude inadvertent emergency core cooling system actuation during heatup and cooldown, blocking is required of the low pressurizer pressure and low steam line pressure safety injection signal actuation logic at 1900 psig.
2. When RCS pressure has decreased below 1000 psig and approximately 425°F during plant cooldown, the SI accumulator isolation valves are closed to prevent injection of the accumulator's volume into the RCS as RCS pressure is reduced.

This action involves energizing the MCCs powering the accumulators' MOV and then closing the valves. These actions are all performed in the control room.

Should a single failure disable the power supply to one or more of the SI accumulator isolation valves, solenoid operated vents are provided on each SI accumulator to allow relieving of the nitrogen overpressure gas to the Containment. These solenoids are Class 1E, powered by the emergency electrical train opposite that powering the SI accumulator isolation valve, and are operable from the control room and the remote shutdown location.

Additionally, during plant cooldown, one centrifugal charging pump, the positive displacement charging pump and both SI pumps will be made inoperable to preclude overpressurization events at low temperatures. This action can also be performed in the control room and the remote shutdown location.

Prior to decreasing RCS temperature below 350°F, the safety injection pumps and the nonoperating charging pumps are made inoperable. It should be noted that the high containment pressure safety injection actuation logic cannot be blocked.

3. Periodic emergency core cooling system pump performance testing requires the testing of the pumps during normal power operation or at hot shutdown conditions, to preclude any potential for developing a cold overpressurization transient.

During shutdown conditions charging pump and SI pump operation are restricted in accordance with the Technical Specifications and their supporting bases.

4. "S" signal circuitry testing, if performed during cold shutdown, will also require RHRS alignment and power lockout of both SI pumps and nonoperating charging pump to preclude developing cold overpressurization transients.

The above procedures, which will be followed for normal operations with a steam bubble, transitional operations where the Reactor Coolant System is potentially water-solid, and during specific testing operations, will provide in-depth cold overpressure prevention or reduction, thereby augmenting the installed Overpressure Relief System.

5.2.3 Reactor Coolant Pressure Boundary Materials

5.2.3.1 Material Specifications

Material specifications used for the principal pressure retaining applications in each component of the RCPB are listed in Table 5.2-2 for ASME Class 1 primary components and Table 5.2-3 for ASME Class 1 and 2 auxiliary components. Tables 5.2-2 and 5.2-3 also include the unstabilized austenitic stainless steel material specifications used for components in systems required for reactor shutdown and for emergency core cooling.

The unstabilized austenitic stainless steel materials for the reactor vessel internals, which are required for emergency core cooling for any mode of normal operation or under postulated accident conditions and for core structural load bearing members, are listed in Table 5.2-4.

In some cases, the tables may not be totally inclusive of the material specifications used in the listed applications. However, the listed specifications are representative of those materials used.

The materials used conform with the requirements of the ASME Code, Section III, plus applicable addenda and Code cases.

The welding materials used for joining the ferritic base materials of the RCPB conform to, or are equivalent to, ASME Material Specifications SFA 5.1, 5.2, 5.5, 5.17, 5.18 and 5.20. They are qualified to the requirements of the ASME Code, Section III.

The welding materials used for joining austenitic stainless steel base materials of the RCPB conform to ASME Material Specifications SFA 5.4 and 5.9. They are qualified to the requirements of the ASME Code, Section III.

The welding materials used for joining nickel-chromium-iron alloy in similar base material combination and in dissimilar ferritic or austenitic base material combination conform to ASME Material Specifications SFA 5.11 and 5.14. They are qualified to the requirements of the ASME Code, Section III.

5.2.3.2 Compatibility with Reactor Coolant

a. Chemistry of Reactor Coolant

The Reactor Coolant System (RCS) chemistry specifications are identified in Technical Specifications 3.4.7 and 3.9.1.b.

The RCS water chemistry is selected to minimize corrosion. A routinely scheduled analysis of the coolant chemical composition is performed to verify that the reactor coolant chemistry meets the specifications.

The Chemical and Volume Control System provides a means for adding chemicals to the RCS which control the pH of the coolant during pre-startup and subsequent operation, scavenge oxygen from the coolant during heatup, and control radiolysis reactions involving hydrogen, oxygen and nitrogen during all power operations subsequent to startup. The limits specified for chemical additives and reactor coolant impurities for power operation are described in the EPRI PWR Primary Water Chemistry Guidelines and implemented in the Chemistry Manual.

The pH control chemical employed is lithium hydroxide monohydrate, enriched in ^7Li isotope to 99.9 percent. This chemical is chosen for its compatibility with the materials and water chemistry of borated water/stainless steel/zirconium/Inconel systems. In addition, ^7Li is produced in solution from the neutron irradiation of the dissolved boron in the coolant. The lithium-7 hydroxide is introduced into the RCS via the charging flow. The solution is prepared in the laboratory and transferred to the chemical additive tank. Reactor makeup water is then used to flush the solution to the suction header of the charging pumps. The concentration of lithium-7 hydroxide in the RCS is maintained in the range specified for pH control. If the concentration exceeds this range, the cation bed demineralizer is employed in the letdown line in series operation with the mixed bed demineralizer.

During a reactor startup from a cold condition (i.e., following a refueling outage), hydrazine may be added to the coolant as an oxygen scavenging agent. The hydrazine is typically added prior to drawing a bubble in the pressurizer. This allows an excess of hydrazine to be present in the system for improved reaction kinetics to take place at higher RCS temperature. Oxygen limits are described in the EPRI PWR Primary Water Chemistry Guidelines and implemented in the Chemistry Manual.

The reactor coolant is treated with dissolved hydrogen to control the products formed by the decomposition of water by radiolysis. The hydrogen reacts with the oxygen to form water and prevent the oxygen from reacting with the nitrogen and forming nitric acid

with a "check source" that is inserted upon the command of the RDMS. Each time the check source is inserted, the microprocessor measures and stores the effect of the check source and compares it to the previous reading to obtain an indication of calibration trends.

5.2.5.9 Technical Specification

The Technical Specification is provided in Section 3/4.4.6.

5.2.6 Reactor Coolant Vent System

5.2.6.1 Design Basis

The Reactor Coolant Vent System is designed to allow venting the large quantities of noncondensable gases that can be generated within the reactor following core damage. It provides a vent path to the containment atmosphere via the pressurizer relief tank to insure that noncondensable gases cannot accumulate in the core to the point where core cooling would be interrupted and further core damage occur.

The design temperature and pressure is the same as the Reactor Coolant System, i.e., 650°F and 2485 psig. Piping and valve material is stainless steel, Type 316. All material is compatible with the reactor coolant chemistry and will be fabricated and tested in accordance with SRP Subsection 5.2.3, "Reactor Coolant Pressure Boundary Materials."

5.2.6.2 System Description

This system (see Figures 5.1-2 and 5.1-4) provides the capability to vent the Reactor Coolant System from two locations: the reactor vessel head and the pressurizer steam space. The vent valves will be manually operated from the control room. The function of these vents is to vent any noncondensable gases that may collect in the reactor vessel head and in the pressurizer following core damage.

a. Reactor Vessel Head Vent

The reactor vessel head vent consists of a single solenoid valve and a motor-operated valve in series. This vent ties into the reactor head vent line which is normally used to vent the vessel for vessel fill. A $\frac{3}{8}$ " flow restricting orifice is provided immediately downstream of the tie-in to the normal vent line. Both valves are powered from the same train emergency power source.

b. Pressurizer Vent

The vent for the pressurizer steam space uses the two parallel, redundant, safety-grade PORVs. The PORVs are 3"x6" pilot-operated

solenoid valves with redundant, direct position indication. Each PORV has its own motor-operated isolation valve.

The PORV and its associated isolation valve are both powered from the same emergency power electrical train. However, each PORV and its associated isolation valve are supplied by opposite train emergency power sources.

5.2.6.3 Safety Evaluation

The RCS vessel head vent piping and valves are Safety Class 1 and 2, seismic Category 1 up to, and including, the second isolation valve. A temperature detector is located immediately downstream of the second isolation valve for leakage detection.

The reactor vessel head vent line has two normally closed valves in series; therefore, a single failure which results in an inadvertent opening of one valve does not initiate venting. The line also contains an orifice on the vessel side of the isolation valves that restricts the flow rate from a pipe break downstream of the orifice to within the makeup capacity of the charging system. Therefore, a break in this line, downstream of the orifice, or an inadvertent actuation of the vent during normal operation does not constitute a LOCA, and does not require ECCS actuation. All piping and components downstream of the flow restricting orifice are Safety Class 2, and seismic Category I. The valve, piping and components downstream of the motor-operated valve are classified Non-Nuclear Safety (NNS).

This valve is designed to withstand the safe shutdown earthquake. In addition, there is no piping which might be affected by spray from a postulated break in the NNS portion of the piping (which is routed to the pressurizer relief tank).

The pressurizer vent consists of the normal pressurizer PORVs and their normally open, motor-operated isolation valves. While inadvertent operation of a PORV would result in RCS depressurization, the effects have been analyzed and are bounded by the analysis presented in Chapter 15 and do not represent an unreviewed safety question. All piping and components upstream of, and including, the PORVs are Safety Class 1 and seismic Category I. All other piping and components downstream of the PORVs are classified Non-Nuclear Safety.

All electrical equipment for both the reactor vessel vent and the pressurizer vent is Class 1E. Motive and control power supplies for these valves are also Class 1E. Equipment within the containment atmosphere is environmentally qualified to insure operability in a hostile environment resulting from an accident.